FFI RAPPORT

LITERATURE REVIEW ON VESSEL DETECTION

ARNESEN Tonje Nanette, OLSEN Richard B

FFI/RAPPORT-2004/02619

LITERATURE REVIEW ON VESSEL DETECTION

ARNESEN Tonje Nanette, OLSEN Richard B

FFI/RAPPORT-2004/02619

FORSVARETS FORSKNINGSINSTITUTT
Norwegian Defence Research Establishment
P O Box 25, NO-2027 Kjeller, Norway

FORSVARETS FORSKNINGSINSTITUTT (FFI)
Norwegian Defence Research Establishment

P O BOX 25
N0-2027 KJELLER, NORWAY

UNCLASSIFIED

SECURITY CLASSIFICATION OF THIS PAGE
(when data entered)

REPORT DOCUMENTATION PAGE

1) PUBL/REPORT NUMBER FFI/RAPPORT-2004/02619	2) SECURITY CLASSIFICATION UNCLASSIFIED	3) NUMBER OF PAGES 168
1a) PROJECT REFERENCE FFI-III/1002/170	2a) DECLASSIFICATION/DOWNGRADING SCHEDULE -	

4) TITLE
LITERATURE REVIEW ON VESSEL DETECTION

5) NAMES OF AUTHOR(S) IN FULL (surname first)
ARNESEN Tonje Nanette, OLSEN Richard B

6) DISTRIBUTION STATEMENT
Approved for public release. Distribution unlimited. (Offentlig tilgjengelig)

7) INDEXING TERMS

	IN ENGLISH:		IN NORWEGIAN:
a)	Ship & vessel detection	a)	Skipsdeteksjon
b)	Target detection	b)	Måldeteksjon
c)	Ship wakes	c)	Kjølvannsstriper
d)	Backscatter	d)	Tilbakespredning
e)	Synthetic Aperture Radar	e)	Syntetisk Apertur Radar

THESAURUS REFERENCE:

8) ABSTRACT

This report presents an overview of available literature on the subject of vessel detection in Synthetic Aperture Radar (SAR) imagery. The review was carried out as part of the EU-funded DECLIMS project, which is aimed at evaluating different methods for monitoring activities of fishing vessels, using spaceborne SAR. Available literature on vessel detection and related topics is vast. The review has been organized according to some key questions and issues that have been presented in the literature body: 1) Generic papers, 2) Signatures and characteristics, 3) Target and wake detection, 4) Wake detection, 5) Target detection, 6) Classification, and 7) HF radar. A table with an overview sorted after the publication year is given in the beginning of each part, and a reference list is given at the end.

9) DATE	AUTHORIZED BY This page only	POSITION
2004-08-18	Johnny Bardal	Director

ISBN-82-464-0859-3

UNCLASSIFIED

SECURITY CLASSIFICATION OF THIS PAGE
(when data entered)

CONTENTS

		Page
1	INTRODUCTION	13
2	GENERIC	17
2.1	Overview	17
2.2	Absolute Calibration of ASAR Level 1 Products Generated by PF-ASAR (50)	24
2.3	Canadian Progress Toward Marine and Coastal Applications of Synthetic Aperture Radar (84)	24
2.4	CDPF/OFW Products from MARCOT (83)	25
2.5	Comparison of Parameter Estimators for K-Distribution	26
2.6	Detecting Surface Vessels by RADARSAT (81)	27
2.7	ERS Detection of Soft and Hard Targets at Sea: What Can Be Operationalized? (54)	28
2.8	Expected Performance of the ENVISAT ASAR for Near Real-Time Maritime Applications (44)	28
2.9	Fishing Boat Detection by Using SAR Imagery (19)	31
2.10	Hough Transform from the Radon Transform (9)	31
2.11	Integrated Use of RADAR Satellites for Fisheries Enforcement Operations (88)	32
2.12	Integrating Spaceborne SAR Imagery into Operational Systems for Fisheries Monitoring (20)	32
2.13	International Fisheries Enforcement Management Using Wide Swath SAR (32)	33
2.14	Maritime Use of Satelliteborne SAR (57)	33
2.15	Mobile Communications Technologies for Ship Detection and Response (18)	34
2.16	Monitoring the Coastal Zone with the RADARSAT Satellite (85)	35
2.17	NATO Naval Exercises As Observed From Civilian Radar satellites (90)	35
2.18	Ocean Applications of RADARSAT (12)	36
2.19	Operational Use of RADARSAT SAR in the Coastal Zone: The Canadian Experience (28)	36
2.20	Radar Satellites and Naval Operations (86)	36
2.21	Remote Vessel Detection on the Grand Banks Using Radarsat Imagery: Early Results (21)	37
2.22	Review of Ship Detection from Airborne Platforms (10)	37

2.23 The Ocean Monitoring Workstation: Experience Gained with RADARSAT (15) 38

2.24 The Role of Wide Swath SAR in High-Latitude Coastal Management (41) 39

2.25 The Use of Satellite-Based SAR in Support of Fisheries Enforcement Applications (33) 40

2.26 Validation of Ship Detection by the RADARSAT SAR (80) 40

2.27 Validation of Ship Detection by the RADARSAT Synthetic Aperture Radar and the Ocean Monitoring Workstation (85) 41

2.28 Vessel Detection with Wide Area Remote Sensing (14) 42

2.29 Literature 42

3 STUDIES ON SIGNATURES AND CHARACTERISTICS 53

3.1 Overview 53

3.2 Detection of point targets in ScanSAR data (In Norwegian) (158) 66

3.3 Detectability of selected phenomena over the ocean in digital ERS-1 images (In Norwegian) (96) 69

3.4 Hull Characteristics from SAR Images of Ship Wakes (272) 69

3.5 Instrumented Ship Imaging Using the AN/APS-506 Spotlight SAR System (154) 70

3.6 K-Distribution (105) 70

3.7 Kelvin and V-like ship wakes affected by surfactants (289) 71

3.8 Neural Processing of Targets in Visible Multispectral IR and SAR Imagery (277) 71

3.9 Nonuniform Azimuth Image Shift Observed in the Radarsat Images of Ships in Motion (207) 72

3.10 Observation of Long Waves Generated by Ferries (201) 72

3.11 Ocean Surveillance with Polarimetric SAR (286) 73

3.12 On the Use of Complex SAR Image Spectral Analysis for Target Detection: Assessment of Polarimetry (249) 74

3.13 On the Use of Polarimetric SAR Data for Ship Detection (256) 74

3.14 Optimization of the Ocean Features Workstation for Ship Detection (115) 75

3.15 Orbital SAR Simulator of Fishing Vessel Polarimetric Signatures Based on High Frequency Electromagnetic Calculations (193) 75

3.16 Results from the Crusade Ship Detection Trial: Polarimetric SAR (287) 76

3.17 SAR Detection of Ships and Ship Wakes (269) 76

3.18 SAR Imaging of Vortex Ship Wakes. Vol. I: Basic Theory and Simulation in L-band Using Bragg Model (247) 77

3.19 SAR Imaging of Vortex Ship Wakes. Vol. II: Simulation in L- and C-Band Comparing the Bragg and HSW Imaging Models (248) 77

3.20 SAR Imaging of Vortex Ship Wakes. Vol. III: An Overview of the Pre-ERS-1 Observations and Models (246) 78

3.21 Satellite SAR Simulator for Fishing Vessels Signature Studies (191) 78

3.22 Sea Surface and Ship Observation with MEMPHIS(111) 79

3.23 Ship Detection Performance Predictions for Next Generation Space borne Synthetic Aperture Radars (244) 79

3.24 Ship Detection Using Polarimetric SAR Data (230) 80

3.25 Ship Surveillance Using RADARSAT ScanSAR Images (231) 81

3.26 Ship Traffic Monitoring Using the ERS-1 SAR (270) 81

3.27 Ship Wakes and Their Radar Images (224) 82

3.28 Ship-Sea Contrast Optimization When Using Polarimetric SARS (260) 82

3.29 Simulation of Polarimetric SAR Vessel Signatures for Satellite Fisheries Monitoring (192) 82

3.30 Statistical Modelling of Ocean SAR Images (131) 83

3.31 Super-Resolution of Polarimetric SAR Images of Ship Targets (210) 83

3.32 Synthetic Aperture Radar Imaging of Ship Wakes in the Gulf of Alaska (239) 84

3.33 Synthetic Aperture Radar Imaging of Surface Ship Wakes (189) 84

3.34 The Ship Detection Capability of ENVISAT's ASAR (205) 85

3.35 Evaluation of ENVISAT ASAR for ship detection (In Norwegian) (97) 86

3.36 Wake Measurements (182) 87

3.37 Literature 87

4 TARGET AND WAKE DETECTION 105

4.1 Overview 105

4.2 An Automatic Ship and Ship Wake Detection System for Spaceborne SAR Images in Coastal Regions (298) 106

4.3 Automatic Moving Target Detection Using a Rule-Based System: Comparison Between Different Study Cases (299) 108

4.4 Automatic Ship and Ship Wake Detection in Spaceborne SAR Images from Coastal Regions (296) 109

4.5 Automatic Ship Detection in SAR Images (293) 109

4.6 Computer-Based Algorithm for Ship Detection from ERS SAR Imagery (301) 110

4.7 Principles and Performance of an Automated Ship detection System for SAR Images (297) 110

4.8 Ship and Ship Wake Detection in the ERS SAR Imagery Using Computer-Based Algorithm (302) 111

4.9 Ship Detection in RADARSAT SAR Imagery (300) 111

4.10 Literature 112

5 WAKE DETECTION PAPERS 115

5.1 Overview 115

5.2 An algorithm for Ship Wake Detection from the Synthetic Aperture Radar Images Using the Radon Transform and Morphological Image Processing (319) 118

5.3 Application of Radon Transform Techniques to Wake Detection in Seasat-A SAR Images (328) 118

5.4 Linear Feature Detection and Enhancement in Noisy Images Via the Radon Transform (324) 119

5.5 Localized Radon Transform-Based Detection of Ship Wakes in SAR Images (309) 119

5.6 Ship Wake Detection in Synthetic Aperture Radar Images Using a Combination of a Wavelet Correlator and Radon Transform (320) 120

5.7 The Application of Wavelets Correlator for Ship Wake Detection in SAR Images (321) 120

5.8 Use of the Dempster-Shafer Algorithm for the Detection of SAR Ship Wakes (327) 121

5.9 Literature 122

6 TARGET DETECTION 127

6.1 Overview 127

6.2 A Neural System for Automatic Target Learning and Recognition Applied to Bare and Camouflaged SAR Targets (350) 135

6.3 A Search Procedure for Ships in RADARSAT Imagery (427) 135

6.4 An Automatic Approach to Ship Detection in Spaceborne Synthetic Aperture Radar Imagery: An Assessment of Ship Detection Capability using RADARSAT (344) 137

6.5 An Automatic Ship Detection System Using ERS SAR Images (404) 138

6.6 Automatic Detection for Ship Targets in RADARSAT SAR Images from Coastal Regions (384) 138

6.7 Automatic Detection for Ship Targets in SAR Imagery Using PNN-model (382) 139

6.8 Automatic Detection of Ships in RADARSAR-1 SAR Imagery (437) 140

6.9 Comparison of Probability Statistics for Automated Ship Detection in SAR Imagery (371) 141

6.10 Context-Based Target Detection with Multi-Pass RADARSAT-1 Data – Application to Coastal Surveillance (388) 141

6.11 Detection of Ships Using Cross-Correlation of Split-Look SAR Images (375) 142

6.12 Exploiting the Polarimetric Information for the Detection of Ship Targets in Non-Homogeneous SAR Images (430) 142

6.13 Model-Based Neural Network for Target Detection in SAR Images (422) 143

6.14 Optimal Target Detection Using One Channel SAR. Complex Imagery: Application to Ship Detection (408) 143

6.15 Probabilistic Winner-Take-All Segmentation of Images with Application to Ship Detection (418) 143

6.16 Results from the Ocean Monitoring Workstation (OMW) Dark Feature Detection Algorithm (433) 144

6.17 SAR ATR Performance Using a Conditionally Gaussian Model (419) 145

6.18 Segmentation-Based Technique for Ship Detection in SAR Images (407) 146

6.19 Ship Detection by the RADARSAT SAR: Validation of Detection Model Predictions (435) 146

6.20 Literature 147

7 CLASSIFICATION 159

7.1 Overview 159

7.2 Composite Filters for Inverse Synthetic Aperture Radar Classification of Small Ships (466) 161

7.3 Classification of ships in SAR images (In Norwegian) (455) 161

7.4 The SSCM for Ship Characterization Using Polarimetric SAR (464) 162

7.5 Vessel Classification as Part of an Automated Vessel Traffic Monitoring System Using SAR Data (461) 162

7.6 Literature 163

8 HF RADAR 165

8.1 Overview 165

8.2 Detection of Ships with Multi-Frequency and CODAR SeaSonde HF Radar Systems (470) 166

8.3 Ship Detection With High-Frequency Phased-Array and Direction-Finding Radar Systems (469) 166

8.4 Surveillance of the 200 Nautical Mile Exclusive Economic Zone (EEZ) Using High Frequency Surface Wave Radar (HFSWR) (473) 167

8.5 Literature 167

LIST OF ABBREVIATIONS

2L-IHP	2-Looks Internal Hermitian Product
ADA	Automatic Detection Algorithm
ADTS	Advanced Detection Technology Sensor
ART-2A	Adaptive Resonance Theory
ASAR	Advanced Synthetic Aperture Radar
ASD	Automatic Ship Detection
ASP	Anne S Pierce
ASW	Anti-Submarine Warfare
ATD&R	Automatic Target Detection and Recognition
BIO	Bedford Institute of Oceanography
BPN	Back Propagation Network
CADA	Complete Automatic Detection Algorithm
C^3	Communication, Command and Control
CCRS	Canada Centre of Remote Sensing
CDPF	Canadian Data Processing Facility
CFAR	Constant False Alarm Rate
CIS	Canadian Ice Service
CRISP	Centre for Remote Imaging, Sensing and Processing
COPE-3	Third Chesapeake Outfall Plume Experiment
DND	(Canadian) Department of National Defence
EEZ	Exclusive Economic Zone
ERS	European Remote Sensing
ESA	European Space Agency
FFI	Forsvarets Forskningsinstitutt
FFT	Fast Fourier Transform
FOM	Figure of Merit
GMTI	Ground Moving Target Indicator
GPS	Global Positioning System
GSS	Gatineau Satellite Station
H	Horizontal polarization
HF	High Frequency
HFSWR	High Frequency Surface Wave Radar
HH	Horizontal sent - Horizontal receive
HULINV	Hull Inversion
HV	Horizontal sent - Vertical receive
IR	Infrared
ISAR	Inverse Synthetic Aperture Radar
ITTC	Information and Instructional Technology Center
KS	Kolmogorov-Smirnov
LDV	Laser Doppler Velocimetry
LUT	Look-Up Table
MARCOT	Maritime Command Coordinated Operational Training
MCR	Multi-Frequency Coastal Radar
ML	Maximum Likelihood
MM	Mathematical Morphology
MML	Mean of the data and Mean of the Log
MMSE	Minimum Mean Square Error
MSAT	Mobile Satellite
MSTAR	Moving and Stationary Target Acquisition and Recognition
MTF	Modulation Transfer Function
MV	Mean and Variance of the data
NAFO	Northwest Atlantic Fisheries Organisation
NDRE	Norwegian Defence Research Establishment
NORCSEX	Norwegian Continental Shelf Experiment
NCRS	Normalised Radar Cross Section
NNDS	Neural-Network-Dempster-Shafer
OFW	Ocean Feature Workstation

OMW	Ocean Monitoring Workstation
OTH	Over-the-Horizon
PDF	Probability Density Function
PIRATA	Pilot Research Moored Array in the Tropical Atlantic
PNN	Probabilistic Neural Networks
POLINSAR	Polarimetric Interferometric Synthetic Aperture Radar
POLSAR	Polarimetric Synthetic Aperture Radar
PWF	Polarimetric Whitening Filter
PWTA	Probabilistic Winner-Take-All
QC	Quality Control
RCS	Radar Cross Section
RSG4	Research Study Group on wake measurements
R&D	Research and Development
SAR	Synthetic Aperture Radar
SCN2	ScanSAR Narrow Far
SDF	Standard Discriminant Function
SGE (HYDRO)	Special Group of Experts on Naval Hydrodynamics and Related Problems
SLAR	Side-Looking Airborne Radar
SLC	Single-Look Complex
SNR	Signal to Noise Ratio
SSCM	Symmetric Scattering Characterization Method
STF	Salvesen-Tuck-Faltinsen
SWDRM	Ship Wake Detection based on Radon transform and Morphological image processing
SWF	Spatial Whitening Filter
TCR	Target to Clutter Ratio
TD/TR	Target Detection/Target Recognition
TopSat	Tactical Optical Satellite
UNCLOS	United Nations Convention on the Law of the Sea
UPC	Universitat Polytècnica de Catalunya
V	Vertical polarization
VMS	Vessel Monitoring System
VTS	Vessel Traffic Services
VTMS	Vessel Traffic Monitoring System
VH	Vertical sent - Horizontal receive
VV	Vertical sent - Vertical receive
WC	Wigley-Cosine
WEAG	Western European Armaments Group

Literature review on vessel detection

1 INTRODUCTION

This report provides an overview of available literature on the subject of vessel detection in Synthetic Aperture Radar (SAR) imagery. The review was carried out as part of the EU-funded DECLIMS project, which is aimed at evaluating different methods for monitoring activities of fishing vessels, using spaceborne SAR.

Ship detection in SAR imagery has become an important routine application in some countries. To illustrate the topics of interest, some examples of images with ships and wakes are given below. Figure 1.1 shows an early example of ships off the Swedish west coast in very stratified waters. The image was one of the fist ERS-1 images acquired in Scandinavian waters. Besides observing the ships themselves, wakes can be detected in this image. Figure 1.2 and Figure 1.3 show examples from ENVISAT acquired over the North Sea and Skagerrak. The first case indicates that in light to moderate winds, it is sometimes possible to observe oil spills from ships. The last case is an example of ENVISAT's Advanced SAR (ASAR) new cross-polarized channel. This channel is good for observing ships, but not wakes, for low incidence angles.

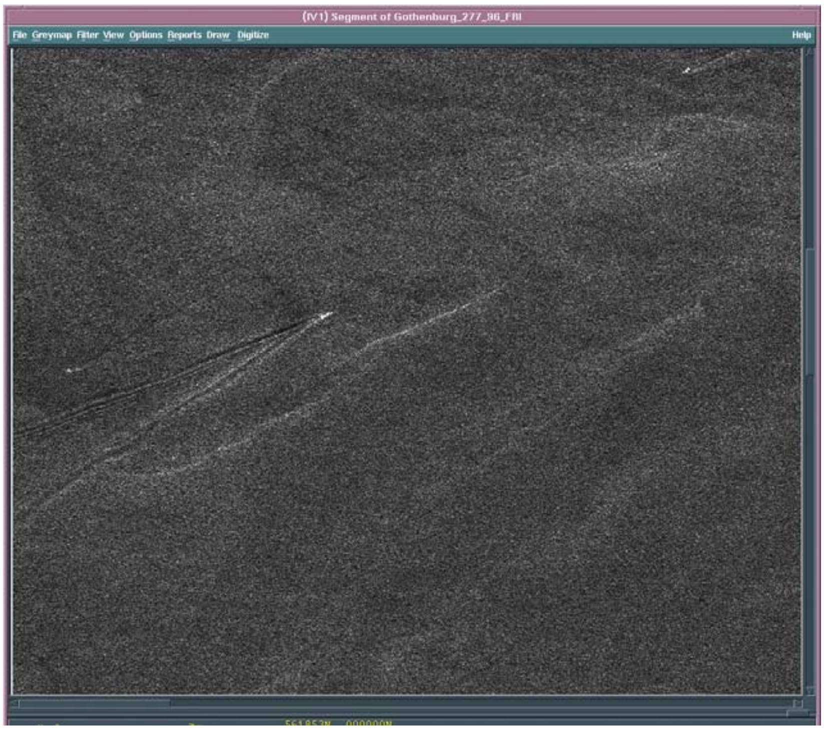

Figure 1.1 *ERS-1 image from 1991 showing ship wakes behind vessels. The dominant wake feature in the image is most likely internal waves set up on a boundary between surface water and deeper water with higher density. © ESA.*

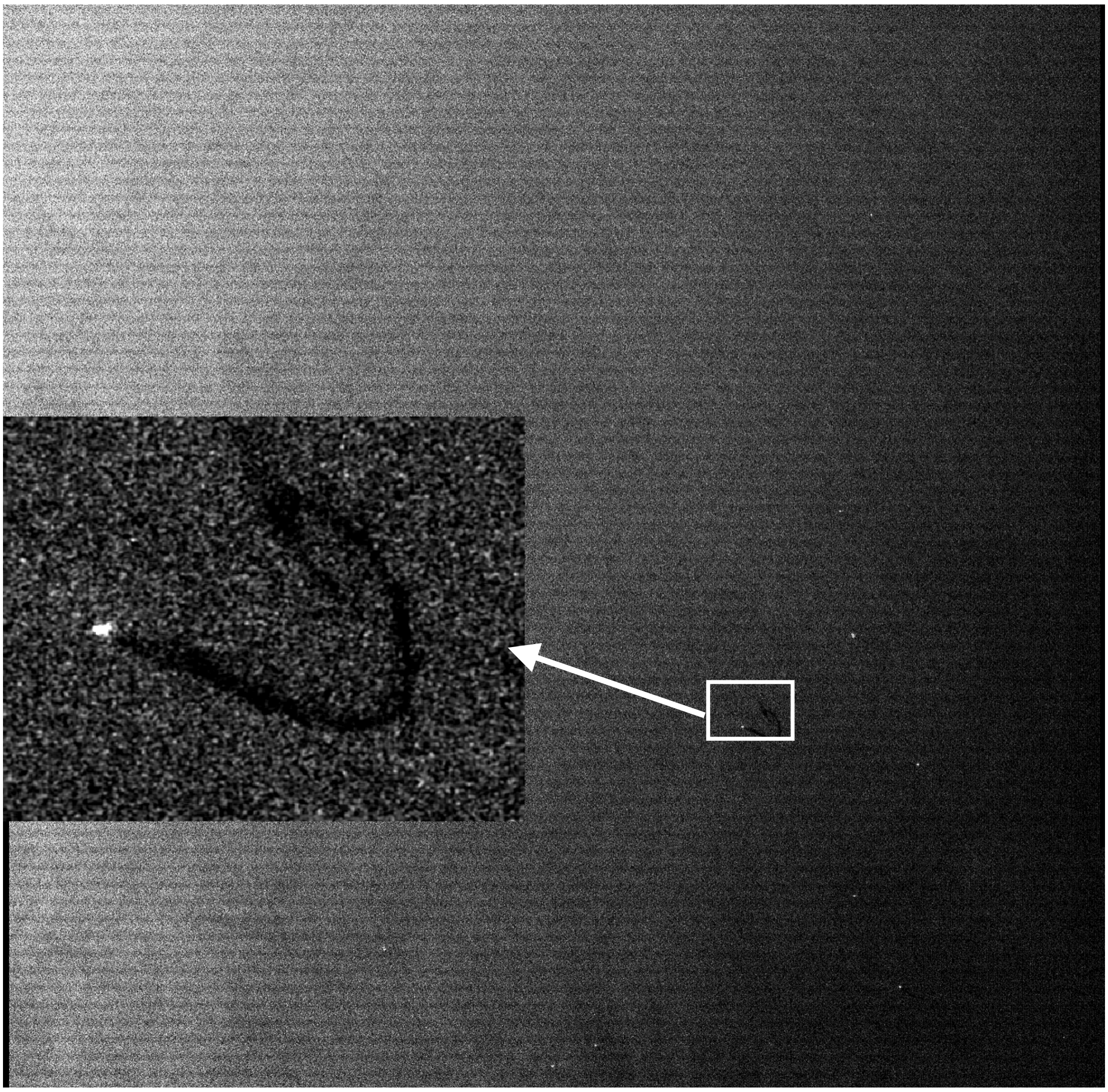

Figure 1.2 Image of the North Sea on June 9, 2004. The data is recorded with ENVISAT ASAR AP mode with VV-polarization and sub-swath IS2. It is possible to detect several vessels. In addition, it is possible to see oil spill behind one of the vessels.

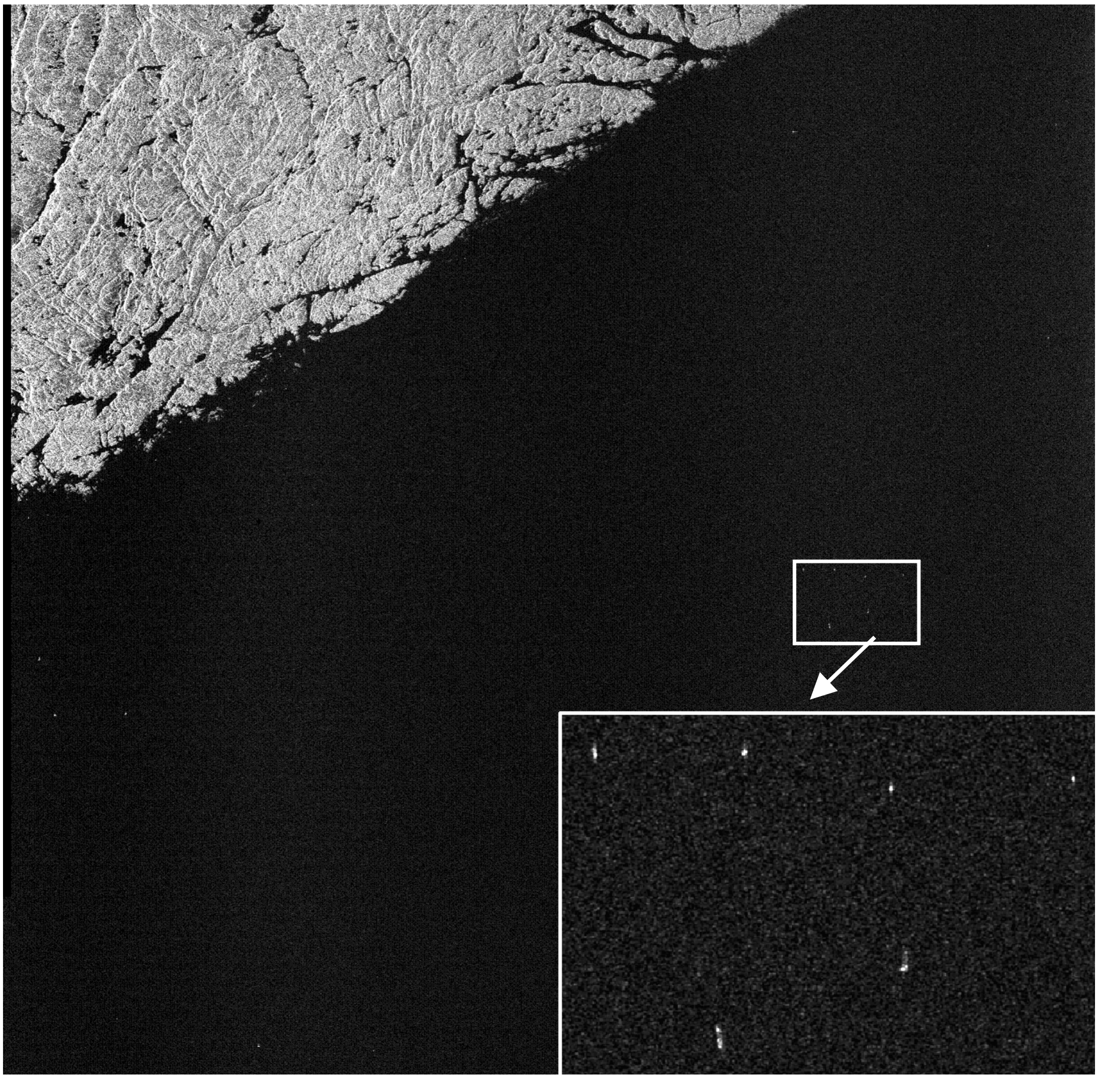

Figure 1.3 ENVISAT image of Skagerrak outside Arendal, Norway May 4, 2004. The data is recorded in sub swath IS1, and it shows that for steep incidence angles, data collected in VH-polarization provides good contrast between vessels and the ocean.

The body of accumulated literature on vessel detection and related topics is vast. In order to provide some structure to the review, we have organised it according to some key questions and issues that have been presented in the literature body:

1. Generic papers – discussing overall approaches to fisheries and vessel traffic monitoring, marine applications of SAR data in general and various other papers not easily categorised.
2. Signatures and characteristics – including measurement trials, campaigns, as well as modelling of wakes and of ship radar signatures. Here we also included at least one paper on statistical properties of ocean images.
3. Target and wake detection – descriptions of approaches for detecting ships and wake-like features in SAR images

4. Wake detection – primarily descriptions of approaches to detecting wake-like features in SAR images
5. Target detection – primarily descriptions of different algorithms for target detection
6. Classification – primarily reports on exploitation of target signatures for determination of classes of various ships
7. HF radar – discussing High Frequency radar used for ship detection.

Some papers may of course be regarded as belonging to more than one of the above categories, in which case the categorisation may seem somewhat arbitrary. The heading under which each paper appears is therefore purely based on subjective choice. As some papers address both ship and wake detection, we have also elected to use a separate category for ship and wake detection (Section 4).

2 GENERIC

2.1 Overview

The following table gives an overview of generic publications sorted after publication year. The generic publications include papers with overall approaches to fisheries and vessel traffic monitoring, marine applications of SAR data in general and various other papers not easily categorised. Summaries of a selection of some of the most important and available papers are given following the table.

YEAR	TITLE	AUTHOR	PUBLISHED
2004	Absolute Calibration of ASAR Level 1 Products Generated by PF-ASAR	Rosich, B and P Meadows	ESA Document, Frascati, Italy.
2004	Study of the Polarimetric Mechanisms on Simulated Vessels with SAR and ISAR Imaging	Margarit, G, X Fabregas and JJ Mallorqui	5th Conference on Synthetic Aperture Radar, EUSAR 2004, Ulm, Germany.
2004	Study of the Vessel Speed and Sea Swell Effects on Simulated Polarimetric High Resolution SAR Images	Margarit, G, JJ Mallorqui and JM Rius	5th Conference on Synthetic Aperture Radar, EUSAR 2004, Ulm, Germany.
2004	Ship Detection in SAR Imagery based on the Wavelet Transform	Tello, M, C Lopez-Martinez and JJ Mallorqui	5th Conference on Synthetic Aperture Radar, EUSAR 2004, Ulm, Germany.
2004	Validation of Predictions Regarding Ship Detection with ENVISAT ASAR in the Alternating Polarization Mode	Olsen, RB, K Eldhuset and T Wahl	5th Conference on Synthetic Aperture Radar, EUSAR 2004, Ulm, Germany.
2003	X-band Wideband Experimental Airborne Radar for SAR, GMTI and Maritime Surveillance	Damini, A, M McDonald and GE Haslam	IEE Proc Radar, Sonar and Navig, Vol. 150, No. 4, pp. 305-312.
2003	Remote Sensing of the Coastal Zone: an Overview and Priorities for Future Research	Malthus, TJ and PJ Mumby	Int J Rem Sens, Vol. 24, No. 13, pp. 2805-2815.
2003	Rapid Environmental Assessment at High Latitudes	Olsen, RB, JK Jensen and Morten Torsås	IEEE Int Geosc and Rem Sensing Symp (IGARSS'03), Toulouse, France.
2003	The Estimation of Ship Velocity from SAR Imagery	Tunaley, JKE	IEEE Int Geosc and Rem Sensing Symp (IGARSS'03), Toulouse, France.
2003	Elimination of Arcross-Track Phase Components in Airborne	Schulz, K, U Soergel, U	IEEE Int Geosc and Rem Sensing Symp

	Along-Track Interferometry Data to Improve Object Velocity Measurements	Thoennessen and U Stilla	(IGARSS'03), Toulouse, France.
2002	Moving Target Detection and Imaging Using an X Band Along-Track Monopulse SAR	Soumekh, M	IEEE Trans on Aerosp and Elect Syst, Vol. 38, No. 1, pp. 315-333.
2002	A Review of Speckle Filtering in the Context of Estimation Theory	Touzi, R	IEEE Trans on Geosc and Rem Sens, Vol. 40, No. 11, pp. 2392-2404.
2001	Modification of the OMW to Include Polarimetric Ship Detection	Plache, B and MD Henschel	Satlantic Document No. SAT-DN-0075, Satlantic, Halifax, NS.
2001	Mobile Communications Technologies for Ship Detection and Response	Jordan, JE	Can J Rem Sens, Vol. 27. No. 4, pp. 345-353, Canada.
2001	The Radar Imaging Instrumentand Its Applications: ASAR	Zink, M, C Buck, JL Suchail, R Torres, A Bellini, J Closa, YL Desnos and B Rosich	ESA Bulletin, No. 106, pp. 46-55.
2001	Review of Ship Detection from Airborne Platforms	Fingas, MF and CE Brown	Can J Rem Sens, Vol. 27. No. 4, pp. 379-385, Canada.
2001	Detection of Targets in Non-Gaussian Sea Clutter	Trunk, GV and SF George	IEEE Trans on Aerosp and Elect Syst, Vol. 6, No. 5, pp. 620-628.
2001	Covert Operations Detection for Maritime Applications	Patton, R, M Webb and R Gaj	Can J Rem Sens, Vol. 27. No. 4, pp. 306-319, Canada.
2001	Integrating Spaceborne SAR Imagery into Operational Systems for Fisheries Monitoring	Kourti, N, I Shepherd, G Scwartz and P Pavlakis	Can J Rem Sens, Vol. 27, No. 4, pp. 291-305, Canada.
2000	Calibrated Polarimetric SAR Data for Ship Detection	Touzi, R	IEEE Trans on Geosc and Rem Sens (IGARSS'00), Honululu, Hawaii, USA.
2000	International Fisheries Enforcement Management Using Wide Swath SAR	Montgomery, DR	Johns Hopkins APL Tech Digest, Vol. 21, No. 1, pp. 41-48.
2000	Applications of SAR Observations to Fisheries in the Bering Sea	Clemente-Colón, P, WG Pichel, K Friedman and X Li	Ship Detection in Coastal Waters Workshop, poster presentation, Nova Scotia, Canada, May 31-June 1, 2000.
2000	Canadian Progress Toward Marine and Coastal Applications of Synthetic Aperture Radar	Vachon, PW, P Adlakha, H Edel, M Henschel, B Ramsay, D Flett, M Rey, G Staples and S Thomas	Johns Hopkins APL Tech Digest, Vol. 21, No. 1, pp. 33-40.
2000	Ship Detection With Satellite-Based Sensors: Summary of Workshop Presentations	Vachon, PW and RB Olsen	Backscatter, Vol 11, No 4, pp 23-26.
2000	Validation of Ship Detection by the RADARSAT Synthetic	Vachon, PB, SJ Thomas, J	Can J Rem Sens, Vol. 26, pp. 200-212, Canada.

	Aperture Radar and the Ocean Monitoring Workstation	Cranton, HR Edel and MD Henschel	
2000	Paramilitary Technologies in Use by a Civilian Company for Canadian Government Ship Detection and Identification Applications	Scott, DF	Proc of a Workshop on Ship Detection in Coastal Waters.
2000	Spaceborne and Airborne SAR for Target Detection and Flood Monitoring	Guo, HD	Photogrammetric Eng and Rem Sens, Vol. 66, No. 5, pp. 611-617.
2000	Generation of "Tactical" Assessments Based on Commercially Available Satellite Data	Teufert, J	WEUSC Res Div, Western EU, Satellite Centre Satellitaire.
2000	Fishing Boat Detection by Using SAR Imagery	Kourti, N, I Shepherd and J Verborgh	AMRS Workshop on Ship Detection (proc), June 2000.
2000	NOAA CoastWatch SAR Applications and Demonstration	Pichel WG and P Clemente-Colón	Johns Hopkins APL Tech Digest, Vol. 21, No. 1, pp. 49-57.
2000	Coastal Observing Systems: The Role of Synthetic Aperture Radar	Johannessen, JA	Johns Hopkins APL Tech Digest, Vol. 21, No., 1, pp. 41-48. Johns Hopkins APL Technical Digest, Vol. 21, No. 1, pp. 41-48.
2000	The Role of Wide Swath SAR in High-Latitude Coastal Management	Olsen, RB and T Wahl	Johns Hopkins APL Tech Digest, Vol. 21, No. 1.
2000	Spaceborne Bistatic Synthetic Aperture Radar for Remote Sensing Applications	Moccia, A, N Chiacchio and A Capone	Int J Rem Sens, Vol. 21, No. 18, pp. 3395-3414.
1999	Radar Observations of Ship-Induced Instabilities in the Ocean-Atmosphere System	Smirnov, AV	Oceanoloica Acta, Vol. 22, No. 1, pp. 45-50.
1998	Validation of Ship Detection by the RADARSAT SAR/Ocean Monitoring Workstation	Thomas, SJ, PW Vachon and J Cranton	20th Canadian Symp on Rem Sens, pp. 165-168, Calgary, Canada.
1998	Demonstration of the RADARSAT SAR/Ocean Monitoring Workstation	Thomas, SJ, PW Vachon, C Bjerkelund, J Cranton, RB Olsen	Proc of GIS'98/RT'98, Toronto, Canada, April 6-9 1998.
1998	The Use of Satellite-Based SAR in Support of Fisheries Enforcement Applications	Montgomery, DR, W Pichel and P Clemente-Colón	Proc of IGARSS'98, Seattle, Washington, 6-10 July, 1998.
1998	Ocean Radar Observations of Ship-Induced Instabilities in the Atmospheric Boundary Layer	Smirnov, AV	J of Atm and Oceanic Tech, Vol. 15, No. 3, pp. 798-803.
1998	Vessel Detection with Wide Area Remote Sensing	Henschel, MD, PA Hoyt, JH Stockhausen, PW Vachon, H Edel, MT Rey and JWM Campbell	Sea Technology, Vol. 39, No. 9, pp. 63-68.

1998	Satellittovervåking	Wahl, T	Norwegian Defence Research Establishment collection of articles, Kjeller, Norway.
1998	RADARSAT: Which Mode Should I Use?	Vachon, PW and RB Olsen	Backscatter, Vol. 9, pp.14-20.
1998	Detecting Surface Vessels by RADARSAT	Vachon, PW, JWM Campbell, C Bjerklund, FW Dobson and MT Rey	Chapter 2.3.7 in Remote Sensing of the Pacific Ocean by Satellites, Earth Ocean and Space, pp. 145-164, PTY Ltd., Glebe, Australia.
1998	Operational Use of RADARSAT SAR in the Coastal Zone: The Canadian Experience	Manore, MJ, PW Vachon, C Bjerklund, HR Edel and B Ramsay	27th Int Symp Rem Sens on the Environment, pp. 115-118, Tromsø, Norway.
1998	Marine Surveillance Using RADARSAT SAR: CCRS Ocean Activities	Cranton J, RA De Abreu, C Bjerkelund, S Thomas and PW Vachon	20th Canadian Symp on Rem Sens, Calgary, Canada.
1998	The Use of Synthetic Aperture Radar as a Potential Indicator of Fishing Activity in the Bering Sea	Clemente-Colón, P, DR Montgomery, WG Pichel, and K Friedman	Proc of the 4th Pacific Ocean Rem Sens Conf (PORSEC'98), pp. 568-572, Qingdao, China.
1998	Integrated Use of RADAR Satellites for Fisheries Enforcement Operations	Wahl, T	Proc of the 27th Int Symp Rem Sens Env, pp. 123-126, Tromsø, Norway, June.
1998	Monitoring the Coastal Zone with the RADARSAT Satellite	Vachon, PW, SJ Thomas, JA Cranton, CA Bjerkelund, FW Dobson and RB Olsen	Oceanology Int 98, 10 p, UK.
1998	Detecting and Mapping Offshore Navigation Hazards Using Synthetic Aperture Radar Data	Lewis, AJ	IEEE.
1997	Recent Advances in Counterdrug OTH Radar Ship Surveillance	Barnum, JR, JA Olkin and JW Ciboci	Proc DoD Counterdrug Workshop at FSSC, Naval Research Laboartory, pp. 11-21.
1997	Using RADARSAT-1 for Fisheries Enforcement Operations	Wahl, T	IEEE Trans on Geosc and Rem Sens, IGARSS'97, "Remote Sensing - A Scientific Vision for Sustainable Development", Vol. 1, pp. 47-49.
1997	Wavelet Analysis of Satellite Images for Coastal Watch	Liu, AK, CY Peng and SYS Chang	IEEE J of Oceanic Eng, Vol. 22, No. 1, pp. 9-17.
1997	The Ocean Monitoring Workstation: Experience Gained with RADARSAT	Henschel, MD, RB Olsen, P Hoyt and PW Vachon	Int Symp, Geomatics in the Era of RADARSAT (GER'97), p. 12, Ottawa, Canada.
1997	Remote Vessel Detection on the Grand Banks Using Radarsat Imagery: Early Results	Larivière, R, H Edel, C Bjerklund, P Vachon, LCdr J Day and M Rey	Fisheries and Oceans Science Directorate, Memorandum, Note de service.
1997	Moving Target Detection in Foliage Using Along Track Monopulse Synthetic Aperture Radar Imaging	Soumekh, M	IEEE Trans on Image Proc, Vol. 6, No. 8, pp. 1148-1163, Aug 1997.

1997	Performance of the CDPF SEA LUT for ScanSAR Ship Detection	Vachon, PW, JWM Campbell, RK Hawkins, J Cranton, R Keeley and H Edel	CCRS Internal Report, Canada.
1997	CDPF/OFW Products from MARCOT	Vachon, PW, JWM Campbell, S Thomas and J Cranton	CCRS Internal Report, Canada.
1997	Operational Evaluation of Radarsat Potential in Fishing Vessel Surveillance: Potential & Test Results	Larivière, R, H Edel, C Bjerklund, P Vachon, R Olsen, S Thomas and D Adair	Fisheries and Oceans Science Directorate, Memorandum, Note de service.
1996	Validation of Ship Detection with the RADARSAT SAR; RADARSAT for Ice and Oceans - Early Experience and Data Access	Vachon PW and JW Campbell	6th Workshop of the Canadian Ice Working Group, Ottawa, Ontario, Canada, November 19-21, 1996.
1996	NATO Naval Exercises As Observed From Civilian Radar Satellites	Wahl, T and Å Skøelv	AGARD MSP 5th Symp on "Space Systems as Contributors to the NATO Defence Mission" (published in CP-580), Cannes, France.
1996	Maritime Use of Satelliteborne SAR	Skøelv, Å, T Wahl, T Jørgensen, ST Dokken	WEAG Euclid CEPA 9, RTP 9.1, WP2300, Final Report (RTP9.1/96/NDRE/2300/FR), FFI/Rapport-96/03203.
1996	Simulated Polarimetric Signatures of Primitive Geometrical Shapes	Cameron, WL, N Youssef and LK Leung	IEEE Trans on Geosc and Rem Sens, Vol. 34, No. 3, pp. 793–803.
1996	RADARSAT SAR Mode Selection for Maritime Applications	Vachon, PW and RB Olsen	Backscatter, Vol. 6, No. 3, pp. 3-4.
1996	Validation of Ship Detection by the RADARSAT SAR	Vachon, PW, JWM Campbell and C Bjerklund	Proc of the Pacific Ocean Rem Sens Conf (PORSEC'96)
1995	ERS Detection of Soft and Hard Targets at Sea: What Can Be Operationalized?	Skøelv, Å and T Wahl	Proc of the Sec ERS Appl Workshop, pp. 193-196, London, 6-8 Dec 1995.
1995	Reduction of Surface Clutter by a Polaimetric FM-CW Radar in Underground Target Detection	Moriyama, T, Y Yamaguchi, H Yamada and M Sengoku	IEEE Trans on Comm, Vol E78B, No. 4, pp. 625-629.
1995	Ship Detection by the RADARSAT SAR (A Working Paper)	Vachon, PW	Tech Report, Canada Centre for Remote Sensing, Ottawa, Ontario, Canada.
1995	Target Detection: Remote Sensing Techniques for Defence Applications	Chaudhuri, BB and SK Parui	Defence Science J, Vol. 45, No. 4, pp. 285-291.
1995	Operational Use of RADARSAT SAR for Marine Monitoring and Surveillance	Olsen, RB, P Bugden, Y Andrade, P Hoyt, M Lewis, H Edel and C Bjerkelund	IEEE Trans on Geosc and Rem Sens (IGARSS'95), pp. 224-226, Firenze, Italy.
1995	Up-coming Radar Satellites and Their Potential for Some	Skøelv, Å, ST Dokken and T Wahl	Progress in Env Rem Sens Res and Appl,

	Maritime Applications		presentation, Switzerland.
1995	Progress in Environmental Remote Sensing and Applications	Parlow, E	Proc of the 15th EARSeL Symphosium, Basel, Switzerland, Sep 4-6, 1995.
1995	Ship Detection by RADARSAT SAR	Vachon, P	Tech Report, Canada Centre for Remote Sensing, Ottawa, Ontario, Canada.
1995	Imaging of Oceanic Features by ERS-1 Synthetic-Aperture Radar	Nilsson, CS and PC Tidesley	J of Geoph Res - Oceans, Vol. 100, No. C1, pp. 953-967.
1994	Ship Traffic Monitoring and Oil Spill Detection Using the ERS-1 SAR	Wahl, T, K Eldhuset and Å Skøelv	Int Symp "Operationalization of Remote Sensing", ITC Enschede, The Netherlands.
1994	Ship Traffic Monitoring and Oil Spill Detection Using the ERS-1 SAR	Skøelv, Å, T Andersen, K Eldhuset and Terje Wahl	Rem Sens from Res to Operational Appl in the New Europe, pp. 19-26, Springer Hungary.
1994	Ship Traffic Monitoring and Oil Spill Detection Using the ERS-1 SAR	Wahl, T, T Andersen, K Eldhuset and Å Skøelv	From Optics to Radar, SPOT and ERS Applications. CNES, Cepadues-Editions, pp. 211-220, Paris.
1993	Ocean Applications of RADARSAT	Gower, JFR, PW Vachon and H Edel	Can J Rem Sens, Vol. 19, No. 4, pp. 372-383, Canada.
1992	Polarimetric Discriminators for SAR Images	Touzi, R, S Goze, T Le Toan, A Lopes and E Mougin	IEEE Trans on Geosc and Rem Sens, Vol. 30, No. 5, pp. 973–980.
1992	The Use of Commercial Radar Satellites in Military Sea Surveillance	Skjelland, E	FFI/Rapport-92/5017 (confidential in Norway), Norwegian Defence Research Establishment, Kjeller, Norway.
1992	Radar Satellites and Naval Operations	Wahl, T	Proc of NATO DRG 25th Anniversary Symp, Vol. 2, London. UK.
1991	A Remote Sensing Technique for the Estimation of a Moving Ship's Velocity and Length from Its Wave Spectra	Wu, Z and GA Meadows	IEEE Proc of Ocean Tech and Opp in the Pacific for the 90's. OCEANS'91, Vol. 2, pp. 810-817.
1991	The Inverse Ship Wave Problem	Newman, JN	The Sixth Int Workshop on Water Waves and Floating Bodies, pp.193-197, MIT, Cambridge, MA, USA.
1991	On the Estimation of a Ship's Velocity and Hull Geometry Information from Its Wave Functions	Wu, Z	The University of Michigan, Program in Ship Hydrodynamics PhD Dissertation, Dep of Naval Arch and Marine Eng.
1991	The Norwegian Coordinated Program for ERS-1 Preparations	Strom, GD	Acta Astronautica, Vol. 24, pp. 115 - 119.
1990	Coastline Detection and Tracking in SAR Images	Lee, JS	IEEE Trans on Geosc and Rem Sens, Vol. 28, No. 4, pp. 662-668.

1987	Ships From Space	Munk, WH, RS Scully-Power and F Zachariasen	Proc of the Royal Society London, A, Vol. 412, pp. 231-254.
1986	A Radar Ocean Imaging Model for Small-To-Moderate Incidence Angles	Holliday, D, G St-Cyr and NE Woods	Int J Rem Sens, Vol. 7, No. 12, pp.1809-1834.
1983	Surveillance of Norway's Economic Zones Using Satellites and Aircraft	Aksnes, K	FFI/Rapport-83/9006, Norwegian Defence Research Establishment, Kjeller, Norway.
1981	Hough Transform from the Radon Transform	Deans, SR	IEEE Trans on Pattern Analysis and Machine Intelligence, Vol. 3, No. 2, pp. 185-188.
1975	Introduction to Non-Parametric Detection with Applications	Gibson, JD and JL Melsa	IEEE press, NJ. Piscataway.
1970	Recent Research of Ship wakes	Newman, JN	8th Symphosium on Naval Hydrodynamics: Hydrodynamics in the Ocean Environment, pp. 519-545, Office of Naval Research, Dep of the Navy, Arlington, Virginia.
1960	Probability of Detection for Fluctuating Targets	Swerling, P	IRE Trans, Vol. IT-6, pp. 269-300.
	RADARSAT	Raney, RK, AP Luscombe, EJ Langham and S Ahmed	Proc of the IEEE, Vol. 79, No. 6, pp. 839-849.
	Expected Performance of the ENVISAT ASAR for Near Real-Time Maritime Applications	Olsen, RB, T Wahl and G Engen	

2.2 Absolute Calibration of ASAR Level 1 Products Generated by PF-ASAR (50)

The paper describes calibration of the different ENVISAT ASAR products in connection with radar backscattering. RCS (Radar Cross Section) depends on the object's size, shape, orientation, the surface of reflection, as well as wavelength and polarization of the incoming signal. The relationship between the value of the pixels (DN), the radar strength (β^0), and the RCS (σ^0), can be written as:

$$DN^2 = K \cdot \beta^0 = \frac{K \cdot \sigma^0}{\sin(\theta)} = K(\theta) \cdot \sigma^0 \tag{2.1}$$

The constant K is the absolute calibration constant, which is obtained from measurements over precision transponders. It depends on the processor and the product type, and can change from one signal to another for the same product type. The RCS for detected products can be obtained by using this relationship:

$$\sigma_{i,j}{}^0 = \frac{DN_{i,j}{}^2}{K} \sin(\theta_{i,j}) \text{, for i = 1…L og j = 1…M} \tag{2.2}$$

L and M are the number of line and column, respectively, in the image. The average RCS for a small area can be obtained by using an average for N pixels within the area:

$$\sigma^0 = \frac{1}{N}\left(\sum_{i=1}^{i=L}\sum_{j=1}^{j=M}\theta^0{}_{i,j}\right) \tag{2.3}$$

If the area is very small, it is possible to use an average incidence angle, θ_d:

$$\sigma^0 = \frac{1}{N}\sum_{i=1}^{i=L}\sum_{j=1}^{j=M}\frac{DN_{i,j}{}^2}{K}\sin(\theta_d) \tag{2.4}$$

The logarithmic RCS (dB) is given by:

$$\sigma^0[dB] = 10 \cdot \log_{10}(\sigma^0) \tag{2.5}$$

All detected ASAR products are delivered with radar strength β^0, i.e. antenna pattern and reflection loss in range direction is corrected, but no correction is done for the incidence angle.

2.3 Canadian Progress Toward Marine and Coastal Applications of Synthetic Aperture Radar (84)

Canada has developed SAR applications that require imagery on operational schedule. RADARSAT-1 is used for the moment, and RADARSAT-2 is being developed for future use. Sea ice surveillance is a near-real-time application, and other marine and coastal roles are emerging, for example ship detection and coastal wind field retrieval. CIS (Canadian Ice Service) uses RADARSAT-1 data regularly as its primary data source. The OMW (Ocean Monitoring Workstation) has, among others, developed automatic algorithms for ship detection, and validated them by using a broad range of image modes and ocean sea states. Using *in situ* information and empirical models, the capability of the ERS (European Remote Sensing) and RADARSAT-1 SARs have been validated to provide wind-vector data. Algorithms for extracting wind-vector information have been developed and are now being tested. RADARSAT-2 and other new satellites will provide increased frequency of radar coverage, selectable modes of operation, and more accurate information retrieval.

27 RADARSAT-1 SAR images, acquired in 1996 and 1997, have been used together with supporting ship validation information (name, type, size, and location) to test the algorithms. The validation information was obtained from Canadian Coast Guard fisheries surveillance, DND (Department of National Defence) Aurora surveillance flight reports, and other dedicated field programs. 174 ships ranging from 20 to 294 m were validated using different RADARSAT-1 beam modes and wind conditions (0.4 to 13.2 m/s). RADARSAT-1 modes with large incidence angles are favourable for ship detection, i.e. fine beams 1 to 5, standard beams 4 to 5, and wide beam 3. Standard beams 1 to 3, and wide beams 1 and 2 are not favourable for ship detection due to the small incidence angles. The detection rate was 77% for less favourable modes for ship detection, 97% for recommended modes for ship detection, and 81% for two ScanSAR narrow far mode images. An overall detection rate of 84% was obtained.

2.4 CDPF/OFW Products from MARCOT (83)

The report describes the Ocean Features Workstation (OFW) and the Canadian Data Processing Facility (CDPF) used in connection with MARCOT, which is a Department of National Defence (DND) training exercise. It occurs every year off Canada’s east coast. RADARSAT-1 SAR images from the MacDonald Dettwiler’s Fast Tracs transportable ground station were analyzed manually for ship detection, within one hour of data acquisition. The RADARSAT-1 data was also processed through the CDPF at Gatineau Satellite Station (GSS), as well as automatically on the OFW, also installed at GSS. The early CDPF/OFW reports showed that there were some problems with large, dense groups of targets in the image far range and near coastal regions. The problems can be categorized into two groups: 1) image saturation by an inappropriate output LUT and 2) image saturation caused by Doppler estimation problems. The report describes the occurrence of these problems as well as mitigation of the problems. A combination of adjusting the OFW ship detection parameters and using an alternate output Look-Up Table (LUT) to reprocess the data helped to solve the problems. The data limitations could not be overcome in some cases. The following recommendations are given in the paper (citation, pp. 3-4):

1. It would be useful to include a significantly reduced resolution image with the OFW product to allow contextual evaluation in the event that the ship product appears to be unusual
2. It is acknowledged that changes in CDPF Doppler estimation algorithms are in progress. However, a limiting property of the data was the inaccurately estimated Doppler centroid, which occasionally resulted in Doppler ambiguities in the coastal zone. As such improved Doppler estimation is required. Furthermore, a means to adjust the Doppler centroid polynomial for ScanSAR reprocessing is needed.
3. The output LUT need to be improved and/or the dynamic range of CDPF products, especially ScanSAR, needs to be increased.
4. A means to delay electronic delivery of CDPF products to OFW until after data QC (Quality Control) is required.

2.5 Comparison of Parameter Estimators for K-Distribution

Blacknell compares three approaches for parameter estimators with the ML (Maximum Likelihood) approach. The first method uses the Mean of Variance of the data (MV method) and equates them with their equivalent theoretical expressions. The second method uses the mean and variance of the log of the data, while the third method uses the Mean of Mean of the natural Logarithm (MML method). Results have shown that the MV method gives better performance at lower wind speeds, while the MML method is slightly more robust at high wind speeds. The expressions for the sample mean and variance of data are given by:

$$E[x] = \mu \tag{2.6}$$

$$Var(x) = \left[\left(1+\frac{1}{\nu}\right)\left(1+\frac{1}{L}\right)-1\right]\mu^2 \tag{2.7}$$

E is the expectation, while *Var* is the variance operators. Moment estimates can be calculated from the histograms of the sampled data from an ocean area. These estimates can then be used to estimate, through the sample mean and variance, the density function’s form and the cumulative probability for the ocean area. Using this information, the CFAR threshold for the detection of ships in the sample area can be set. The second method uses the mean and variance of the natural log of the data:

$$E[\ln(x)] = \ln(\mu) + [\psi(\nu) - \ln(\nu)] + [\psi(L) - \ln(L)] \tag{2.8}$$

$$Var[\ln(x)] = \psi^{(1)}(\nu) + \psi^{(1)}(L) \tag{2.9}$$

$\psi(x)$ is the digamma function and the superscript, n, is the nth derivative. The third method to obtain the parameter estimates is to use the sample mean of the data and the sample mean of the log of the data. An ML analysis of the L-look, K-distribution, can be used to derive the choice of moments.

2.6 Detecting Surface Vessels by RADARSAT (81)

The paper presents a statistical model, which gives predictions of the ship detection performance of RADARSAT-1 SAR. Ocean clutter, image PDF, and ship cross section elements are included in the model. Figure 2.1 summarizes the model results. It is shown that SCNfar represents a good compromise between ship detectability and swath coverage. Data has been collected off the coast of Halifax, Nova Scotia in March/April 1996 in a ship detection field program. *In situ* wind and wave data as well as image signatures of known ships were also available. Amazon rain forest images were used to calibrate the data to derive antenna patterns and a calibration constant. The calibration is accurate to ± 0.5 dB. The relationship between the output image and the calibrated cross section is given by:

$$\sigma^0 = \left(\langle I \rangle \frac{R^3}{G^2(\theta)} \right) \frac{\sin\theta}{K} \tag{2.10}$$

$\langle I \rangle$ is the mean image intensity for the region of interest, $G^2(\theta)$ is the two-way elevation antenna pattern gain, R is the range, θ is the local incidence angle, and K is the calibration constant.

There is a risk of underestimating the Radar Cross Section in near coastal regions due to small signal suppression, and thus there is a potential calibration error. It is shown that the hybrid C-band HH-polarized cross section model is excellent under the test conditions, and that the K-distribution is appropriate for RADARSAT-1 ocean scenes. The simple cross section model is based upon the ship length alone. It is shown that it is within the correct order of magnitude, but it tends to underestimate the ship cross section, especially with increasing incidence angle. The model underestimates the ship detectability for RADARSAT-1 in most cases. The incidence angle and ship orientation dependence are not addressed in detail.

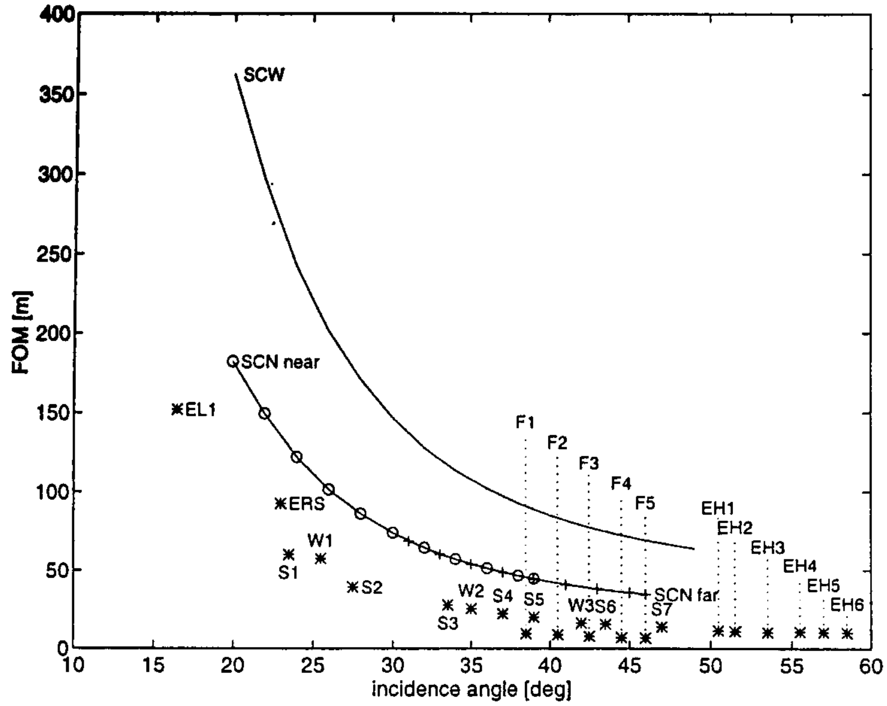

Figure 2.1: *The ship detection Figure of Merit (FOM) as a function of the incidence angle for the different beams and modes on RADARSAT-1.*

2.7 ERS Detection of Soft and Hard Targets at Sea: What Can Be Operationalized? (54)

The paper describes the possibilities of using ERS SAR images for near real time ocean surveillance applications such as detection of ships, ship wakes, icebergs, and oil slicks. It is shown that most ships can be visualized as bright spots under calm sea conditions (0-2 m/s wind speed). Ships longer than 50 m are visible at wind speeds above 5 m/s. Ships smaller than 100 m may be lost when the wind speed is above 10 m/s. Steeper incidence angles give stronger backscatter from the sea. Since ERS uses a steep incidence angle, it is not optimal for detection of smaller fishing vessels and icebergs. Oil slick detection is far more effective because of the large dynamic variation that occurs at low wind speeds as well as the low noise-equivalent σ_0. Oil slick detection has been developed into a pre-operational level.

2.8 Expected Performance of the ENVISAT ASAR for Near Real-Time Maritime Applications (44)

The paper presents the expected performance of the ENVISAT ASAR instrument, which provides a diversity of imaging geometry and polarization. Modes are available for ship detection at all incidence angles. The swath width is limited to less than 100 km. The performance is examined in terms of geometry, coverage, spatial resolution and radiometric characteristics. Based on these results, the applicability of the different beams and modes for near real-time monitoring of the marine environment are examined. Recommendations for beams and modes for the most important applications, seen from a Norwegian perspective, are given. Cross-polarized channels are recommended to use for ship detection at steep incidence angles. Either AP mode or Image mode are recommended for the outer swaths. The cross-polarized channel on ENVISAT is expected to provide good images of ships, while the co-polarized channel is best for detection of ship wakes, natural slicks, oil slicks, oceanographic and meteorological features. Figure 2.2 shows that the VH-polarized backscatter is more than 20 dB below VV. It is not likely that VH-polarized data will give useful returns from the ocean surface using ENVISAT.

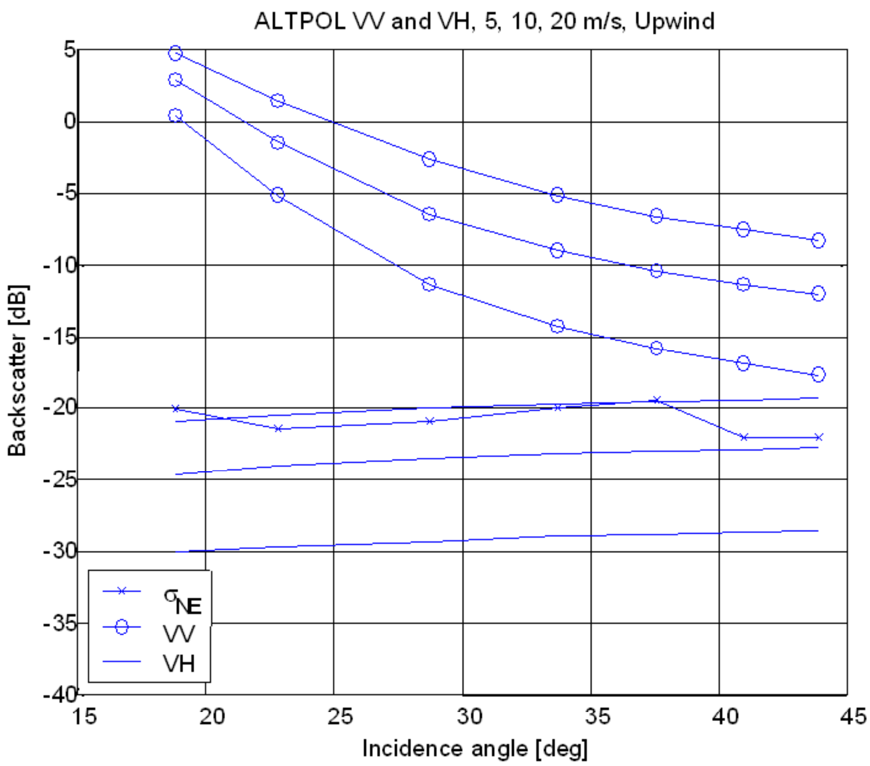

Figure 2.2 The ocean backscatter depends on the incidence angle, polarization, wind speed and wind direction. The figure shows the relationship for upwind at 5, 10 and 20 m/s for VV- and VH-polarized data for the Image mode.

By using the AP mode with VV and HH, it is expected to obtain further insight into Modulation Transfer Functions (MTFs) for wave spectral estimates.

Wide Swath mode, VV-polarized data is recommended for oil slick detection, because the signal levels are expected to be above the noise floor under most conditions (see Figure 2.3). The resolution is also satisfactory.

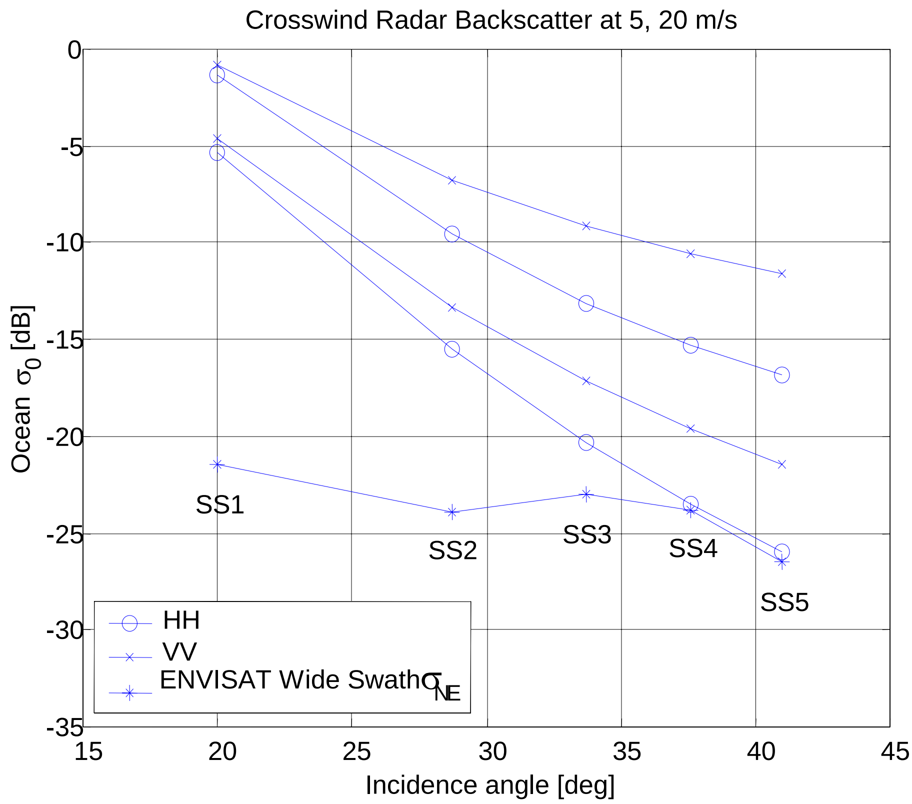

Figure 2.3 *The ocean backscatter depends on the incidence angle, polarization, wind speed and wind direction. The figure shows the relationship for crosswind at 5 and 20 m/s. The ocean backscatter is compared to the ENVISAT ASAR Wide Swath mode noise floor.*

Vachon's modified version of Skolnik's relationship between the RCS (Radar Cross Section - σ_{skip}) and ship length (l) is used to determine the ship detection performance:

$$l = \frac{\sigma_{skip}}{0.08R(\theta)} \tag{2.11}$$

R is the ratio between measured and expected value of the RCS, while θ is the incidence angle in degrees, $\theta \in [15°,45°]$:

$$R(\theta) = 0.78 + 0.11\theta \tag{2.12}$$

To be able to calculate the RCS for the smallest ship that is possible to detect, a threshold value (T) of the average backscattering or noise floor is used:

$$\sigma_{skip}^{\min} = \rho_r \rho_a 10^{(\sigma_{sjø}+T)/10} \tag{2.13}$$

ρ_r and ρ_a are the resolutions in range and azimuth direction, and σ_{sea} is the RCS from the sea surface. Table 2.1 shows the smallest detectable ship lengths for selected swaths.

	5 m/s	10 m/s	20 m/s
Upwind/Crosswind min. ship length [m] VV-polarization			
IS1	74 / 65	88 / 79	124 / 90
IS4	17 / 13	25 / 17	44 / 28
IS7	10 / 7	16 / 9	30 / 19
SS1	174 / 152	215 / 186	306 / 220
SS5	36 / 26	59 / 35	109 / 68
Upwind/Crosswind min. ship length [m] HH-polarization			
IS1	70 / 62	87 / 77	122 / 89
IS4	12 / 10	18 / 12	29 / 19
IS7	7 / 7	9 / 7	17 / 11
SS1	162 / 141	204 / 176	291 / 210
SS5	23 / 16	36 / 22	65 / 40

Table 2.1 The smallest detectable ship length estimates for selected swaths.

2.9 Fishing Boat Detection by Using SAR Imagery (19)

To counteract fish stock collapses, it is necessary to have sustainable fisheries, stable extraction rates and stock robustness. Uncontrolled exploitation of the sea and industrialization of fishing have often in past years led to fishing stock collapses. The paper presents a project, which uses spaceborne SAR for ship detection, that was initiated to modernize the control of the Common Fisheries Policy adopted by the European Union.

The test region was in international waters in the 3M division of the Northwest Atlantic Fisheries Organisation (NAFO) in the area around the Flemish cap. The objective of NAFO is “to contribute towards the optimum utilization, rational management and conservation of the fishery resources of the Convention Area”. There is considerable information available on the maritime traffic in the NAFO area 3M, which mainly consists of fishing vessels. Using ScanSAR imagery it is shown that fishing vessels longer than 35 m can be detected. Comparing the SAR data with Vessel Monitoring System (VMS) data showed that it is possible for the inspectors to identify these vessels. Thus, SAR data can be used to detect vessels that are not subject to the VMS or not using their VMS. Using SAR data can help the surveillance aircrafts and patrol vessels can better be coordinated.

2.10 Hough Transform from the Radon Transform (9)

The paper presents techniques for application of the Radon transform to lines and pixels through examples, as well as an appropriate generalization to arbitrary curves. J. Radon developed the Radon transform in 1917, and it is shown that a special case of this transform has the major properties of the Hough transform. This provides a natural formalism for further efforts to generalize the Hough transform. The Hough transform is useful to find line segments in digital pictures. The two-dimensional Radon transform for an arbitrary generalized function *F(x,y)* defined on the *xy* plane *D* is given by:

$$f(\theta, p) = R\{F\} = \iint_D F(x, y)\delta(p - x\cos\theta - y\sin\theta)dxdy \qquad (2.14)$$

If θ and/or p remain fixed, then one has a sample of the transform. To get the full transform, θ and p vary, so f is determined for arbitrary values of θ and p. The paper gives further references to mathematical literature for more literature on the Radon transform. In addition it gives references to review articles in the area of using Radon transform inversion in a digital setting. Simple examples of the use of the transform over a line segment and over a pixel are given. Generalizations to more complicated curves and regions are given.

2.11 Integrated Use of RADAR Satellites for Fisheries Enforcement Operations (88)

The paper presents results from tests and demonstrations of RADARSAT-1's capabilities for detection of fishing vessels. A chain for acquisition, processing and analysis of RADARSAT-1 images in Norwegian waters has been created and an operational radar satellite image analysis centre has been established. Regular reports were generated for use in fisheries enforcement operations in the Barents Sea and around Jan Mayen RADARSAT-1 observations are used in addition to aircraft, helicopters, and ships to optimise the use of national assets in sovereignty and fisheries enforcement operations. The chain has shown promising results for ship detection in Norwegian waters. RADARSAT-1 ScanSAR Narrow Far (block averaged to 50 m x 50 m pixel size) is most effective, but it has limitations during the winter storms. RADARSAT's Fine Modes and the Standard Beams S6-S7 can be used to estimate the number of fishing vessels in a limited ocean area.

2.12 Integrating Spaceborne SAR Imagery into Operational Systems for Fisheries Monitoring (20)

The paper shows that there is a good agreement of the vessels' positions obtained from spaceborne SAR imagery and VMS position reports. By correlating the two sources of information, information about vessels not using the VMS and ships that are not subject to the VMS can be obtained, and surveillance and control can be concentrated on these vessels. Detection results can be available to the inspectors two hours after the image recording, but it must be planned, because programming of the RADARSAT-1 beam requires some time. The West Freugh ground station covers southern European waters, while the Mediterranean remains uncovered. The coverage problem will be solved with the ENVISAT and RADARSAT-2 satellites.

Fishing vessels longer than 26 m have a 92% probability of being detected by ScanSAR imagery. ScanSAR and VMS information about position correlate well. 73% of the vessels in the Flemish Cap and 92% in the North Sea could be identified. In the Azores, where spun glass and wooden vessels predominate, it was difficult to detect the vessels subject to VMS. The mean distance between the VMS position and the detected position was about 0.3 nautical miles. SAR imagery can be used as a complementary tool to VMS or other surveillance aircraft on ships not using their VMS or not subject to it. SAR imagery gives a real view of the traffic in the area, while VMS only gives the positions. The main reasons for not being able to detect vessels are incidence angle, image errors, and weather effects. Detection in the near swath (low incidence angle) is difficult due to sea clutter. Narrow Far imagery only affects detection if it is combined with high wind speeds. Image errors are shown in bright areas or bright spots at edges of the different beam modes. Reasons for wrongly identifying image noise as a vessel are time difference between image acquisition, vessel position report, and low frequency of the VMS.

2.13 International Fisheries Enforcement Management Using Wide Swath SAR (32)

Wide Swath SAR can be used for surveillance of commercial fishing grounds, help detecting illegal fishing activities, and make the use of limited aircraft or patrol craft resources more efficient. Many nations with vast economic enterprise zones, for example small Pacific Island nations, do not have effective monitoring methods with available patrol resources. It is necessary with an efficient method to prevent fish stocks to decline and collapse. Wide Swath SAR can frequently monitor large ocean areas, and detected ships can be observed and monitored by patrols. RADARSAT-1's standard mode (100 km swath and 25 m resolution) is better than ERS-1 SAR for ship detection due to reduced backscattering from the ocean using HH-polarization in RADARSAT-1. Increasing the incidence angle increases ship detection probability due to reduced backscatter from the ocean. RADARSAT-1's fine beam modes (45 km swath and 10 m resolution) are best for ship detection performance due to the high resolution and large incidence angle. The large incidence angles are best to use for the ScanSAR mode (up to 500 km swath and 100 m resolution). But due to the large resolution cells, the ship detection performance is not as good as for the standard beam modes. An integrated SAR and VMS (Vessel Monitoring System) system is able to detect vessels greater than 20 m, and provides global, all weather, day-night capability. The system will quickly show vessels that are not using their VMS to report their position.

2.14 Maritime Use of Satelliteborne SAR (57)

The report describes the results from a work package on maritime use of spaceborne SAR, which was proposed and approved as a part of the Norwegian activity under WEAG (Western European Armaments Group) Euclid RTP 9.1. SAR imaging models have been reviewed in the paper and simulations of the interaction between satellites, ships, and aircrafts has been studied. Some predictions for the future have also been done.

ERS-1 and ERS-2 have mostly been used to perform the experiments. Wide Swath ScanSAR is efficient for ocean applications. Sufficient dynamic range is necessary for both hard target and soft target detection. Cross-polarized mode is good for hard target detection. The radar frequencies, X- and S-band, are acceptable for a maritime point of view. The S-band frequency will probably be the best for military use. Spatial resolution is a key parameter for ship classification and identification (favours X-band frequency). Cross-polarization vs. co-polarization is more important than the choice of radar frequency for ship detection.

Note: Access to this report is limited to participants in the RTP 9.1 project.

2.15 Mobile Communications Technologies for Ship Detection and Response (18)

The paper reviews useful available technologies for agencies that need to be able to respond to ships detected in coastal waters. The focus is mainly on affordable commercial civilian technologies available or that could be developed. Mobile communications technologies provide communication, command and control (C^3), and are expected to play an important role as an enabling technology for ship detection and response scenarios. A low data-rate satellite telephone on an NCR Convair aircraft us used to illustrate the practical use of currently available technology. It can be used for voice communications for airborne scientific experiments as well as for access to the Internet, transfer of meteorological information, and radar images. Current developments in mobile communications technology, which may be used for these purposes, are also summarized. Low-bandwidth commercial satellite telephone technology, such as Mobile Satellite (MSAT), has given indications to be useful in ship detection and response, because it is cost-effective and an effective tool for communications in an airborne environment.

The group of authors who have written the paper have developed an airborne system, which is capable of receiving imagery broadcast by the polar-orbiting weather satellite in real time in the VHF band. Traditionally, it has been used to transmit low-resolution weather satellite imagery, but it can also be used to transmit radar and radiometer imagery using the analogue transmission format. Higher resolution capabilities have been provided with new digital transmission formats, while higher data/image transmission capabilities with higher frequency bands have been used for real-time broadcast.

2.16 Monitoring the Coastal Zone with the RADARSAT Satellite (85)

The report presents coastal zone applications of RADARSAT-1 SAR data, as well as guidelines for beam mode selection. The applications ship detection, oil spill detection, and wind vector retrieval are considered in detail using the Ocean Monitoring Workstation (OMW). The OMW system can be used to extract ocean information from RADARSAT-1 images. 187 collocated ships have been identified, which shows good agreement between RADARSAT-1/OMW detected targets and the VTS/GPS/DND (Vessel traffic Services/Global Positioning System/Department of National Defence) Aurora ship surveillance data. Larger ships are easier to detect. It is shown that larger incidence angles and lighter winds decrease the background clutter, which increases the detecting probability. This is consistent with theoretical predictions. OMW ship products can be used to cue other operational surveillance activities.

2.17 NATO Naval Exercises As Observed From Civilian Radar satellites (90)

Spaceborne SAR data has been used in NATO naval exercises in Norwegian waters for near real-time information (less than 2 hours). ESA's ERS-1 satellite has been used under five major NATO naval exercises: "North Star 1991", "TEAMWORK 1992", "Battle Griffin 1993", "Strong Resolve 1995", and "Battle Griffin 1996". Major participating naval vessels were detected at least once during the exercise. SAR images with low resolution (about 30 m for typical civilian satellites) have in many cases been satisfactory for detection of ships, while full resolution images have given more information about the ships. Large transport ships give quite different signatures than dedicated military vessels. It is shown that it is possible to estimate the ship's length in many cases.

Ship wakes can also be seen in SAR images. This can provide information about the ship's direction of motion. Ocean features of possible relevance for sonar operations have also been observed. No oil spills were detected in the SAR images during the five NATO exercises.

ERS-1 has a steep incidence angle, and this is a limiting factor for detection of smaller ships. RADARSAT-1 and ENVISAT will be better to detect smaller ships due to more flexible instruments with modes that are better suited for ship detection. For ship detection, cross-polarization channels are believed to be optimal, while co-polarization gives most information about ship wakes and ocean features.

2.18 Ocean Applications of RADARSAT (12)

The paper discusses potential applications by using examples from past airborne and satellite SARs as well as Space Shuttle sun-glint photographs. It also gives references to important papers defining the various applications. RADARSAT-1 SAR gives a large volume of radar imagery and has wide and rapid coverage, and is therefore more "operational" than previous space mission. Using RADARSAT-1's broad ScanSAR mode, it is possible to image large ocean surface (mesoscale) features, monitor large areas for oil spills, monitor coastal areas, and map the surface wind patterns. But this mode is limited by the sensitivity, and to be able to study surface waves during storms and smaller-scale oil spills, higher resolution modes are needed.

It is shown that ships longer than about 30 m can be detected in Seasat SAR images with wind speeds less than 5 m/s (calm conditions). Airborne SARs are able to detect small coastal fishing vessels. Higher wind speeds make it harder to detect ships due to increased sea clutter. Ships travelling at full speeds are easier to detect due to visible wakes after the ships. There are three types of wake features visible in SAR images: 1) the normal Kelvin wide-V bow wake, 2) the narrow-V wake due to short, Bragg-resonant waves which are slower moving, and 3) the linear turbulent wake along the ship's track where surface waves are disrupted.

2.19 Operational Use of RADARSAT SAR in the Coastal Zone: The Canadian Experience (28)

RADARSAT-1 SAR is a flexible and operational system for monitoring dynamic coastal zones. The paper describes the Canadian activities in the areas sea ice monitoring (by the Canadian Ice Service), vessel detection, and oil slick detection. The status and development of automated algorithms for these applications are summarized. Focus has been on vessel detection algorithms, which have been validated over a broad range of image modes and sea states. The future with multiple satellites (RADARSAT-1, ENVISAT, and RADARSAT-2) operating simultaneously can solve the problem of conflicting use of different imaging parameters for the various applications.

29 RADARSAT-1 SAR images have been used in the experiment, which have supporting ship validation information such as ship name, type, size, and location. 187 validation collocations have been identified. The detection rate is 93% for beams that are most favourable for ship detection.

2.20 Radar Satellites and Naval Operations (86)

The paper describes the importance of spaceborne SAR. Spaceborne SAR may give information about ships and oceanographic features of importance for naval operations. The information is important in tomorrow's naval warfare, and military radar satellites will have a clear role. Civilian SAR satellites are also important, and capable of producing imagery of military interest. The optical SPOT satellite played an important role before and during the Gulf War, and it is to be shown the importance of radar satellites in future conflicts and crisis.

2.21 Remote Vessel Detection on the Grand Banks Using Radarsat Imagery: Early Results (21)

The paper presents early results for the ship detection capability using RADARSAT-1 SAR. The first acquisition was composed of three images off the Flemish cap. An image in the Standard beam mode (S7) gave optimal coverage and resolution of the targeted area. The study indicated that image processing using the K-distribution is expected to provide improved results in ship detection. The K-distribution improves the precision of the ship location (86 % of all targets were detected) and reduces the occurrence of false alarms with 72 %. It is possible to detect ships closer to the coastline by performing land masking. Enhancement of the OFW (Ocean Feature Workstation), improved synchrony with ancillary data, and standardized Swath Planner configuration files give the users a cost-effective ship detection product. It can be delivered within three hours after the pass.

2.22 Review of Ship Detection from Airborne Platforms (10)

The paper summarizes and describes spaceborne and airborne ship detection techniques. Detection done from airborne platforms has been the most common method for surveillance. The two most common sensors for ship detection used are search radar and Side-Looking Airborne Radar (SLAR). Usually search radars are used for detection, while visible, low-altitude passes are used for identification and verification. The detection is usually performed manually, while the identification and documentation are done with video and photographic cameras due to the low cost. Laser and strobe lights have been used in specialized systems for scene illumination, while infrared sensors have been used to detect ships. SLAR is often used for ship detection. The ship detection algorithms are not used due to the positional uncertainty in the imagery. SLAR on board aircraft uses radar to first manually detect the ship, and afterwards the vessel is identified visually. In addition determining compliance to legislation related to discharge or fishing is also done.

Synthetic Aperture Radar (SAR) can provide additional useful information about ship position, heading, and speed, as well as relative size and type of vessel under certain conditions. The reflection of the ship, which is usually strong because of corner reflection, and the ship’s wake are used to detect ships. SAR interpretation algorithms, that are also applicable for airborne systems, have been extensively developed for SAR systems on board satellites. Several automatic ship detection algorithms have been developed for satellite-acquired data.

The ship’s wake is usually 15 km behind the boat, and is a V-shaped feature with less sea clutter (sometimes called the turbulent wake). The backscatter from the ship and the ship’s wake strongly depends on the wind speed and sea state. It is easier to detect the Kelvin arms at lower wind speeds. The visibility is also higher with HH-polarization than with VV-polarization. The minimum size of a vessel that can be detected at different wind speeds has been estimated for typical airborne system. The numbers are based on similar estimations for satellite systems. Better TCR (Target to Clutter Ratio) can be obtained using HH-polarization, while VV-polarization gives more information about the sea conditions.

The paper also describes work that has been done by using a combination of sensors, for example visible, InfraRed (IR), and SAR. Image recognition analysis has also been done.

2.23 The Ocean Monitoring Workstation: Experience Gained with RADARSAT (15)

The Ocean Monitoring Workstation (OMW) has been developed to extract marine information from RADARSAT-1 SAR ocean images. The system uses state of the art algorithms to obtain wind and wave information, information about the vessels, and the location of ocean and atmospheric features. The information is formatted, interpreted, and transmitted to operational centers on land and at sea. Applications of the OMW that have been explored are ship detection, wind measurements, and estimates of wave conditions. The three main uses are vessel detection, oil spill monitoring, and environmental monitoring. The system overview is given in Figure 2.4. The Vessel Detection Module detects at least 90% of the vessel targets in a SAR image.

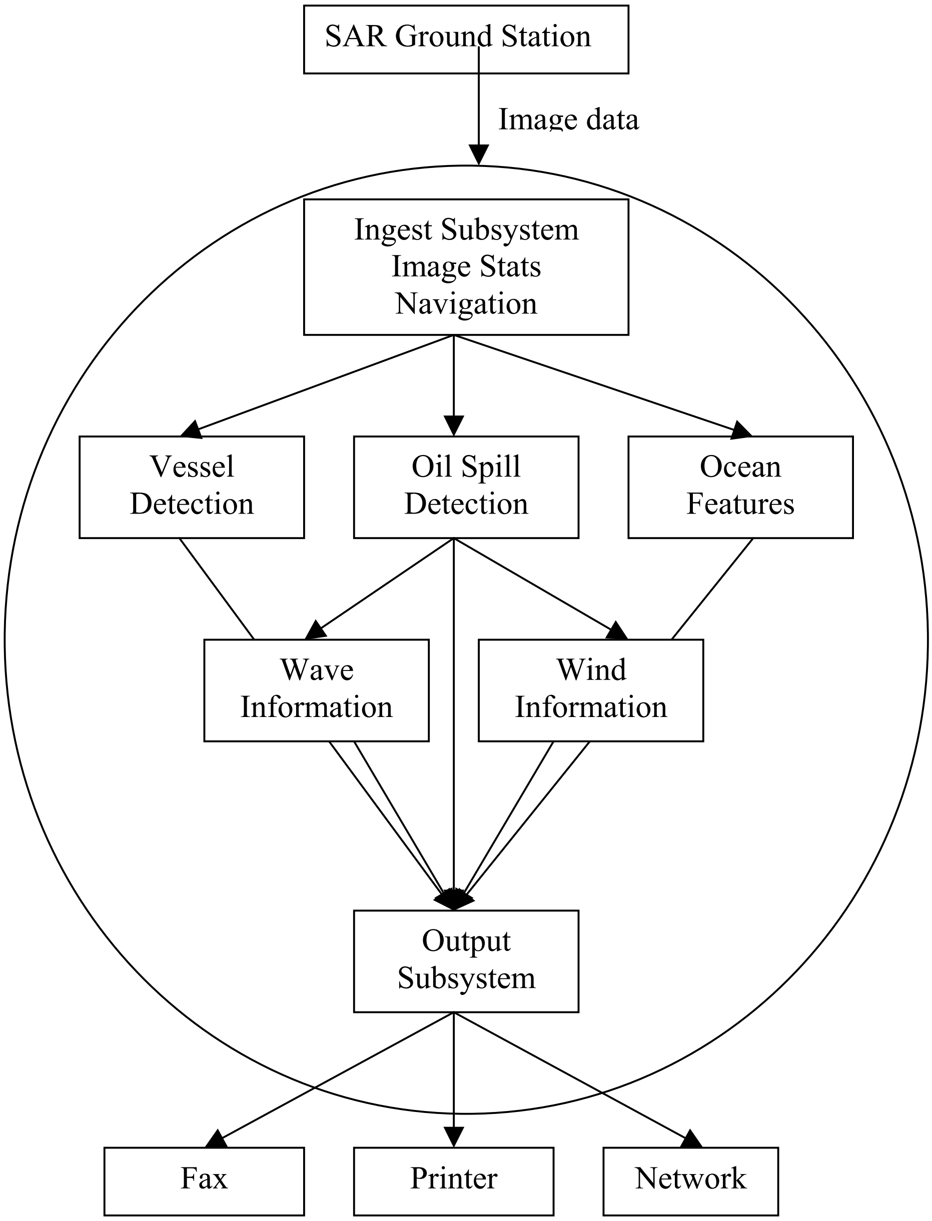

Figure 2.4 System overview of the Ocean Monitoring Workstation

2.24 The Role of Wide Swath SAR in High-Latitude Coastal Management (41)

Norway is responsible for managing economic zones that stretch from 56 °N to 82 °N, and has taken advantage of satellites swaths providing frequent coverage over the region. Even in high wind and rough sea states, the RADARSAT-1 ScanSAR narrow-far mode provides satisfactory spatial resolution for monitoring fishing activities. ENVISAT's Wide Swath mode is not suitable for this application, even though a subset of it can provide some satisfying data. Cost-benefit analysis in the 1980s showed that radar satellites could be used to cut the cost of patrolling waters under Norwegian jurisdiction. Relative to equatorial waters, the SAR coverage is twice as frequent for the North Sea and 4.5 times as frequent for the Barents Sea.

SAR can reveal many meteorological phenomena that cannot be captured by other observational methods or models, and they can contribute to understand phenomena that may be related to certain meteorological situations. A significant advantage of the wide area coverage, over narrow swath modes, is that it enables observations of weather systems and ocean circulation patterns at synoptic scales. In addition Wide Swath SAR gives several opportunities over a few days to cover a particular area at different incidence angles. The ability to use different incidence angles makes it possible to use the observations for specific applications. Large incidence angles should be used for ship detection, while steeper incidence angles should be used for ocean surface observations such as ship wakes. Algorithms to reduce data to geophysical parameters require access to details of the acquisition and SAR correlation process, as well as access to data in other forms than the traditional multilook detected image.

2.25 The Use of Satellite-Based SAR in Support of Fisheries Enforcement Applications (33)

The paper presents the use of spaceborne SAR to improve the existing fisheries aircraft and patrol vessel reconnaissance methods. Spaceborne SAR gives unique surveillance and monitoring capability. Three different experiments using SAR have been defined and implemented to assess the utility for fisheries enforcement applications:

1) SAR and Acoustic Measurements of Fishing Vessels in the Donut Hole Region of the Bering Sea. The experiment included detection of fishing vessels and ship wake detection. The measurements were done undersea to study the effect of blended SAR and acoustic signatures. Results indicate that fishing vessels may be differentiated from other classes of ships because they can have unique acoustic signatures.
2) SAR Measurements of the Columbia River Salmon Habitat. The experiment included observations of salmon spawning and nursery habitat. With this monitoring toll, large habitat regions can be monitored, which are not patrolled by conventional means.
3) SAR Measurements of Large-Scale Pelagic Driftnets. This experiment assessed the capability to detect large-scale pelagic driftnets. SAR observations were not done.

2.26 Validation of Ship Detection by the RADARSAT SAR (80)

The paper presents a statistical approach that is used to detect point targets in a clutter background. The model includes ocean clutter, image PDF, and ship cross section elements. Previous experience with ERS-1 SAR data was used to derive the ocean clutter and image PDF. The model is used to evaluate the expected ship detection performance of the RADARSAT-1 SAR as well as comparing the expected ship detection performance for the different modes on RADARSAT-1 SAR. Large incidence angle, low wind speed, and finer resolution increase the ship detection capability of smaller ships. A good compromise between spatial coverage and detection probability is the ScanSAR Narrow Far mode. Data acquired during a RADARSAT-1 SAR ship detection/validation field program in March/April 1996 off the coast of Halifax, Nova Scotia is used to quantitatively validate the model predictions. Measurements by buoys of a long time series of wind and directional wave spectra were used together with RADARSAT-1 C-band HH-polarized SAR passes over known ships. Validation of some of the model's key assumptions is presented. Focus is on the hybrid C-band HH-polarized ocean cross-section model, image probability density function, as well as ship radar signatures. The following conclusions are obtained from the ocean cross-section model:

- The largest σ^0's are for upwind directions (i.e. wind blowing towards the radar look direction)
- The smallest σ^0's are for (nearly cross wind directions (i.e. wind blowing across the radar look direction.
- σ^0 increases for increasing wind speed
- σ^0 for C-band VV is larger than σ^0 for C-band HH for all wind speeds and directions.
- σ^0 for C-band HH decreases more rapidly with increasing incidence angle than σ^0 for C-band VV. They should converge as the incidence angle becomes smaller.

The ship weight in tons (D) and length in meters (l) for the Bedford Institute of Oceanography (BIO) fleet and for some of the ships in the MARCOT'95 exercise are related, as a rule of thumb:

$$\sigma \equiv D = 0.08 l^{7/3} \tag{2.15}$$

σ is the RCS of the ship in square meters. The minimum point target RCS for detection at a chosen probability level is given by:

$$\sigma = I_c \sigma^0 \rho_a \rho_r \tag{2.16}$$

I_c is the critical image intensity of the relevant PDF (for unity mean image clutter), σ^0 is the ocean's normalized RCS, ρ_a is the azimuth resolution cell size, and ρ_r is the ground range resolution cell size.

2.27 Validation of Ship Detection by the RADARSAT Synthetic Aperture Radar and the Ocean Monitoring Workstation (85)

The paper presents the capability of RADARSAT-1 SAR used in combination with the Ocean Monitoring Workstation (OMW) for automatic ship detection. The validation has been done using *in situ* information collected during the field experiments performed in 1996 and 1997. The RADARSAT-1 single beam modes with large incidence angles are best suited for ship detection. The detection rates for these modes are 97 %, and 84 % overall. The validation ships used are 120 m long in average, and data with low winds are used. The RADARSAT/OMW combination indicates reliable ship detection performance.

2.28 Vessel Detection with Wide Area Remote Sensing (14)

The paper describes how Synthetic Aperture Radar (SAR) can be used to locate ships within an exercise area. The main information is from ERS-1 and RADARSAT-1 images. The real-time operational surveillance trial was carried out by Satlantic and Iosat for the Maritime Command coordinated Operational Training (MARCOT) and NATO Unified Spirit 1998 (US 98). The task of the experiment was to provide locations of the ships within the exercise area in less than one hour. The exercise area was off the East coast of Canada during June 1998.

Satlantic has developed the Ocean Monitoring Workstation (OMW) to enable real-time image exploitation and to take advantage of the wide area of coverage. Areas up to 500 m x 500 m were used. The OMW ship detection algorithm reduces the information to include the ship's location, extent of oil spills as well as wind and wave fields. The OMW software automatically analyses SAR imagery in 3-5 minutes. It can either be implemented as a stand-alone workstation or integrated directly into ground station infrastructure. The OMW is essentially a Constant False Alarm (CFA) rate algorithm, which is driven by a 1-look, K-distribution PDF. The automated OMW has a ship detection rate of 97 % for specific beam modes of RADARSAT-1. The satellite surveillance requirements for the MARCOT/US 98 operations were met using a combination of satellite, ground station, and the OMW.

2.29 Literature

(1) Aksnes, K (1983): Surveillance of Norway's Economic Zones Using Satellites and Aircraft, FFI/Rapport-83/9006, Norwegian Defence Research Establishment, Kjeller, Norway.

(2) Barnum, JR, JA Olkin and JW Ciboci (1997): Recent Advances in Counterdrug OTH Radar Ship Surveillance, Proc DoD Counterdrug Workshop at FSSC, Naval Research Laboartory, pp. 11-21.

(3) Cameron, WL, N Youssef and LK Leung (1996): Simulated Polarimetric Signatures of Primitive Geometrical Shapes, *IEEE Trans on Geosc and Rem Sens*, Vol. 34, No. 3, pp. 793–803.

(4) Chaudhuri, BB and SK Parui (1995): Target Detection: Remote Sensing Techniques for Defence Applications, Defence Science J, Vol. 45, No. 4, pp. 285-291.

(5) Clemente-Colón, P, DR Montgomery, WG Pichel, and K Friedman (1998): The Use of Synthetic Aperture Radar as a Potential Indicator of Fishing Activity in the Bering Sea, Proc of the 4th Pacific Ocean Rem Sens Conf (PORSEC'98), pp. 568-572, Qingdao, China.

(6) Clemente-Colón, P, WG Pichel, K Friedman and X Li (2000): Applications of SAR Observations to Fisheries in the Bering Sea, Ship Detection in Coastal Waters Workshop, poster presentation, Nova Scotia, Canada, May 31-June 1, 2000.

(7) Cranton J, RA De Abreu, C Bjerkelund, S Thomas and PW Vachon (1998): Marine Surveillance Using RADARSAT SAR: CCRS Ocean Activities, 20th Canadian Symp on Rem Sens, Calgary, Canada.

(8) Damini, A, M McDonald and GE Haslam (2003): X-band Wideband Experimental Airborne Radar for SAR, GMTI and Maritime Surveillance, IEE Proc Radar, Sonar and Navig, Vol. 150, No. 4, pp. 305-312.

(9) Deans, SR (1981): Hough Transform from the Radon Transform, *IEEE Trans on Pattern Analysis and Machine Intelligence*, Vol. 3, No. 2, pp. 185-188.

(10) Fingas, MF and CE Brown (2001): Review of Ship Detection from Airborne Platforms, *Can J Rem Sens*, Vol. 27. No. 4, pp. 379-385, Canada.

(11) Gibson, JD and JL Melsa (1975): Introduction to Non-Parametric Detection with Applications, IEEE press, NJ. Piscataway.

(12) Gower, JFR, PW Vachon and H Edel (1993): Ocean Applications of RADARSAT, Can J Rem Sens, Vol. 19, No. 4, pp. 372-383, Canada.

(13) Guo, HD (2000): Spaceborne and Airborne SAR for Target Detection and Flood Monitoring, *Photogrammetric Eng and Rem Sens*, Vol. 66, No. 5, pp. 611-617.

(14) Henschel, MD, PA Hoyt, JH Stockhausen, PW Vachon, H Edel, MT Rey and JWM Campbell (1998): Vessel Detection with Wide Area Remote Sensing, Sea Technology, Vol. 39, No. 9, pp. 63-68.

(15) Henschel, MD, RB Olsen, P Hoyt and PW Vachon (1997): The Ocean Monitoring Workstation: Experience Gained with RADARSAT, Int Symp, Geomatics in the Era of RADARSAT (GER'97), p. 12, Ottawa, Canada.

(16) Holliday, D, G St-Cyr and NE Woods (1986): A Radar Ocean Imaging Model for Small-To-Moderate Incidence Angles, *Int J Rem Sens*, Vol. 7, No. 12, pp.1809-1834.

(17) Johannessen, JA (2000): Coastal Observing Systems: The Role of Synthetic Aperture Radar, Johns Hopkins APL Technical Digest, Vol. 21, No. 1, pp. 41-48.

(18) Jordan, JE (2001): Mobile Communications Technologies for Ship Detection and Response, *Can J Rem Sens*, Vol. 27. No. 4, pp. 345-353, Canada.

(19) Kourti, N, I Shepherd and J Verborgh (2000): Fishing Boat Detection by Using SAR Imagery, AMRS Workshop on Ship Detection (proc), June 2000.

(20) Kourti, N, I Shepherd, G Scwartz and P Pavlakis (2001): Integrating Spaceborne SAR Imagery into Operational Systems for Fisheries Monitoring, *Can J Rem Sens*, Vol. 27, No. 4, pp. 291-305, Canada.

(21) Larivière, R, H Edel, C Bjerklund, P Vachon, LCdr J Day and M Rey (1997): Remote Vessel Detection on the Grand Banks Using Radarsat Imagery: Early Results, Fisheries and Oceans Science Directorate, Memorandum, Note de service.

(22) Larivière, R, H Edel, C Bjerklund, P Vachon, R Olsen, S Thomas and D Adair (1997): Operational Evaluation of Radarsat Potential in Fishing Vessel Surveillance: Potential & Test Results, Fisheries and Oceans Science Directorate, Memorandum, Note de service.

(23) Lavrova, OY, TY Bocharova and MI Mityagina (2003): SAR Observations of Typical Phenomena in the Black Sea Shore Area, IEEE Int Geosc and Rem Sensing Symp (IGARSS'03), Toulouse, France.

(24) Lee, JS (1990): Coastline Detection and Tracking in SAR Images, *IEEE Trans on Geosc and Rem Sens*, Vol. 28, No. 4, pp. 662-668.

(25) Lewis, AJ (1998): Detecting and Mapping Offshore Navigation Hazards Using Synthetic Aperture Radar Data, IEEE.

(26) Liu, AK, CY Peng and SYS Chang (1997): Wavelet Analysis of Satellite Images for Coastal Watch, *IEEE J of Oceanic Eng*, Vol. 22, No. 1, pp. 9-17.

(27) Malthus, TJ and PJ Mumby (2003): Remote Sensing of the Coastal Zone: an Overview and Priorities for Future Research, *Int J Rem Sens*, Vol. 24, No. 13, pp. 2805-2815.

(28) Manore, MJ, PW Vachon, C Bjerklund, HR Edel and B Ramsay (1998): Operational Use of RADARSAT SAR in the Coastal Zone: The Canadian Experience, 27th Int Symp Rem Sens on the Environment, pp. 115-118, Tromsø, Norway.

(29) Margarit, G, JJ Mallorqui and JM Rius (2004): Study of the Vessel Speed and Sea Swell Effects on Simulated Polarimetric High Resolution SAR Images, 5th Conference on Synthetic Aperture Radar, EUSAR 2004, Ulm, Germany.

(30) Margarit, G, X Fabregas and JJ Mallorqui (2004): Study of the Polarimetric Mechanisms on Simulated Vessels with SAR and ISAR Imaging, 5th Conference on Synthetic Aperture Radar, EUSAR 2004, Ulm, Germany.

(31) Moccia, A, N Chiacchio and A Capone (2000): Spaceborne Bistatic Synthetic Aperture Radar for Remote Sensing Applications, *Int J Rem Sens*, Vol. 21, No. 18, pp. 3395-3414.

(32) Montgomery, DR (2000): International Fisheries Enforcement Management Using Wide Swath SAR, *Johns Hopkins APL Tech Digest*, Vol. 21, No. 1, pp. 41-48.

(33) Montgomery, DR, W Pichel and P Clemente-Colón (1998): The Use of Satellite-Based SAR in Support of Fisheries Enforcement Applications, Proc of IGARSS'98, Seattle, Washington, 6-10 July, 1998.

(34) Moriyama, T, Y Yamaguchi, H Yamada and M Sengoku (1995): Reduction of Surface Clutter by a Polaimetric FM-CW Radar in Underground Target Detection, *IEEE Trans on Comm*, Vol E78B, No. 4, pp. 625-629.

(35) Munk, WH, RS Scully-Power and F Zachariasen (1987): Ships From Space, Proc of the Royal Society London, A, Vol. 412, pp. 231-254.

(36) Newman, JN (1970): Recent Research of Ship wakes, 8th Symphosium on Naval Hydrodynamics: Hydrodynamics in the Ocean Environment, pp. 519-545, Office of Naval Research, Dep of the Navy, Arlington, Virginia.

(37) Newman, JN (1991): The Inverse Ship Wave Problem, The Sixth Int Workshop on Water Waves and Floating Bodies, pp.193-197, MIT, Cambridge, MA, USA.

(38) Nilsson, CS and PC Tidesley (1995): Imaging of Oceanic Features by ERS-1 Synthetic-Aperture Radar, *J of Geoph Res - Oceans*, Vol. 100, No. C1, pp. 953-967.

(39) Nilubol, C, RM Mersereau and MJT Smith (2002): A SAR Target Classifier Using Radon Transforms and Hidden Markov Models, Digital Signal Processing, Vol. 12, No. 2-3, pp. 274-283.

(40) Olsen, RB, K Eldhuset and T Wahl (2004): Validation of Predictions Regarding Ship Detection with ENVISAT ASAR in the Alternating Polarization Mode, 5th Conference on Synthetic Aperture Radar, EUSAR 2004, Ulm, Germany.

(41) Olsen, RB and T Wahl (2000): The Role of Wide Swath SAR in High-Latitude Coastal Management, *Johns Hopkins APL Tech Digest*, Vol. 21, No. 1.

(42) Olsen, RB, P Bugden, Y Andrade, P Hoyt, M Lewis, H Edel and C Bjerkelund (1995): Operational Use of RADARSAT SAR for Marine Monitoring and Surveillance, *IEEE Trans on Geosc and Rem Sens* (IGARSS'95), pp. 224-226, Firenze, Italy.

(43) Olsen, RB, JK Jensen and Morten Torsås (2003): Rapid Environmental Assessment at High Latitudes.

(44) Olsen, RB, T Wahl and G Engen: Expected Performance of the ENVISAT ASAR for Near Real-Time Maritime Applications, *IEEE Int Geosc and Rem Sensing Symp* (IGARSS'03), Toulouse, France.

(45) Parlow, E (1995): Progress in Environmental Remote Sensing and Applications, Proc of the 15th EARSeL Symphosium, Basel, Switzerland, Sep 4-6, 1995.

(46) Patton, R, M Webb and R Gaj (2001): Covert Operations Detection for Maritime Applications, *Can J Rem Sens*, Vol. 27. No. 4, pp. 306-319, Canada.

(47) Pichel WG and P Clemente-Colón (2000): NOAA CoastWatch SAR Applications and Demonstration, *Johns Hopkins APL Tech Digest*, Vol. 21, No. 1, pp. 49-57.

(48) Plache, B and MD Henschel (2001): Modification of the OMW to Include Polarimetric Ship Detection, Satlantic Document No. SAT-DN-0075, Satlantic, Halifax, NS.

(49) Raney, RK, AP Luscombe, EJ Langham and S Ahmed: RADARSAT, Proc of the IEEE, Vol. 79, No. 6, pp. 839-849.

(50) Rosich, B and P Meadows (2004): Absolute Calibration of ASAR Level 1 Products Generated by PF-ASAR, ESA Document, Frascati, Italy.

(51) Schulz, K, U Soergel, U Thoennessen and U Stilla (2003): Elimination of Arcross-Track Phase Components in Airborne Along-Track Interferometry Data to Improve Object Velocity Measurements, *IEEE Int Geosc and Rem Sensing Symp* (IGARSS'03), Toulouse, France.

(52) Scott, DF (2000): Paramilitary Technologies in Use by a Civilian Company for Canadian Government Ship Detection and Identification Applications, Proc of a Workshop on Ship Detection in Coastal Waters.

(53) Skjelland, E (1992): The Use of Commercial Radar Satellites in Military Sea Surveillance, FFI/Rapport-92/5017 (confidential in Norway), Norwegian Defence Research Establishment, Kjeller, Norway.

(54) Skøelv, Å and T Wahl (1995): ERS Detection of Soft and Hard Targets at Sea: What Can be Operationalized?, Proc of the Sec ERS Appl Workshop, pp. 193-196, London, 6-8 Dec 1995.

(55) Skøelv, Å, ST Dokken and T Wahl (1995): Up-coming Radar Satellites and Their Potential for Some Maritime Applications, Progress in Env Rem Sens Res and Appl, presentation, Switzerland.

(56) Skøelv, Å, T Andersen, K Eldhuset and Terje Wahl (1994): Ship Traffic Monitoring and Oil Spill Detection Using the ERS-1 SAR, Rem Sens from Res to Operational Appl in the New Europe, pp. 19-26, Springer Hungary.

(57) Skøelv, Å, T Wahl, T Jørgensen, ST Dokken (1996): Maritime Use of Satelliteborne SAR, WEAG Euclid CEPA 9, RTP 9.1, WP2300, Final Report (RTP9.1/96/NDRE/2300/FR), FFI/Rapport-96/03203.

(58) Smirnov, AV (1998): Ocean Radar Observations of Ship-Induced Instabilities in the Atmospheric Boundary Layer, *J of Atm and Oceanic Tech*, Vol. 15, No. 3, pp. 798-803.

(59) Smirnov, AV (1999): Radar Observations of Ship-Induced Instabilities in the Ocean-Atmosphere System, Oceanoloica Acta, Vol. 22, No. 1, pp. 45-50.

(60) Soumekh, M (2002): Moving Target Detection and Imaging Using an X Band Along-Track Monopulse SAR, *IEEE Trans on Aerosp and Elect Syst*, Vol. 38, No. 1, pp. 315-333.

(61) Soumekh, M. Moving Target Detection in Foliage Using Along Track Monopulse Synthetic Aperture Radar Imaging, IEEE Trans on Image Proc, Vol. 6, No. 8, pp. 1148-1163, Aug 1997.

(62) Strom, GD (1991): The Norwegian Coordinated Program for ERS-1 Preparations, Acta Astronautica, Vol. 24, pp. 115 - 119.

(63) Swerling, P (1960): Probability of Detection for Fluctuating Targets, IRE Trans, Vol. IT-6, pp. 269-300.

(64) Tello, M, C Lopez-Martinez and JJ Mallorqui (2004): Ship Detection in SAR Imagery based on the Wavelet Transform, 5th Conference on Synthetic Aperture Radar, EUSAR 2004, Ulm, Germany.

(65) Teufert, J (2000): Generation of "Tactical" Assessments Based on Commercially Available Satellite Data, WEUSC Res Div, Western EU, Satellite Centre Satellitaire.

(66) Thomas, SJ, PW Vachon and J Cranton (1998): Validation of Ship Detection by the RADARSAT SAR/Ocean Monitoring Workstation, 20th Canadian Symp on Rem Sens, pp. 165-168, Calgary, Canada.

(67) Thomas, SJ, PW Vachon, C Bjerkelund, J Cranton, RB Olsen (1998): Demonstration of the RADARSAT SAR/Ocean Monitoring Workstation, Proc of GIS'98/RT'98, Toronto, Canada, April 6-9 1998.

(68) Touzi, R (2000): Calibrated Polarimetric SAR Data for Ship Detection, *IEEE Trans on Geosc and Rem Sens* (IGARSS'00), Honululu, Hawaii, USA.

(69) Touzi, R (2002): A Review of Speckle Filtering in the Context of Estimation Theory, *IEEE Trans on Geosc and Rem Sens*, Vol. 40, No. 11, pp. 2392-2404.

(70) Touzi, R, S Goze, T Le Toan, A Lopes and E Mougin (1992): Polarimetric Discriminators for SAR Images, *IEEE Trans on Geosc and Rem Sens*, Vol. 30, No. 5, pp. 973–980.

(71) Trunk, GV and SF George (1970): Detection of Targets in Non-Gaussian Sea Clutter, *IEEE Trans on Aerosp and Elect Syst*, Vol. 6, No. 5, pp. 620-628.

[72) Tunaley, JKE (2003). The Estimation of Ship Velocity from SAR Imagery, *IEEE Int Geosc and Rem Sensing Symp* (IGARSS'03), Toulouse, France.

(73) Vachon PW and JW Campbell (1996): Validation of Ship Detection with the RADARSAT SAR; RADARSAT for Ice and Oceans - Early Experience and Data Access, 6th Workshop of the Canadian Ice Working Group, Ottawa, Ontario, Canada, November 19-21, 1996.

(74) Vachon, P (1995): Ship Detection by RADARSAT SAR, Tech Report, Canada Centre for Remote Sensing, Ottawa, Ontario, Canada.

(75) Vachon, PW, SJ Thomas, J Cranton, HR Edel and MD Henschel (2002): Validation of Ship Detection by the RADARSAT Synthetic Aperture Radar and the Ocean Monitoring Workstation, *Can J Rem Sens*, Vol. 26, pp. 200-212, Canada.

(76) Vachon, PW (1995): Ship Detection by the RADARSAT SAR (A Working Paper), Tech Report, Canada Centre for Remote Sensing, Ottawa, Ontario, Canada.

(77) Vachon, PW and RB Olsen (1996): RADARSAT SAR Mode Selection for Maritime Applications, *Backscatter*, Vol. 6, No. 3, pp. 3-4.

(78) Vachon, PW and RB Olsen (1998): RADARSAT: Which Mode Should I Use?, *Backscatter*, Vol. 9, pp.14-20.

(79) Vachon, PW and RB Olsen (2000): Ship Detection With Satellite-Based Sensors: Summary of Workshop Presentations, *Backscatter*, Vol 11, No 4, pp 23-26.

(80) Vachon, PW, JWM Campbell and C Bjerklund (1996): Validation of Ship Detection by the RADARSAT SAR, Proc of the Pacific Ocean Rem Sens Conf (PORSEC'96)

(81) Vachon, PW, JWM Campbell, C Bjerklund, FW Dobson and MT Rey (1998): Detecting Surface Vessels by RADARSAT, Chapter 2.3.7 in Remote Sensing of the Pacific Ocean by Satellites, Earth Ocean and Space, pp. 145-164, PTY Ltd., Glebe, Australia.

(82) Vachon, PW, JWM Campbell, RK Hawkins, J Cranton, R Keeley and H Edel (1997): Performance of the CDPF SEA LUT for ScanSAR Ship Detection, CCRS Internal Report, Canada.

(83) Vachon, PW, JWM Campbell, S Thomas and J Cranton (1997): CDPF/OFW Products from MARCOT, CCRS Internal Report, Canada.

(84) Vachon, PW, P Adlakha, H Edel, M Henschel, B Ramsay, D Flett, M Rey, G Staples and S Thomas (2000): Canadian Progress Toward Marine and Coastal Applications of Synthetic Aperture Radar, *Johns Hopkins APL Tech Digest*, Vol. 21, No. 1, pp. 33-40.

(85) Vachon, PW, SJ Thomas, JA Cranton, CA Bjerkelund, FW Dobson and RB Olsen (1998): Monitoring the Coastal Zone with the RADARSAT Satellite, Oceanology Int 98, 10 p, UK.

(86) Wahl, T (1992): Radar Satellites and Naval Operations, Proc of NATO DRG 25th Anniversary Symp, Vol. 2, London. UK.

(87) Wahl, T (1992): Using RADARSAT-1 for Fisheries Enforcement Operations, *IEEE Trans on Geosc and Rem Sens*, IGARSS'97, "Remote Sensing - A Scientific Vision for Sustainable Development", Vol. 1, pp. 47-49.

(88) Wahl, T (1998): Integrated Use of RADAR Satellites for Fisheries Enforcement Operations, Proc of the 27th Int Symp Rem Sens Env, pp. 123-126, Tromsø, Norway, June.

(89) Wahl, T (1998): Satellittovervåking, Norwegian Defence Research Establishment collection of articles, Kjeller, Norway.

(90) Wahl, T and Å Skøelv (1996): NATO Naval Exercises As Observed From Civilian Radar Satellites, AGARD MSP 5th Symp on "Space Systems as Contributors to the NATO Defence Mission" (published in CP-580), Cannes, France.

(91) Wahl, T, K Eldhuset and Å Skøelv (1993): Ship Traffic Monitoring and Oil Spill Detection Using the ERS-1 SAR, Int Symp "Operationalization of Remote Sensing", ITC Enschede, The Netherlands.

(92) Wahl, T, T Andersen, K Eldhuset and Å Skøelv (1994): Ship Traffic Monitoring and Oil Spill Detection Using the ERS-1 SAR, From Optics to Radar, SPOT and ERS Applications. CNES, Cepadues-Editions, pp. 211-220, Paris.

(93) Wu, Z (1991): On the Estimation of a Ship's Velocity and Hull Geometry Information from Its Wave Functions, The University of Michigan, Program in Ship Hydrodynamics PhD Dissertation, Dep of Naval Arch and Marine Eng.

(94) Wu, Z and GA Meadows (1991): A Remote Sensing Technique for the Estimation of a Moving Ship's Velocity and Length from Its Wave Spectra, IEEE Proc of Ocean Tech and Opp in the Pacific for the 90's. OCEANS'91, Vol. 2, pp. 810-817.

(95) Zink, M, C Buck, JL Suchail, R Torres, A Bellini, J Closa, YL Desnos and B Rosich (2001): The Radar Imaging Instrument and Its Applications: ASAR, ESA Bulletin, No. 106, pp. 46-55.

3 STUDIES ON SIGNATURES AND CHARACTERISTICS

3.1 Overview

The following table gives an overview of publications on the theme "Studies on Signatures and Characteristics" sorted after publication year. The papers include measurement trials, campaigns, as well as modelling of wakes and of ship radar signatures. Papers on statistical properties of ocean images are also included. Summaries of a selection of some of the most important and available papers are given following the table.

YEAR	TITLE	AUTHOR	PUBLISHED
2004	Vurdering av ENVISAT ASAR for Skipsdeteksjon	Arnesen, T and RB Olsen	FFI/Rapport-2004/02121, Norwegian Defence Research Establishment, Kjeller, Norway.
2004	Ultra High Resolution Spaceborne SAR Processing	Eldhuset, K	IEEE Trans on Aerosp and Elect Syst, Vol. 40, No. 1, pp. 370-378.
2004	Reconsideration of Coherency Matrix Parameters for Target Scattering Characterization	Touzi, R	5th Conference on Synthetic Aperture Radar, EUSAR 2004, Ulm, Germany.
2004	First Polish SAR Trials	Gados, A, A Gorzelanczyk, A Jarzebska, M Mordzonek, M Smolarczyk, KS Kulpa and B Dawidowicz	5th Conference on Synthetic Aperture Radar, EUSAR 2004, Ulm, Germany.
2004	ISAR Target Simulation and Matching	Kolev, NZ and CI Alexandrov	5th Conference on Synthetic Aperture Radar, EUSAR 2004, Ulm, Germany.
2004	Analysis of the Propeller-Hull Interaction by LDV Phase Sampling Techniques	Felli, M and F Di Felice	J of Visualization.
2004	Satellite Synthetic Aperture Radar Detection of Delaware Bay Plumes: Jet-Like Feature Analysis	Zheng, QN, P Clemente-Col?n, XH Yan, WT Liu and NE Huang	J of Geoph Res - Oceans, Vol. 109, No. C3, pp. 953-967.
2003	The Use of Fully Polarimetric Information for the Fuzzy Neural Classification of SAR Images	Chen, CT, KS Chen and JS Lee	IEEE Trans on Geosc and Rem Sens, Vol. 41, No. 9, pp. 2089-2100.
2003	Super-Resolution of Polarimetric SAR Images of Ship	Pastina, D, P Lombardo, A	Signal Proc, Vol. 83, No. 8, pp. 1737-1748.

	Targets	Farina and P Daddi	
2003	Study on Detection of Information on the Sea Surface in SAR Imagery	Obi, S and M Murata	NEC R&D, Vol. 44, No. 2, pp. 165-169.
2003	Orbital SAR Simulator of Fishing Vessel Polarimetric Signatures Based on High Frequency Electromagnetic Calculations	Margarit, G, P Blanco, J Sanz and JJ Mallorqui	IEEE.
2003	Multiple Moving Target Detection and Trajectory Estimation Using a Single SAR Sensor	Dias, JMB and PAC Marques	IEEE Trans on Aerosp and Elect Syst, Vol. 39, No. 2, pp. 604-624.
2003	The Ship Detection Capability of ENVISAT's ASAR	Olsen, RB and T Wahl	IEEE Int Geosc and Rem Sensing Symp (IGARSS'03), Toulouse, France.
2003	3-D E-CSAR Imaging of a T-72 Tank and Synthesis of Its SAR Reconstructions	Bryant, ML, LL Gostin and M Soumekh	IEEE Trans on Aerosp and Elect Syst, Vol. 39, No. 1, pp. 211-227.
2003	Detection and Imaging of Arbitrarily Moving Targets with Single-Channel SAR	Kirscht, M	IEE Proc Radar, Sonar and Navig, Vol. 150, No. 1, pp. 7-11.
2003	Results of Flight Tests of a Two-Channel Radar System with Real-Time MTI Processing	Meyer-Hilberg, J, B Bickert and KP Schmitt	IEE Proc Radar, Sonar and Navig, Vol. 150, No. 1, pp. 23-27.
2003	Scattering-Based Tomography for HRR and SAR Prediction	Denney, BS and RJP De Figueiredo	Multidim Systems and Signal Proc, Vol. 14, No. 1-3, pp. 207-222.
2003	Toward Target Recognition from Synthetic Aperture Radar Imagery Using Electromagnetics-Based Signatures	Yeang, CP, CY Cho and JH Shapiro	Optical Eng, Vol. 42, No. 7, pp. 2129-2149.
2003	On the Use of Complex SAR Image Spectral Analysis for Target Detection: Assessment of Polarimetry	Souyris, JC, C Henry and F Adragna	IEEE Trans on Geosc and Rem Sens, Vol. 41, No. 12, pp. 2725-2734.
2003	Satellite Image Fusion with Multiscale Wavelet Analysis for Marine Applications: Preserving Spatial Information and Minimizing Artifacts (PSIMA)	Du, Y, PW Vachon and JJ van der Sanden	Can J Rem Sens, Vol. 29, No. 1, pp. 14-23, Canada.
2003	Detection of Invisible Moving Targets in Foliage Penetration Ultra-Wide-Band Synthetic Aperture Radar Images	Guo, HW, DN Liang, Y Wang and XT Huang	Optical Eng, Vol. 42, No. 10, pp. 2796-2797.
2002	Nonuniform Azimuth Image Shift Observed in the Radarsat Images of Ships in Motion	Ouchi, K, M Lehara, K Morimura, S Kumano and I Takami	IEEE Trans on Geosc and Rem Sens, Vol. 40, No. 10, pp. 2188-2195.
2002	Ship Wakes and Their Radar Images	Reed, AM and JH Milgram	Annual Review of Fluid Mechanics, Vol. 34, pp. 469-502.
2002	Simulation of Polarimetric SAR Vessel Signatures for Satellite Fisheries Monitoring	Mallorqui, JJ, JM Rius and M Bara	IEEE Trans on Geosc and Rem Sens (IGARSS'02), Vol. 5, pp. 2711-2713, Toronto, Canada.

2002	Satellite SAR Simulator for Fishing Vessels Signature Studies	Mallorqui, JJ, JM Rius and M Bara	EUSAR 2002, Cologne, Germany.
2002	Derivation of RCS and s0 from ASAR products. ESA. ASAR Calibration Review	Zink, M	ESTEC, the Netherlands.
2002	Results from the Crusade Ship Detection Trial: Polarimetric SAR	Yeremy, ML, G Geling and M Rey	IEEE Trans on Geosc and Rem Sens (IGARSS 02), Vol. 2, pp. 711-713.
2002	Free-Surface Turbulent Wake Behind Towed Ship Models: Experimental Measurements, Stability Analyses and Direct Numerical Simulations	Shen, L, C Zhang and DKP Yue	J of Fluid Mech, Vol. 469, pp. 89-120.
2002	A Simple Model for SAR Azimuth Speckle, Focusing, and Interferometric Decorrelation	Gabriel, AK	IEEE Trans on Geosc and Rem Sens, Vol. 40, No. 8, pp. 1885-1889.
2002	Characterization of Target Symmetric Scattering Using Polarimetric SARs	Touzi, R and F Charbonneau	IEEE Trans on Geosc and Rem Sens, Vol. 40.
2002	Estimating the Effective Number of Looks in Interferometric SAR Data	Gierull, CH and IC Sikaneta	IEEE Trans on Geosc and Rem Sens, Vol. 40, No. 8, pp. 1733-1742.
2002	A Comparison Between Different Polarimetric Measurement Schemes	Santalla, V and YMM Antar	IEEE Trans on Geosc and Rem Sens, Vol. 40, No. 5, pp. 1007-1017.
2002	Measured and Predicted Synthetic Aperture Radar Target Comparison	Douville, PL	IEEE Trans on Aerosp and Elect Syst, Vol. 38, No. 1, pp. 25-37.
2002	Using Similarity Parameters for Supervised Polarimetric SAR Image Classification	Xu, JY, J Yang, YN Peng, C Wang and YA Liou	IEEE Trans on Comm, Vol E85B, No. 12, pp. 2934-2942.
2001	Kelvin and V-like Ship Wakes Affected by Surfactants	Zilman, G and T Miloh	J of Ship Res, Vol. 45, No. 2, pp. 150-163.
2001	Ship Detection Using Airborne Polarimetric SAR	Hawkins, RK, KP Murnaghan, M Yeremy and M Rey	CEOS SAR Workshop Proc, pp. 6-15, Tokyo, Japan.
2001	Ship-Sea Contrast Optimization When Using Polarimetric SARS	Touzi, R, F Charbonneau, RK Hawkins, K Murnaghan and X Kavoun	Proc of IGARSS'01, Australia.
2001	Contextual Information in SAR Target Detection	Blacknell, D	IEE Proc Radar, Sonar and Navig, Vol. 148, No. 1, pp. 41-47.
2001	Extraction of Moving Ground Targets by a Bistatic Ultra-Wideband SAR	Pettersson, MI	IEE Proc Radar, Sonar and Navig, Vol. 148, No. 1, pp. 35-40.
2001	Three-Dimensional ISAR Imaging of Maneuvering Targets Using Three Receivers	Wang, GY, XG Xia and VC Chen	IEEE Trans on Image Proc, Vol. 10, No.35, pp. 436-447, March 2001.

2001	Theory of Synthetic Aperture Radar Imaging of a Moving Target	Jao, JK	IEEE Trans on Geosc and Rem Sens, Vol. 39, No. 9, pp. 1984-1992.
2001	On the Monitoring of Illicit Vessel Discharges Using Spaceborne SAR Remote Sensing - a Reconnaissance Study in the Mediterranean Sea	Pavlakis, P, D Tarchi and AJ Sieber	Annales des Telecommunications-Annals of Telecommunications, Vol. 56, No. 11-12, pp. 700-718.
2001	Ship Detection Performance Predictions for Next Generation Spaceborne Synthetic Aperture Radars	Simoes, MVS	Thesis Naval Postgraduate School, Monterey, CA, USA.
2001	Observation of Long Waves Generated by Ferries	Neumann, DG, E Tapio, D Haggard, KE Laws and RW Bland	Can J Rem Sens, Vol. 27. No. 4, pp. 361-370, Canada.
2001	Ocean Surveillance with Polarimetric SAR	Yeremy, M, JWM Campbell, K Mattar and T Potter	Can J Rem Sens, Vol. 27. No. 4, pp. 328-344, Canada.
2000	Potential of Radar Satellite Remote Sensing for Estimating Underwater Ambient Noise	Hutt, D, P Chevret and ME Zakharia	Proc of the Fifth European Conference on Underwater Acoustics, ECUA 2000, Lyon, France.
2000	Detection of Ship Wakes Using an Airborne Magnetic Transducer	Zou, N and A Nehorai	IEEE Trans on Geosc and Rem Sens, Vol. 38, No. 1, pp. 532-539.
2000	Object-Based SAR Image Compression Using Vector Quantization	Venkatraman, M, H Kwon and NM Nasrabadi	IEEE Trans on Aerosp and Elect Syst, Vol. 36, No. 4, pp. 1036-1046.
2000	Statistical Target Behaviour in SAR Images	Blacknell, D	IEE Proc Radar, Sonar and Navig, Vol. 147, No. 3, pp. 143-148.
2000	Target Detection in Correlated SAR Clutter	Blacknell, D	IEE Proc Radar, Sonar and Navig, Vol. 147, No. 1, pp. 9-16.
2000	Preliminary Results from Polarimetric SAR in the Crusade-2000 Experiment on Ship Detection	Rey, M, RK Hawkins, M Yeremy, B Noise, B Bayer and K Murnaghan	Ship Detection in Coastal Waters Workshop, poster presentation, Nova Scotia, Canada, May 31-June 1, 2000.
2000	Ship Surveillance Using RADARSAT ScanSAR Images	Robertson, N, P Bird and C Brownsword	
1999	Wakes and Spokes: New Motion-Induced Brightness Illusions	Holcombe, AO, SL Macknik, J Intriligator, AE Seiffert and PU Tse	Perception 28, pp. 1231-1242.
1999	Aerosol Dynamics in Ship Tracks	Russel, LM, JH Seinfeld, RC Flagan, RJ Ferek, DA Hegg, PV Hobbs, W Wobrock, AI Flossmann, CD O'Dowd, KE	J of Geoph Res, Vol. 104, No. 24, pp. 31,077-31,095.

		Nielsen and PA Durkee	
1999	Cell-Averaging CFAR Detection in Compound Clutter with Spatially Correlated Texture and Speckle	Barkat, M and F Soltani	IEE Proc Radar, Sonar and Navig, Vol. 146, No. 6, pp. 279-284.
1999	An Appraisal of Literature on the Simulation of the SAR Imaging of Turbulent Ship Wakes	Waymont, DK and IOG Davies	Tech Note-90/515/1.0, Smith Associates, Guilford, UK.
1999	SAR Imaging and Moving Targets	Perry, PP, RC Dipietro and RL Fante	IEEE Trans on Aerosp and Elect Syst, Vol. 35, No. 1.
1999	Ship Detection Using Polarimetric SAR Data	Ringrose, R and N Harris	Proc of the CEOS SAR workshop, ESASP-450.
1999	Radar Imaging of Kelvin Arms of Ship Wakes	Hennings, I, R Romeiser, W Apers and A Viola	Int J Rem Sens, Vol. 20, pp. 2519-2543.
1999	Instrumented Ship Imaging Using the AN/APS-506 Spotlight SAR System	Godbole, M, PE Dimini and GE Haslam	Proc of the 21st Int Airborne Rem Sens Conf, pp. 550-557, Ottawa, Ont.
1999	On the Use of Polarimetric SAR Data for Ship Detection	Touzi, R	Proc of IGARSS'99, 3p, Hamburg, Germany, June 28-July 2 1999.
1998	Radar Beamwidth Reduction Techniques	Suzuki, T	IEEE Aerospace and Electronic Systems Magazine, Vol. 13, No. 5, pp. 43-48.
1998	Measurements of Ship-Induced Tracks in Clouds off the Washington Coast	Ferek, RJ, DA Hegg, PV Hobbs, P Durkee and K Nielsen	J of Geoph Res - Atmospheres, Vol. 103, No. D18, pp. 23,199-23,206.
1998	Analysis of Speckle Noise Contribution on Wavelet Decomposition of SAR Images	Simard, M, G DeGrandi, KPB Thomson and GB Beniev	IEEE Trans on Geosc and Rem Sens, Vol. 36, No. 6, pp. 1953-1962.
1998	Feature Extraction of SAR Targets Consisting of Trihedral and Dihedral Corner Reflectors	Liu, ZS and J Li	IEE Proc Radar, Sonar and Navig, Vol. 145, No. 3, pp. 161-172.
1998	Sea Surface and Ship Observation with MEMPHIS	Boehmsdorff, S and H Essen	Proc of IGARSS'98, Seattle, USA.
1998	K-Distributed Model for the Statistics of RADARSAT Imagery	Jiang, Q, D Ziou, GB Benie and A El Zaart	Tech Report, University of Sherbrooke.
1998	Deteksjon av Punktmål Ved Hjelp av ScanSAR	Grønlien, TR	Diploma thesis in physics, University of Oslo.
1997	Degree of Polarization of Radar Backscatters from a Mixed Target	Hirosawa, H	IEEE Trans on Geosc and Rem Sens, Vol. 35, No. 2, pp. 466-470.
1997	On the Positioning of Multisensor Imagery for Exploitation and Target Recognition	Chellappa, R, QF Zheng, P Burlina, C Shekhar and KB Eom	Proc of the IEEE, Vol. 85, No. 1, pp. 120-138.
1997	The Effect of Median Filtering on Synthetic Aperture Radar Images	Rees, WG and MJF Satchell	Int J Rem Sens, Vol. 18, No. 13, pp. 2887-2893.

1997	Target Angular Motion Effects on ISAR Imaging	Berizzi, F and M Diani	IEE Proc Radar, Sonar and Navig, Vol. 144, No. 2, pp. 87-95.
1997	Single Point and Spatial Statistics of Polarimetric SAR Imagery	Blacknell, D and AP Blake	Int J Rem Sens, Vol. 18, No. 3, pp. 629-649.
1997	VSAR: A High Resolution Radar System for Detection of Moving Targets	Friedlander, B and B Porat	IEE Proc Radar, Sonar and Navig, Vol. 144, No. 4, pp. 205-218.
1997	Multi-Frequency SAR Images of Ship-Generated Internal Waves	Ouchi, K, NR Stapleton and BC Barber	Int J Rem Sens, Vol. 18, No. 18, pp. 3709-3718.
1997	Statistical Modelling of Ocean SAR Images	Delignon, Y, R Garello and A Hillion	IEE Proc Radar, Sonar and Navig, Vol. 144, No. 6.
1997	Maximum Likelihood Estimation of the Number of Looks in SAR Images	Foucher, S, GB Benie and J Boucher	Mikon, pp. 657-660, Pologne, Wroclaw.
1997	Optimization of the Ocean Features Workstation for Ship Detection	Campbell, JWM and PW Vachon	CCRS Internal Report, Canada.
1997	Ship Wakes in Radar Imagery	Stapleton, NR	Int J Rem Sens, Vol. 18, No. 6, pp. 1381-1386, 1997.
1997	Ocean Surface Feature Detection With the CCRS Along-Track InSAR	Campbell, JWM, AL Gray, KE Mattar, JH Clarke and MWA van der Kooij	Can J Rem Sens, Vol. 23. No. 1, pp. 24-37, Canada.
1997	Propageringsfaktorens Betydning for Radar Deteksjon av Mål i Sjøbakgrunn	Nordland, R	Kompendium for UNIKF361, Universitetsstudiene på Kjeller.
1996	Understanding of Partial Polarization in Polarimetric SAR Data	Dong, Y and B Forster	Int J Rem Sens, Vol. 17, No. 12, pp. 2467-2475.
1996	Detection and Estimation of Moving Target Signals by Multi-Channel SAR	Ender, JHG	Archiv fur Elektronik und Ubertragungstechnik (AEU) - Int J of Electronics and Comm, Vol. 50, No. 2, pp. 150-156.
1996	Experimental Moving Target Detection Results from a Three-Beam Airborne SAR	Coe, DJ and RG White	Archiv fur Elektronik und Ubertragungstechnik (AEU) - Int J of Electronics and Comm, Vol. 50, No. 2, pp. 157-164.
1996	Simulation of Ship Wakes Image by an Along-Track Interferometric SAR	Shemer, L, L Kagan and G Zilman	Int J Rem Sens, Vol. 17, No. 18, pp. 3577-3597.
1996	Observations of Ship-Generated Internal Waves in SAR Images from Loch Linnhe, Scotland, and Comparison with Theory and In Situ Internal Wave Measurements	Hogan, GG, RD Chapman, G Watson and DR Thompson	IEEE Trans on Geosc and Rem Sens, Vol. 34, No. 2, pp. 532-542.
1996	A Low-Cost Space-Based Radar System Concept	Curry, GR	IEEE Aerospace and Electronic Systems Magazine, Vol. 11, No. 9, pp. 21-24.

1996	Multifrequency SAR Observation of a Ship Wake	Oumansour, K, Y Wang and J Saillard	IEE Proc Radar, Sonar and Navig, Vol. 143, No. 4, pp. 275-280.
1996	SAR Observations of Iinternal Wave Wakes from Sea Mounts	Cresswell, G, C Zhou, PC Tildesley and CS Nilsson	Marine and Freshwater Res, Vol. 47, No. 3, pp. 489-495.
1996	Ship Hull Characteristics from Surface Wake Synthetic Aperture Radar (SAR) Imagery	Griffin, OM, HT Wang and GA Meadows	Ocean Eng, Vol. 23, No. 5, pp. 363-383.
1996	Mystery Ship Detected in SAR Image	Liu, AK, CY Peng and Y-S Chang	EOS, Transactions, American Geophysical Union, Vol. 77, No. 3, pp. 17-18.
1996	RCS Studier av Skip og Sjø ved Bruk av RADARSAT	Waastad, H	Internal paper, SATOV-project, FFI/E.
1995	Neural Processing of Targets in Visible Multispectral IR and SAR Imagery	Waxman, AM, MC Seibert, A Gove, DA Fay, AM Bernardon, C Lazott, WR Steele and RK Cunningham	Neural Networks, Vol. 8, No. 7-8, pp. 1029-1051, 1995.
1995	Frequency and Azimuthal Variations of Radar Cross-Section and Their Influence Upon Low-Frequency SAR Imaging	Axelsson, SRJ	IEEE Trans on Geosc and Rem Sens, Vol. 33, No. 5, pp. 1258-1265.
1995	Polarimetric Calibration of SIR-C Using Point and Distributed Targets	Sarabandi, K, LE Pierce, MC Dobson, FT Ulaby, JM Stiles, TC Chiu, R Deroo, R Hartikka, A Zambetti and A Freeman	IEEE Trans on Geosc and Rem Sens, Vol. 33, No. 4, pp. 858-866.
1995	A New Look at Spotlight Mode Synthetic-Aperture Radar as Tomography - Imaging 3-D Targets	Jakowatz, CV and PA Thompson	IEEE Trans on Image Proc, Vol. 4, No. 5, pp. 699-703, May 1995.
1995	Clutter Statistics Along Edge Features in Synthetic-Aperture Radar Imagery	Caves, RG, PJ Harley and S Quegan	J of Electromag Waves and Appl, Vol. 9, No. 3, pp. 327-353.
1995	An Approach to Radar Imaging Using the Spherical Projection Density Concept	Elassad, S and I Lakkis	Annales des Telecommunications-Annals of Telecommunications, Vol. 50, No. 7-8, pp. 695-704.
1995	Assessing the Feasibility of a Vessel Monitoring System in the Western Pacific Pelagic Longline Fishery	Yamashita, S and G Hornhof	Draft Report forwarded by Robert Harman, NMFS, Honolulu, HI.
1994	Analysis of Marine Radar Image Spectra Collected During the Grand-Banks ERS-1 SAR Wave Experiment	Trask, J, M Henschel and B Eid	Atmosphere-Ocean, Vol. 32, No. 1, pp. 215-236.
1994	Detection of Whale Wakes with Synthetic-Aperture Radar	Radford, SF, RL Gran and RV Miller	Marine and Tech Soc J, Vol. 28, No. 2, pp. 46-52.
1994	Calibration of a Polarimetric Synthetic-Aperture Radar	Sarabandi, K	IEEE Trans on Geosc and Rem Sens, Vol. 32, No. 3, pp. 575-

	Using a Known Distributed Target		582.
1994	Detection of Moving-Objects with Airborne SAR	Daddio, E, M Dibisceglie and S Bottgalico	Signal Proc, Vol. 36, No. 2, pp. 149-162.
1994	Optimum Classification of Non-Gaussian Processing Using Neural Networks	Blacknell D and RG White	IEE Proc Vision Image and Signal Proc, Vol. 141, No. 1, pp. 56-66.
1994	On the Determination of Density Profiles in Stratified Seas from Kinematical Patterns of Ship-induced Internal Waves	Avital, E and T Miloh	J of Ship Res, Vol. 38, No. 4, pp. 308-318.
1994	Effect of Doppler Centroid Mis-Tracking on the Parameter Estimation of Point Target Complex Signals	Touzi, R and K Raney	IEEE Trans on Geosc and Rem Sens (IGARSS'94), Pasadena, California, USA.
1994	Generalizations of the Nonlinear Ocean-SAR Transform and a Simplified SAR Inversion Algorithm	Krogstad, HE, O Samset and PW Vachon	Atmosphere-Ocean, Vol. 32, No. 1, pp. 61-82.
1994	New Method for the Simulation of Correlated K-Distributed Clutter	Blacknell, D	IEE Proc Radar, Sonar and Navig, Vol. 141, No. 1, pp. 53-58.
1994	Radar Detection in K-Distributed Clutter	Conte, E, M Lops and G Ricci	IEE Proc Radar, Sonar and Navig, Vol. 141, No. 2, pp. 116-118.
1994	Comparison of Parameter Estimators for K-Distribution	Blacknell, D	IEE Proc Radar, Sonar and Navig, Vol. 141, No. 1, pp. 45-52.
1994	Hull Characteristics from SAR Images of Ship Wakes	Wang, HT, OM Griffin and GA Meadows	IEEE Trans on Geosc and Rem Sens (IGARSS '94), "Surface and Atmospheric Remote Sensing: Technologies, Data Analysis and Interpretation", Vol. 3, pp. 1278-1280.
1994	K-Distribution	Blacknell, D	IEE Proc Radar, Sonar and Navig, Vol. 141, No. 1.
1993	Target Detection in a Jamming Background in Partially Coherent Synthetic-Aperture Radars	Dorosinskiy, IG and SI Timoshenko	Telecomm and Radio Eng, Vol. 48, No. 8, pp. 74-78.
1993	Characterization of a Spatial Statistics of Distributed Targets in SAR Data	Rignot, E and R Kwok	Int J Rem Sens, Vol. 14, No. 2, pp. 345-363.
1993	2-Dimensional SAR Imaging Using Linear Arrays with Transverse Motion	Mahafza, BR	J of the Franklin Inst - Eng and Applied Mathematics, Vol. 330, No. 1, pp. 95-102.
1993	Modeling Short Sea Wave Energy-Distributions in the Far Wakes of Ships	Milgram, JH, RA Skop, RD Peltzer and OM Griffin	J of Geoph Res - Oceans, Vol. 98, No. C4, pp. 7115-7124.
1993	Suppression of Short Sea Waves in Ship Wakes - Measurements and Observations	Milgram, JH, RD Peltzer and OM Griffin	J of Geoph Res - Oceans, Vol. 98, No. C4, pp. 7103-7114.
1992	High-Resolution Measurement of Surface-Active Film Redistribution in Ship Wakes	Peltzer, RD, OM Griffin, WR Barger and JAC Kaiser	J of Geoph Res - Oceans, Vol. 97, No. C4, pp. 5231-5252.

1992	Extraction of Point Target Response Characteristics from Complex SAR Data	Touzi, R	IEEE Trans on Geosc and Rem Sens, Vol. 30, pp. 1158–1161.
1992	Remote-Sensing of Surface Ship Wakes	Perceival, RC, OM Griffin, RD Peltzer, AM Reed and RF Beck	Naval Eng J, Vol. 104, No. 4, pp. 122-123.
1992	SAR Ocean Image Decomposition Using the Gabor Expansion	Teti, JG Jr. and HN Kritikos	IEEE Trans on Geosc and Rem Sens, Vol. 30, No. 1, pp. 192-196.
1992	SAR ISAR Imaging of a Nonuniformly Rotating Object	Jain, A and I Patel	IEEE Trans on Aerosp and Elect Syst, Vol. 28, No. 1, pp. 317-321.
1992	Measurements of the Internal Wave Wake of a Ship in a Highly Stratified Sea Loch	Watson, G, RD Chapman and JR Apel	J of Geoph Res - Oceans, Vol. 97, No. C6, pp. 9689-9703.
1992	Low-Grazing Angle Radar Measurements of Ship Generated Internal Waves in Scotland 1989-1991	Ward, KD	Memorandum 4589, Defence Research Agency, Malvern, UK.
1992	Ship Traffic Monitoring Using the ERS-1 SAR	Wahl, T, K Eldhuset and Å Skøelv	Proc of the 1st ERS-1 Symp, pp. 823-828, Cannes, France.
1992	Inner Angle Wave Packets in an Unsteady Wake	Cao, Y, W Schultz and RF Beck	Proc of the 19th ONR Symposium in Naval Hydrodynamics, Seoul, Korea.
1992	Radar Detection of Targets Located in a Coherent K Distributed Clutter Background	Pentini, FA, A Farina and F Zirilli	IEEE Proc for Radar and Signal Processing, Vol. 139, No. 3, pp. 239-245.
1992	Detekterbarheten av Utvalgte Fenomener Over Sjø i Digitale ERS-1 Bilder	Andersen, T	Thesis, University of Oslo.
1992	Remote Sensing of Surface Ship Wakes	Griffin, OM, RD Peltzer, AM Reed and RF Beck	Naval Eng J, Vol. 104, pp. 245-258.
1991	SAR Application of a Signal Coding Technique for Single-Hit Measurement of the Target Scattering Matrix	Giuli, D and L Facheris	European Trans on Telecomm, Vol. 2, No. 6, pp. 675-688.
1991	Image Simulation of Geometric Targets for Spaceborne Synthetic Aperture Radar	Nasr, JM and D Vidalmadjar	IEEE Trans on Geosc and Rem Sens, Vol. 29, No. 6, pp. 986-996.
1991	Scattering Matrix Representation for Simple Targets	Van Zyl, JJ and FT Ulaby	Radar Polarimetry for Geosc Appl, chapter 2, pp. 17-50, The Artech House Remote Sensing Library.
1991	The Simulation of the SAR Image of a Ship Wake	Tunaley, JKE, EH Buller, KH Wu and MT Rey	IEEE Trans on Geosc and Rem Sens, Vol. 29, No. 1, pp. 149-156.
1991	The Detection of Ship Wakes in Remote Sensed Imagery	Cowderoy, RI and JG Jones	Conference, Defence Oceanology Int '91, Brigthon, UK.
1991	Estimation of Radar Detection and False Alarm Probabilities	Echard, JD	IEEE Trans on Aerosp and Elect Syst, Vol. 27, No. 2, pp. 255-260.

1990	Ship Trails and Ship Induced Cloud Dynamics	Porch, WM, CYJ Kao and RG Kelley	Atmospheric Environment Part A - General Topics, Vol. 24, No. 5, pp. 1051-1059.
1990	Wake Measurements	Lemche, V et al	North Atlantic Treaty Organization Defence Research Group, RSG.4 on Wake Measurements.
1990	Synthetic Aperture Radar Imaging of Ship Wakes in the Gulf of Alaska	Shemdin, OH	J of Geoph Res, Vol. 95, No. C9, pp. 16,319-16,338.
1990	Considerations of Uniqueness in the Inverse Kelvin Wake Problem	Kuhn, JC	SNAME, H-5 Panel, Analytic Ship Wave Relations, Meeting 90, Jersey City, NJ.
1990	Detailed Analysis of Spaceborne Synthetic Aperture Radar Images of Ship Wakes	Meadows, L and G Meadows	The University of Michigan, Ocean Eng Report, OEL-9004-DTRC-0001.
1990	Hybrid SAR-ISAR Imaging of Ships	Ward, KD, RJ Tough amd B Haywood	Record of the IEEE 1990 National Radar Conf, pp.64-69, Arlington, VA.
1990	SAR Imaging of Vortex Ship Wakes. Vol. III: An Overview of the Pre-ERS-1 Observations and Models	Skøelv, Å and T Wahl	FFI/Notat-90/7055, Norwegian Defence Research Establishment, Kjeller, Norway.
1990	Functional and Software Specification for a Model of the SAR Igamging of Turbulent Wakes	Waymont, DK and IOG Davies	Smith Associates Tech Proposal, TR-90/173/1.0.
1990	Hydrodynamics of Ship Wake Surfactant Films	Peltzer, RD, JH Milgram, RA Skop, JAC Kaiser, OM Griffin and WR Barger	Proc of the 18th Symposium on Naval Hydrodynamics University of Michigan, Aug 20-23, 1990.
1990	Hydrodynamics of Remotly Sensed Surface Ship Wakes	Reed, AM, RF Beck, OM Griffin and RD Peltzer	SNAME Trans., Vol. 98, pp. 319-363.
1989	A Workstation for the Fast Detection of Ships	Rye, AJ, FG Sawyer and R Sothinathan	Proc of IGARSS'90, pp. 2263-2266, Vancouver, Canada.
1989	A Proposal for the Simulation of the SAR Imaging of Turbulent Wakes Smith Associayes Technical Proposal	Davies, IOG and NR Bruke	Smith Associates Tech Proposal, TP-89/376.
1989	Synthetic Aperture Radar Imaging of Ship-Generated Internal Waves	Gasparovic, RF, DR Thompson and JR Apel	Johns Hopkins APL Tech Digest, Vol. 10, No. 4, pp. 326-331.
1989	Observations of a Nonlinear Solitary Wave Packet in the Kelvin Wake of a Ship	Brown, ED, SB Buchsbaum, RE Hall, JP Penthume, KF Schmitt, KM Watson and DC Watson	J of Fluid Mech, Vol. 204, pp. 263-293.
1989	The Radar Image of the Turbulent Wake Generated by a Moving Ship	Tunaley, KE, JR Dubois and JBA Mitchell	Proc of IGARSS'89.
1989	The Effect of the Ship's Screws on the Ship Wake and its Implications for the Radar Image of the Wake	Buller, EH and JKE Tunaley	Proc of IGARSS'89, Vol. 1, pp. 362-365, Vancouver, BC, Canada.

1989	Detection Performance in K-Distributed and Correlated Rayleigh Clutter	Hou, XY and N Moringa	IEEE Trans on Aerosp and Elect Syst, Vol. 25, No. 5, pp. 634-641.
1989	Radar Characterization of Ship Wake Signatures of Ambient Ocean Clutter Features	Shurman, SR	IEEE Proc of the National Radar Conference, pp. 3-8, Dallas, Texas, USA.
1988	A Survey of the Hough Transform	Illingworth, J and J Kittler	Computer Vision, Graphics, and Image Processing, Vol. 44, No. 1, pp. 87-116.
1988	Synthetic Aperture Radar Detection of Surface Ship Wakes	Lyden, JD, DR Lyzenga and RA Schuman	J of Geoph Res, Vol. 93, No. C10, pp. 12,293-12,303.
1988	Synthetic Aperture Radar Imaging of Surface Ship Wakes	Lyden, JD, RR Hammond, DR Lyzenga and RA Schuman	J of Geoph Res, Vol. 93, pp. 12,293-12,303.
1988	SAR Imaging of Vortex Ship Wakes. Vol. I: Basic Theory and Simulation in L-band Using Bragg Model	Skøelv, Å, T Wahl and SS Eriksen	FFI/Notat-88/9001, Norwegian Defence Research Establishment, Kjeller, Norway.
1988	Ship Detection Using the ASAR Instrument	Olsen, RB, T Wahl and K Eldhuset	FFI.
1988	Wakex 86, A Ship Wake/Films Exploratory Experiment	Kaiser, JAC, SE Ramberg, RD Peltzer, MD Andrews and WD Garrett	NRL Memo Report 6270.
1988	Ship Wave Modification by a Surface Current Field	Griffin, OM	J of Ship Res, Vol. 32, No. 3, pp. 186-193.
1988	WAVEAMP: A Program for Computation of Wave Elevations Created by a Ship Travelling at a Constant Speed	Fotis, A	Tech Rep No. 88-03, Department of Naval Arch and Marine Eng, University of Michigan, Ann Arbour, Michigan.
1988	Theory of Radar Backscatter from Short Waves Generated by Ships, with Application to Radar (SAR) Imagery	Milgram, JH	J of Ship Res, Vol. 32, pp. 54-69.
1988	Generation of K-Distributed Random Variables	D'Addio E, S Giannatempo and G Galati	Trans of the Soc for Computer Simulations, Vol. 5, pp. 159-174.
1988	SAR Imaging of Vortex Ship Wakes. Vol. II: Simulation in L- and C-Band Comparing the Bragg and HSW Imaging Models	Skøelv, Å, T Wahl and SS Eriksen	FFI/Notat-88/9001, Norwegian Defence Research Establishment, Kjeller, Norway.
1987	Generalized K Distribution: A Statistical Model for Weak Scattering	Jakeman, E	J of Optical. Society of America A: Optics, Image Science, and Vision, Vol. 4, No. 9, pp. 1764-1772.
1987	SAR Imaging of Ship Wakes in the Gulf of Alaska	Shemdin, OH	Report, JPL/Ocean Res and Eng, Pasadena, CA, USA.
1987	Numerical Simulation of the Wake Downstream of a Twin-	Swean, TF Jr	Naval Res Lab Memorandum Report 6131, 41 p.

	Screw Destroyer Model		
1987	A Remote Sensing Study of a Surface Ship Wake	Peltzer, RD, WD Garrett and P Smith	Int J Rem Sens, Vol. 8, No. 5, pp. 689-704.
1987	Radar Detection Prediction in K-Distributed Sea Clutter and Thermal Noise	Watts, S	IEEE Trans on Aerosp and Elect Syst, Vol. 28, No. 1.
1987	Imaging Radar Polarization Signatures: Theory and Observation	Van Zyl, HA Zebker and C Elachi	Radio Science, Vol. 22, pp. 529-543.
1987	Phenomenological Theory of Radar Targets	Huynen, JR	PhD Thesis, P.Q. Research, Polarimetric Quest, Los Altos Hills, CA, USA.
1986	SAR Detection of Ships and Ship Wakes	Wahl, T, K Eldhuset and K Asknes	SAR Applications Workshop (ESA Special Publication SP-264), p. 61, Paris, France.
1986	Ship Wake Detection in Speckle Noise Using a Modified Hough Transform	Wilmut, MJ and RF MacKinnon	Proc of the Tenth Canadian Symp on Rem Sens, Edmonton, Alberta.
1985	Analysis of Seasat Revolution 407 Ship Wake Data	Lyden, JD	Topic Report 155900-32-T, ERIM, MI.
1985	Analysis of Narrow Ship Wakes in the Georgia Strait SAR Data	Lyden, JD, DR Lyzenga, RA Schuman and ES Kasischke	Topic Report 155900-20-T, ERIM, MI.
1985	Correlated K-Distributed Clutter Models	Oliver, CJ	Optica Acta, Vol. 32, No. 12, pp. 1515-1547.
1985	Mechanisms and Models of Narrow-V Wakes	Witting, JM and R Vaglio-Laurin	ORI Inc Tech Report 2529, 120 p.
1984	Surface Signature of Ship-Generated Internal Waves	Liu, AK, DA Berge and SR Borchardt	Rep DT-8311-01, Dyn Technologies, Torrance, CA, USA.
1984	White-Water Wake Characteristics of Surface Vessels	Peltzer, RD	NRL Memo Report 5335.
1984	The Radon Transform and Its Properties	Durrani, TS and D Bisset	Geophysics, Vol. 49, No. 8, pp. 1180-1187.
1984	Radar Observability of Ship Wakes	Swanson, CF	Cortana Corporation Report. Falls Church, VA, USA.
1983	SAR Ship Wake Signatures	Schuman, RA, ES Kasischke, DR Lyzenga and A Klooster	Topic Report 157700-1-X, ERIM, MI.
1980	On the Statistics of K-Distributed Noise	Jakeman, E	J of Phys America: Mathematical and General, Vol. 13, pp. 31-48.
1979	A Point Target Model for the Synthetic Aperture Radar Detection Ships and Ice Conditions During a Swell	Evans, DD	IEEE Trans on Antennas and Propagation, Vol. 27, No. 1, pp. 30-34.
1978	Object Detectability in Speckle Noise	Christensen, CR	Int Conf on Lasers, pp. 637-645, Orlando, Florida.

1978	Phenomenological Theory of Radar Targets	Huynen, JR	Electromagnetic Scattering, Uslenghi, PL (ed), New York: Academic.
1977	On the Detection of Structures in Noisy Pictures	Cohen, M and GT Toussaint	Pattern Recognition Letters, Vol. 9, pp. 95-98.
1973	An Empirical Formula for the Radar Cross Section of Ships at Grazing Incidence	Skolnik, MI	IEEE Trans on Aerosp and Elect Syst, Vol. 10.
1971	A Ship's Wave and Its Wake	Peregrine, DH	J of Fluid Mech, Vol. 49, pp. 353-360.
1971	On Ship Wave Pattern and Their Spectra	Tuck, EO, JL Collins and WH Wells	J of Ship Res, Vol. 15, pp.11-21.
1971	Synthetic Aperture Imaging Radar and Moving Targets	Raney, RK	IEEE Trans on Aerosp and Elect Syst, Vol. 7, pp. 499-505.
1970	Turbulent Energy Balance and Spectra of the Axisymmetric Wake	Uberoi, MS and P Freymuth	Physics of Fluids, Vol. 13, No. 9, pp. 2205-2210.
1967	Radar Resolution of Moving Targets	Rihaczek, AW	IEEE Trans on Information Theory, Vol. 13, pp. 51-56, Jan 1967.
1960	On Kelvin's Ship Wave Pattern	Ursell, F	J of Fluid Mech, Vol. 8, pp. 418-432.
1946	Physics of Sound in the Sea, Part IV - Acoustic Properties of Wakes	National Defense Research Committee Division 6	Summary of Tech Report Vol. 8.
	Fast Curve Estimation Using Preconditioned Generalized Radon Transform	Hansen, KV and PA Toft	IEEE Trans on Image Proc, Vol. 5, No. 12, pp. 1651-1661, Dec 1996.

3.2 Detection of point targets in ScanSAR data (In Norwegian) (158)

The thesis uses ScanSAR to analyse point targets. It adds new knowledge about radar satellites, as well as giving good advice on ENVISAT's possible user areas. Based on earlier work at the Norwegian Defence Research Establishment (Forsvarets Forskningsinstitutt - FFI), a threshold value of 10 dB (higher than the value for the sea clutter) is suggested to be a reasonable value for ship detection in radar satellite images with more than 3 looks. To be able to find the accurate threshold for a specific false alarm rate, it is necessary to estimate the speckle probability for the specific image.

A surface, which is rough for one radar beam, might be specular for another beam. The Rayleigh criterion gives the condition for a smooth surface:

$$h < \frac{\lambda}{8\cos\theta} \tag{3.1}$$

h is the height of the surface variations, while θ is the radar's incidence angle. ENVISAT operates in the C-band with a wavelength of 5.62 cm. The incidence angle varies between 18° and 44°. A surface will appear as rough if the surface variations are more than approximately 0.7-1.0 cm. Thus, the ocean will almost always appear as a rough surface when using radar.

Skolnik's equation shows how the radar backscatter (in square meters) depends on the ships weight displacement in tons:

$$\sigma_{ship}\left[m^2\right] = ship's\_displacement\left[tons\right] \tag{3.2}$$

The equation doesn't give correct values when it is used on radar satellite images, which indicates that ships reflect more than what is believed from the equation. The RCS (Radar Cross Section) value is larger for larger incidence angles. Oceangoing fishing vessels have larger weight displacement compared to the ship's length than navy vessels. Vachon's equation seems to give the minimum value for the ship's length or expected RCS value for a ship, where D is the ship's displacement in tons and l is the ship's length in meters:

$$\sigma_{ship} \equiv D = 0.08048 \cdot l^{2.31} \approx 0.08 \cdot l^{7/3} \tag{3.3}$$

A ship's RCS depends on the following parameters:

- Whether the ship is fully loaded or not (especially if the ship is oriented with the long side towards the satellite and is situated far away from the satellite in the range direction.
- Ship's orientation
- Ship's building materials
- Ship's 3D structure

- Ship reflectors coherence
- Multi reflection (including the sea surface)

Fishing boats are harder to detect due to their size. The radar reflection is largest when the ship has its long side towards the radar. The radar reflection is considerable smaller with greater angle of attack (α = 90° - θ). Ships situated far away in the range direction give a larger RCS compared to the situation where the ship is situated closer to the satellite in range direction. Vachon's additional equation seems to give the average value or expected value for a ship. *R* is the ratio between measured and expected value of the RCS, while θ is the incidence angle in degrees, $\theta \in [15°,45°]$:

$$R(\theta) = 0.78 + 0.11\theta \tag{3.4}$$

The equation shows that ships far away from the satellite in the range direction give larger measured RCS value in the image. Variation in the average value, which is measured to be 6 dB, may be caused by the variations in the incidence angle. Because of the changes in the assumptions in Vachon's equation, it is expected to be able to detect smaller ships in the radar images than expected earlier.

If the sea surface is almost still, RADARSAT-1's S5 mode has a limit of detection of approximately 20-25 meters, while the F5 mode seems to be the best for ships around 8 meters. ENVISAT has better possibilities to detect ships than RADARSAT-1's HH-polarization, but RADARSAT-1 has better solution between resolution, incidence angle and swath width. ENVISAT's modes IS3, IS4, IS5, IS6 and IS7 are expected to give reliable detection of ships with length larger than 50 meters in HH-polarization in wind speeds up to 10 m/s. The SS3, SS4 and SS5 modes are best in the Wide Swath mode. These are expected to be able to detect clusters of ships with approximate lengths of about 55-60 meters in HH-polarization and wind speeds up to 10 m/s, if the data is processed with 3-look in azimuth and one in range.

Two new non-linear models relating ship length to displacement are investigated. The first model has the form:

$$D = \alpha l^{\beta} \tag{3.5}$$

while the second model has the following form:

$$D = (\alpha + \beta l)^2 \tag{3.6}$$

The investigation concluded that there is no general relationship between displacement and a ship's length for an arbitrary vessel. When *a priori* knowledge about the vessel target is not available, the relationship (3.5) is as follows:

$$D = kl^2, \quad k \in \langle 0.27, 0.60 \rangle \tag{3.7}$$

When *a priori* knowledge is available that the vessels are military navy vessels, the constant k is defined as $k \in \langle 0.27, 0.30 \rangle$. When *a priori* knowledge is available that the vessels are ocean going fishing vessels, the relationship is given by:

$$D \in \langle 0.25 l^{2.1}, 0.60 l^{2} \rangle \tag{3.8}$$

Vachon's equation is useful as a simple and general formula to give rough estimates, and the formula (3.7) should also be taken into account. Model 2 seems to give better correlation than model 1 for larger data sets.

The results when using the two models on different data sets are given in Table 3.1 and Figure 3.1. Formula (3.5) holds well for all cases, while model 2 (3.6) gives a slightly better correlation for the total data set.

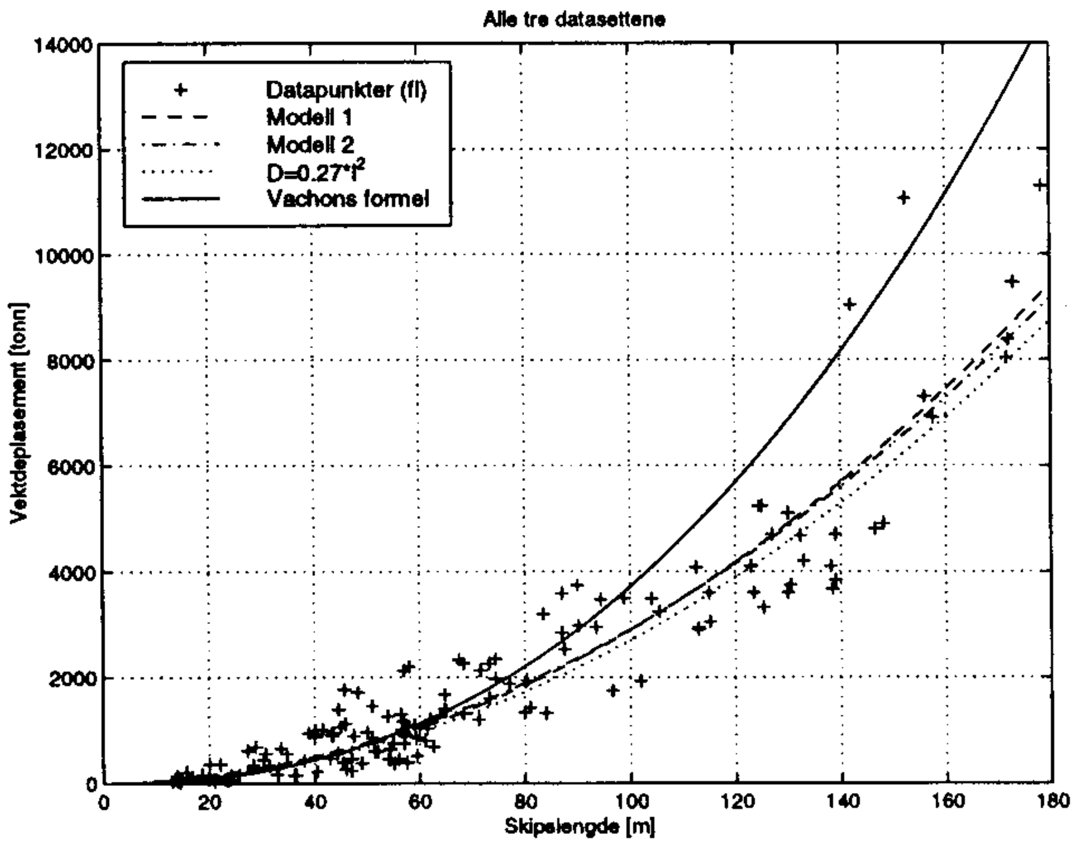

Figure 3.1 Model relationships between ship length and displacement for all three data sets.

Data set	Model	α	β	Correlation
A	1	0.08	2.31	0.9850
	2	0.19	0.55	0.9769
B	1	0.64	1.98	0.9649
	2	0.38	0.76	0.9598
C	1	0.07	2.31	0.9512
	2	0.56	-2.64	0.9529
Combined	1	0.27	2.01	0.9257
	2	1.65	0.52	0.9478

Table 3.1 Summary of data sets

3.3 Detectability of selected phenomena over the ocean in digital ERS-1 images (In Norwegian) (96)

FFI has developed an automatic algorithm for detection of ships and wakes in high resolution SAR imagery. The algorithm is mainly developed for use in open sea and near land. Due to the noise in the images, low-resolution images have shown advantages for detection of some phenomena. Possibilities for detection of icebergs, oil spills and ships in low-resolution images are studied. The analysis, as well as visual inspection of the ERS-1 scenes, broadens the knowledge for detection of the objects. Automatic detection in low-resolution imagery requires low wind speeds. The scattering distribution function for dark sea is low, and this will give sufficient contrast for a good segmentation result. In the vicinity and within the ice edge, the assumptions for the FFI algorithm may change due to the change of possible wakes. A description of wakes close to the ice edge compared to FFI's ship detector is also given.

3.4 Hull Characteristics from SAR Images of Ship Wakes (272)

The paper presents how SAR images of ship wakes can be used to obtain estimates of the Kelvin wake amplitude function ($A(\theta)$), ship speed (V), and ship heading (α). The Fourier transform (Z) of the ship's Kelvin wakes can be used to get the information. This information can be used to derive additional information about the hull characteristics. The distance between two successive peaks (or valleys) of $A(k_x)$, with $\Delta k_x \approx 2\pi/L$, is used to estimate L. The relation is given in terms of the fundamental wave number, k_0:

$$\frac{\Delta k_x}{k_0} = \frac{\lambda_{0x}}{L} = \frac{2\pi U^2}{gL} = 2\pi Fn^2 \tag{3.9}$$

Fn is the Froude number. The Fourier transform of the magnitude of the slope amplitude function $|kA(k_x/k_0)|$ is used to estimate the ship length (L) instead of $|A|$ since it tends to enhance the dominant wake length scale. The accuracy increases with the longitudinal symmetry of the hull and the Froude number, Fn.

Using *A*, *L*, and the draft, *H*, the HULINV code can be used to calculate offsets $\zeta(x,z)$ for a general hull such as the WC (Wigley-Cosine). HULINV code is short for Hull Inversion code, and was developed at the University of Michigan by Wu (1991). The ship's volume can also be calculated from the information.

3.5 Instrumented Ship Imaging Using the AN/APS-506 Spotlight SAR System (154)

The paper describes the AN/APS-506 Spotlight Synthetic Aperture Radar System that has been developed by the Canadian Department of National Defence. An ocean-going ship was instrumented with motion sensors, and high-resolution data sets were collected using the radar from a full range of aspect angles. Imagery collected during the trial is presented, and key aspects to be able to obtain good ship imagery for very high-resolution airborne radar systems are described. The paper also presents the unique aspects of the AN/APS-506 Spotlight SAR system. It is a significant improvement over the existing capabilities of the CP-140, because it allows the operator to classify at long range as combatant or non-combatant. It is also a very useful tool to classify small ships.

3.6 K-Distribution (105)

Parameter estimation is necessary when analysing coherent imagery such as SAR images. Parameter estimation makes it possible to characterise the statistical properties of homogenous regions for use in segmentation and target detection algorithms. K-distribution can be used to model the statistics of the SAR imagery, and this paper presents methods for estimating the parameters of the K-distribution. The K-distribution for a given radar signal X is given by:

$$p_X(I) = \frac{2}{I\Gamma(\nu)\Gamma(L)}\left(\frac{L\nu I}{\langle I\rangle}\right)^{(L+\nu)/2} K_{L-\nu}\left\{2\sqrt{\frac{L\nu I}{\langle I\rangle}}\right\} \tag{3.10}$$

where $p_X(I)$ is the probability distribution function for the image intensity *I*, *L* is the number of effective independent looks, Γ is the gamma function, and $K_{L-\nu}(z)$ is the modified Bessel function of order L-ν. ν is an order parameter for the distribution that defines the skewness and shape of the tail. Thus, it is important to obtain a good estimate for this parameter to be able to set a proper threshold. Above this threshold, detected pixels will be expected to belong to a different population with a given probability.

The estimation errors of three moment-based estimation schemes are compared with the maximum likelihood estimation errors (calculated from the Cramer-Rao lower bound) in the paper. These methods are alternatives to the Maximum Likelihood (ML) estimates that only can be calculated by cumbersome numerical techniques.

Based on the comparison, recommendations are given on the number of looks and which parameter estimation scheme that is best to use. The goal is to obtain near optimum estimation performance without being forced to do cumbersome numerical evaluations of the ML solution. An estimator based on the Mean and the Variance of the data gives large errors, while an estimator based on the Mean of the data and Mean of the Log (MML) is almost optimum.

3.7 Kelvin and V-like ship wakes affected by surfactants (289)

The paper presents a study of ship-generated wakes and their Radar Cross Section (RCS) in SAR images. Ship wakes in light wind and calm sea conditions often appear as a bright V with a half-angle of 2 to 3 degrees. The Bragg scattering mechanism has been used as a basis to explain this phenomenon. It is believed that the narrow V-wake is not a part of the Kelvin wake. Alternatively, it is suggested that short divergent Kelvin waves may contribute to the V-wake, even though the waves are mixed with unsteady surface waves, which are generated by ship-induced turbulence.

A single layer of hydrodynamic singularities represents the hull of the ship. The Green function of a point target moving below a free surface covered by surfactants is derived. A closed-form asymptotic solution for the far ship wake is obtained by isolating the steady Kelvin waves from the unsteady waves. The corresponding RCS is calculated analytically using the closed-form asymptotic solution. The paper also discusses the radiative, viscous and surfactant-induced decay of the V-wake brightness along the arms of the V-wake. Experimental data is used to compare the theoretical results. The amplitudes of the short divergent waves do not depend on the specific form of the submerged portion of the ship. The amplitudes are larger for ships with fuller waterline. The decay of the RCS is weak and the V-wake becomes very persistent for relatively large values of the resolution cells. Increasing the ship's speed increases the RCS strongly and leads to a narrower V-form. Both arms of the V-wake can be visible for several kilometres in calm water, azimuthal directions and for favourable SAR parameters. It seems that the complex V-wake phenomenon is a result of the Bragg scattering from a sea surface with many waves, which is disturbed by breaking waves, the steady Kelvin waves and the ship-induced turbulence.

3.8 Neural Processing of Targets in Visible Multispectral IR and SAR Imagery (277)

The paper describes the design and implementation of computational neural systems for target enhancement, detection, learning, and recognition. Multispectral infrared and SAR imagery have been used. The following motivates the system architecture:

- Designs of biological vision systems.
- Drawing insights from retinal processing of contrast and colour.
- Occipital lobe processing of shading, colour, and contour.
- Temporal lobe processing of pattern and shape.

The paper also describes how discrimination among similar targets and accumulation of evidence across image sequences are done. It also shows how 3D target learning and recognition from visible silhouettes and SAR return patterns are related. Models of contrast enhancement, contour, shading and colour vision can aid target detection by enhancing targets in multispectral IR and SAR imagery.

3.9 Nonuniform Azimuth Image Shift Observed in the Radarsat Images of Ships in Motion (207)

The paper describes nonuniform azimuth image shift of a rigid body, focusing on cruising ships, observed in RADARSAT-1 SAR images. The different slant-range velocities of coherent scatterers across the hull associated with the ship motions cause the phenomenon. The identified ship in a SAR image is used to estimate the slant-range velocity. Then the velocity is compared with the velocity computed from the STF (Salvesen-Tuck-Faltinsen) numerical model using the ship's specification in addition to meteorological data. The pitching motion of the ship is the dominant factor in the nonuniform image shift. The results are in good agreement when compared with the wave orbital velocity. Yawing contribution to the velocity cannot be ignored even though it is found to be small. Reasonable agreement is also obtained when comparisons are made between the SAR-derived slant-range velocities of two unknown ships and the wave orbital velocities. One of the ships investigated exhibits image skew in addition to the nonuniform shift, which may be caused by the rolling of the ship. Taking into account rolling in addition to pitching gives a closer fit to the observed skew. Without knowing the ship's specification, the exact cause of the skewing is not certain.

3.10 Observation of Long Waves Generated by Ferries (201)

The paper presents analysis of ship wakes in the San Francisco Bay. Many wakes from high-speed ferries make long waves that are apparently travelling ahead of the boat. They display all the properties of solitons, and are much longer than the waves that make up the Kelvin-wake. For this reason they might be better for spaceborne detection of ship wakes. The measurements are done with an apparatus for measuring current speed designed and built by the San Francisco State University (SFSU). A 200 MHz carrier phase-modulated with a pseudo-random binary sequence is used, which makes it possible to measure the water motion by timing the propagation of ultrasound signals.

One group of waves that has been observed is the usual Kelvin wakes (large waves) with amplitude up to 0.3 m/s and periods of 4 to 6 seconds. The other group with periods of 30 to 40 seconds arrives well before the Kelvin wake, and sometimes before the boat. There are several features separating these wakes from the Kelvin wakes. The wake's propagation velocities are supercritical (exceeding $\sqrt{gh}$), and they lack dispersive effects, which is characteristic of solitons. It is believed that non-linear effects cancel dispersion to produce solitons continuously emitted in the direction of the boat's motion. The long waves are absent for the ferries travelling northwards through deeper water. For the ferries travelling southward, the waveform varies considerably. To understand these features completely, more direct observations of current distributions, consideration of bathymetry, speed and course of the boat, hull type as well as tidal motion and vertical stratification are required. Spaceborne SAR has before been tested for detection of wakes of ocean-going ships and internal waves in the ocean. SAR observations sensitive to suppression of surface waves due to velocity strain is the most promising method to observe this type of wake. By approximating the velocity wave, the velocity strain corresponding to the solitons observed can be found.

3.11 Ocean Surveillance with Polarimetric SAR (286)

The Aurora CP-140 patrol flights and naval ship reports have historically been used by the Canadian Department of National Defence (DND) to provide surveillance over Canadian waters. RADARSAT-1 and ENVISAT, as well as the future RADARSAT-2 can be used for ship detection applications. ENVISAT has the possibility of dual polarization, while RADARSAT-2 will give quad-polarized SAR modes, which make it possible to get information about a target's structure.

The paper presents two studies: Target to Clutter Ratio (TCR) studies and a ship detection study using polarimetric methods. Polarimetric image data from the sea trial acquisitions MARCOT'98 (Maritime Command Coordinated Operational Training) and CRUSADE'00 have been used. It is shown that target decomposition methods for polarimetric data are suitable for both detection and classification applications, as well as providing information about the scatterer's physical structure. The TCR study indicates that the HH and HV channels are more optimal for ship detection applications for incidence angles >45° and <45° respectively. This gives useful information when choosing polarization combination on ENVISAT and on the future RADARSAT-2.

Polarimetric methods improve the ship detection capabilities compared to single channel results. A method developed by Van Zyl discerns from polarimetric data, whether the received backscattered data has bounced of an odd, even or several number of times. The data that doesn't fit any of these categories is considered unclassified. The other method, the Cameron method, detects an elemental scatterer, or primitive, based on the physical scattering mechanism associated with the image backscatter. The five elemental scatterers: cylinder, dihedral, narrow diplane, quarter wave, and dipole primitives (derived from the method) are studied. This method is a very robust target detection method for the maritime environment, and it provides structural information, which is suitable for classification. Both decomposition methods reject false alarms quite well. Buoys were discriminated from the ships, and this is important for automatic ship detection capabilities. The Cameron method showed promising results for ship classification, and the classification was used to discern false targets successfully from the data set. Data from the CRUSADE Trial indicates that some aspects of a ship may be possible, but this requires further investigation. It is also shown that saturated signal data degrades the polarimetric detection rates.

3.12 On the Use of Complex SAR Image Spectral Analysis for Target Detection: Assessment of Polarimetry (249)

The paper describes how the magnitude and the phase of polarimetric SAR imagery can be used for point target detection and analysis. An analysis is first done on a Single-Look Complex (SLC) image, which is a single polarized radar image. The image included point targets embedded in clutter. The inherent speckle effects are analysed by generating a number of sub looks in azimuth and range from the SLC image. The paper defines the 2-Looks Internal Hermitian Product (2L-IHP), which qualitatively increase the TCR. The derivation of the 2L-IHP includes spectral whitening, generation, and overlapping sub looks. The processing of azimuth and range spectra before the derivation is also described. To be able to model the point target behaviour, a simulation tool is developed. The way the method has been used has several limitations:

- The IHP works properly only if the target response remains constant in magnitude and phase throughout the whole illumination time.
- The performances of the algorithm could not be quantified accurately, because the ground data was too poor.
- Only fully developed speckle was considered.
- Only airborne SAR data was used, which gives better spatial resolution and TCR than spaceborne SAR data.

The paper also proposes a polarimetric extension of 2L-IHP, and defines the optimised polarimetric 2L-IHP. The polarimetry enhances the detection capabilities, and provides additional information for target analysis compared to single polarization. Ship detection, mapping of permanent scatterers in interferometry, and mapping of stationary point targets in radar grammetry are possible applications.

3.13 On the Use of Polarimetric SAR Data for Ship Detection (256)

The paper investigates the polarization information for ship detection by using polarimetric SAR images from the airborne Convair-580. The data set is collected off the Nova Scotia coast in Canada, Polarimetric signatures of ships are analysed for incidence angles between 45º and 70º. At incidence angles lower than 45º, circular polarization is better suited, because the ocean backscattering is mainly dominated by specular scattering. The ocean signature and the ship response are both low at HV-polarization. VV-polarization provides best information on the sea state, and more ships are missed at this polarization. HH-polarization gives the best TCR at grazing angles, out of the three classical polarization channels HH, VV and HV. The TCR starts to be significant at incidence angles larger than 55º. The radiometric information from the three channels does not provide enough information for ship detection. The detection methods, which are based on the thresholding decision over the sea clutter K-distribution, are also limited.

The polarization entropy improves the TCR for incidence angles up to 60º, because the Bragg ocean mechanism has lower entropy compared to the ship's polarization entropy. The ships can hardly be seen in HH-polarization. The efficiency of the polarization entropy is reduced at larger incidence angles, because the increasing heterogeneity of the ocean scattering mechanism. RADARSAT-2, which has the capability to use full-polarized data, will improve ship detection capabilities provided that the modes are well calibrated.

To validate the method at lower incidence angles (20º- 40º), other campaigns will be done with the Convair-580. Tests will be performed for different types of ships with different orientations in varying wind conditions.

3.14 Optimization of the Ocean Features Workstation for Ship Detection (115)

The paper presents how the use of the Ocean Features Workstation (OFW) for ship detection can be optimized. It is designed for unattended analysis of RADARSAT-1 ocean scenes. Ship detection is a focal point of most OFW operations. The final goal for the workstation is also to be able to extract wind speed and direction, calculate two dimensional wave spectra, as well as detection and classification of ocean surface features such as fronts, slicks, and eddies. The limitations using the K-distribution based ship detection algorithm (81) were demonstrated while using the OFW during the MARCOT'97 military exercises (83). The limitations are due to: 1) the hardware and beam table parameters on board RADARSAT-1, 2) the processing algorithms and resultant outputs from the Canadian Data Processing Facility (CDPF), and 3) the OFW itself. One solution that minimizes the problem is to carefully select some parameters within the OFW. Modifications to the CDPF and the OFW will also improve the use of the OFW. The report presents five recommended separate OFW configuration files for different combinations of beam mode and product type.

3.15 Orbital SAR Simulator of Fishing Vessel Polarimetric Signatures Based on High Frequency Electromagnetic Calculations (193)

A preliminary numerical simulator able to simulate the full-polarimetric raw data for a given orbital SAR system from a realistic vessel model was presented in (192). This paper presents applications of the simulator. Using the simulator, it is possible to construct a precise database of vessel signatures, which can be used to develop classification algorithms. Determination of system parameters of a future SAR sensor that will be used for ocean monitoring is also an important application of the simulator. Validation tests and development of new improvements of the simulator are also presented. The improved simulator is more realistic with respect to the vessel speed and the rotation of the vessel during acquisition due to sea state. Verifications of the accuracy on the reconstruction of point targets and the correct polarimetric behaviour of the simulator have been done.

3.16 Results from the Crusade Ship Detection Trial: Polarimetric SAR (287)

The experiment presented in the paper is performed offshore of Newfoundland's coastline in Canada in March 2000. It assessed ship detection capabilities for several radar systems. Image data was collected over a period of ten days from:

- RADARSAT-1
- Polarimetric C/X SAR at Cape Race, Newfoundland
- High Frequency Surface Wave Radar (HFSWR) also at Cape Race

Three ships remained on site at specified positions during the entire period. The extensive data set included 60 PolSAR (Polarimetric Synthetic Aperture Radar) images. The results indicate that dual use of HH- and HV-polarization is efficient for wide area ship detection applications. 96 % (67 out of 70) of the ships were detected by using a moment analysis (4^{th}) method. Even a 20 m wooden hull vessel was detected. Polarimetric target decomposition methods indicated that false target discrimination is more robust with PolSAR data compared to single channel data. The results also indicate capability for recognition of ships.

3.17 SAR Detection of Ships and Ship Wakes (269)

The paper presents some results obtained using spaceborne SAR for detection of ships and ship wakes in an ESA contract study in 1996. Analyses have been done on more than 200 ship wake appearances in Seasat images. An example of an image from the English Channel shows that the dominant wake feature is the dark turbulent wake. Some Kelvin arms can also be seen. Two of the wakes showed interesting features. They both have one bright and one dark Kelvin arm displaced in azimuth, and the opening angle is much less than the predicted angle (2 x 19.5°). The turbulent wakes typically persist for about 7 minutes assuming typical ship speed of 8 m/s. Wind speeds of about 4-5 m/s are very favourable for wake imaging, while no wakes were reported in Seasat images at wind speeds greater than 10 m/s. The visibility of the wakes depends on the environmental conditions, radar wavelength, and resolution.

Some digital techniques for detection and analysis of wakes are presented. There are several ways to determine a ship's speed and direction of motion. ERS-1 data have been used in the experiment.

3.18 SAR Imaging of Vortex Ship Wakes. Vol. I: Basic Theory and Simulation in L-band Using Bragg Model (247)

The report describes a numerical simulation scheme for detection of ship wakes, which is able to model SAR imaging of different current-induced ocean phenomena. The simulations of ship wakes are performed in the L-band using the Bragg model. Parameters describing the wind and wave environment, ship and SAR characteristics, as well as grid sizes and spacing could be varied in the model. Even though the spatial resolution is 25 m, useful information can be inferred from the following scene parameters:

- Number of ship pixels
- Length of ship
- Spatial distribution of strong scatterers on board the ship
- Direction of motion
- Velocity
- Wake length
- Wake width
- Wind measurements or forecasts
- Wake measurements or forecasts

The model has many shortcomings. The ship is assumed to have constant velocity parallel to the satellite's flight direction, which is not always the case. The size and hull form of the ships and the weather conditions may not be constant in a real SAR image. The Bragg waves have no azimuth component, because it is assumed that the wind blows in range direction. Axial flow and initial circulation are not included. The model can be useful as a first attempt to model the wake imaging mechanisms for ships not moving in the range direction. The results from the simulations are compared with empirical wake data obtained from Seasat SAR images, and the model gives reasonable values.

3.19 SAR Imaging of Vortex Ship Wakes. Vol. II: Simulation in L- and C-Band Comparing the Bragg and HSW Imaging Models (248)

The report describes two imaging models used to simulate SAR imaging of ship wakes in L- and C-band. The first model is the naive Bragg model and the second is the HSW model, which includes contributions from the full ocean wave spectrum. Holliday et al proposed the HSW model in 1986 (16). Parameters describing the wind and wave environment, ship and SAR characteristics, as well as grid sizes and spacings could be varied in the model. Results using the HSW model showed that the Bragg resonant component is the main contribution to the radar backscatter in L-band.

The rest of the backscatter comes from longer waves, and increases with increasing wind speed, because the significance of tilting and quasi-specular effects increase with increasing wind speed. This fraction is larger for the C-band frequency (in accordance with the HSW model). The turbulent wakes are as visible in C-band as in L-band.

Results indicated that the naive Bragg model is not always enough to fully describe the radar backscatter mechanisms. Using C-band, the model breaks down. Increasing wind speed decreases the peak values of the bands. A complete parameter study was not possible due to the extensive amount of CPU time needed to run the program.

Two shortcomings of the simulation model, in addition to the ones described in (320) are 1) that velocity bunching is not included in the HSW model and 2) that each wave packet that crosses the wake is treated as it is experiencing a “frozen” current profile.

3.20 SAR Imaging of Vortex Ship Wakes. Vol. III: An Overview of the Pre-ERS-1 Observations and Models (246)

The report presents an overview of the pre-ERS-1 observations and models. It describes the various turbulent wake observations, including previously not discussed Seasat SAR scenes, amateur photos of wakes behind different sized ships, as well as results from the 1988 NORCSEX (Norwegian Continental Shelf Experiment) campaign at Haltenbanken. Three models make a complete simulation scheme for the SAR imaging of turbulent wakes: 1) a model for the generation and development of the surface currents behind the ship, 2) a model for the wave-current interaction, and 3) a radar backscatter model. Requirements for a complete turbulent wake model are also discussed. Analyses are done to see to what extent the qualitative implications of the various models are consistent with the empirical data available. Finally, conclusions for ERS-1 applications are presented.

3.21 Satellite SAR Simulator for Fishing Vessels Signature Studies (191)

The paper presents a satellite SAR simulator for detection of fishing vessels, which is a modified version of the RCS prediction code developed at the Universitat Polytècnica de Catalunya (UPC). The characteristics of the chirp radar as well as the orbit of the satellite are taken into account. Commercial computer-aided-design with a high degree of detail and fidelity has been used, which makes it possible to generate the vessel models. The SAR simulator can be used to calculate the full-polarimetric raw data. Based on polarimetric decompositions, it is possible to develop vessel classification algorithms. The simulator can also be used to simulate existing or new sensors to study its limitations and applications for vessel classification.

3.22 Sea Surface and Ship Observation with MEMPHIS(111)

The mmW radar MEMPHIS of FGAN-FHP has been used to measure many scenes in SAR geometry. The purpose of the research presented in the paper was to investigate the ability of SAR to detect natural and manmade disturbances on the water surface. The scattering mechanism on the sea surface showed significant scattering on two frequencies that were used, 35 GHz and 94 GHz. The dominant interaction can be modelled by the Bragg resonance at 35 GHz, but this is not valid at 94 GHz. Changes in the local incidence angle due to modulations of spectral components (whose wavelength are not compatible with the Bragg criterion) are important at 35 GHz, and even more important at 94 GHz. Thus, special care should be taken when the upper mm-wave radar bands are considered for applications of indirect signatures on the sea surface, for example ship wakes or oil spill.

3.23 Ship Detection Performance Predictions for Next Generation Space borne Synthetic Aperture Radars (244)

The thesis focuses on the strong and weak points of using Synthetic Aperture Radar (SAR) for ship detection. Spaceborne radars will have a main role in ship detection for civilian and military purposes in the future. The well-known and reliable ship detection model by Vachon et al in 1997 is tested in the Canadian Ocean Monitoring Workstation as well as in some validation field programs. The RCS as a function of wind speed and incidence angle is represented in Vachon et al's model. The minimum ship length that can be found against the ocean sea clutter is determined by using the critical intensity level obtained from a statistical relationship between ship size and RCS. Wind speed changes the ocean RCS and the critical intensity, thus the minimum detectable ship length is strongly dependent on wind speed.

The upcoming RADARSAT-2 S1 mode has 3.1 Number of Looks, incidence angle of 23.5°, and 99.5 % confidence. For this mode, it is expected that a change in the wind speed from 2 to 10 m/s will change the minimum detectable ship length from 24 to 37 m in the best case and from 29 to 54 m in the worst case. The PIRATA (Pilot Research Moored Array in the Tropical Atlantic) project will survey areas on the north coast of Brazil. With wind speeds of 6 m/s, it is expected that the minimum detectable ship length is 32 m in the best case and 42 m in the worst case. The minimum detectable ship length is dependent on the wind speed, incidence angle and radar resolution.

Larger incidence angles reduce the ocean RCS, due to a reduction in Bragg scattering, and increase the ship RCS, due to increase in corner reflections back to the radar. Using the upcoming RADARSAT-2 standard mode for a wind speed of 10 m/s, the minimum detectable ship length is 20 m for an incidence angle of 20° and 99 m for an incidence angle of 45°.

A reduction of the pixel size increases the probability that the ship reflects photons from that pixel. By changing RADARSAT-2 modes from ScanSAR mode to Ultrafine Narrow mode, it will increase the area resolution by a factor of 10^3 for wind speed of 10 m/s, incidence angle of 20° and 1-look, and the minimum detectable ship length will decrease from 280 m to 15 m. Using RADARSAT-2 Fine Resolution modes, it is possible to detect ships that are as small as 1.5 m to 3.5 m. This is a large improvement in ship detection, and it also gives the possibility of recognizing the ship in good conditions (wind, sea clutter etc). The possibility of using cross-polarization also improves the ship detection capabilities. The new resolution modes and the possibility of using cross-polarization are the main reasons for improving the ship detection capability. On future missions, the main SAR characteristics desired are high incidence angle orbits, shorter repeat cycle, multi-polarization, and large swath widths at high resolution.

3.24 Ship Detection Using Polarimetric SAR Data (230)

The paper presents polarimetric techniques used to get information from spaceborne SAR data. Target feature vectors are being extracted from polarimetric data for use in classification algorithms. An alternative analysis technique, land-use, has been investigated. The full scattering matrix is decomposed for each image pixel into three orthogonal components, and then a series of matrix manipulations are performed. Corresponding to one of the various physical elemental scatterer types, the radar return image pixel is characterized. The advantage of this method can be utilized in ship detection, because polarimetric analysis is carried out for each individual pixel. Areas of a typical polarimetric content may characterize the vessel well enough, so it is possible to mitigate the backscatter from the sea clutter. The method is reliable for ship detection if the target is made up of different scatterer types than what is found in the surrounding ocean. Data used in the experiment is taken from a SIR-C experiment in 1994, in addition to simulated SAR data of ships. SIR-C operates in the L-band, and the data used are full-polarimetric single-look complex data. The simulated SAR data is of a small commercial ship of about 50 m, and the resolution is approximately half of that. This image was found to contain dihedrals, narrow dihedrals, and quarter waves, while the ocean in the images from SIR-C primarily consists of cylinders at thresholds as low as -15 dBm. At this level all the ocean clutter is visible. The ship is at least as bright as this threshold value, thus the ship’s main scatterer types will be visible and become distinct from the ocean clutter.

The spatial resolution is not so important for the scatterer classification, and thus it can be used for wide area surveillance. A better understanding of how the scattering matrix changes over the sea states can be obtained by analysing more images of ocean. This can be fed back into the ship detection algorithm, and all sea clutter can be eliminated, leaving only targets behind. The paper also investigates implications using fully polarimetric SAR data for ship detection, which is required for this system of ship detection. The requirements for full-polarimetric SAR images and better resolution are important.

3.25 Ship Surveillance Using RADARSAT ScanSAR Images (231)

The paper presents the ship detection performance of the wide area RADARSAT-1 ScanSAR imaging modes. The sensitivity to imaging geometry, environmental conditions, ship size, and SAR processing algorithms is analysed. RADARSAT-1 images used in the exercise have been acquired over the English Channel during 1996-1998 using mainly the ScanSAR Narrow Far (SCN2) mode. The average detection rate for all ships was 64 %, while it was 77 % for shipping lanes. The ships that were not detected are believed to be smaller fishing vessels and pleasure craft. The smallest vessels visible in the SAR imagery were about 30-40 m. The detection rate increased at larger incidence angles. An experimental processor was used to investigate different SAR processing algorithms, and it produced a detection rate 4.6 % better than with standard processors due to better image focusing and sharper output. Few wakes were detected in the SCN2 mode due to the shallow incidence angle and system noise. The ScanSAR Narrow Near mode has a steeper incidence angle, which improves sea feature visibility, and thus more ship wakes can be seen using this mode. A standard CFAR algorithm together with a neural network post-processor was used to develop an automatic ship detection process. An average detection rate of 88 % was achieved with a false alarm rate of 12 % (using three SCN2 images).

3.26 Ship Traffic Monitoring Using the ERS-1 SAR (270)

The paper presents a fast processing and distribution chain for ERS-1 SAR images, which has been developed in Norway. Large quantities of ERS-1 images have been analysed to be able to analyse the ship and ship wake detection capability of the satellite. Analyses of ships and ship wakes, as well as automatic detection have been done using the 30 m resolution Fast Delivery product. Ships larger than 120 m can be automatically detected in ERS-1 SAR images, while ships shorter than 100 m may become invisible at some wind speeds because of high backscatter from the sea. Medium sized ships are problematic to detect at wind speeds greater than 10 m/s. Detection of ships smaller than 50 m is very unlikely due to ERS-1’s steep incidence angle. The very far range part of the swath is better to use than the near range part of the swath. Signatures from ship wakes are very similar to those observed from the Seasat satellite. The dark turbulent wake is the most frequent wake. A bright line along the upwind side of the wake often accompanies the wake. The ship itself is seen more often than the ship’s wake.

The 100 m resolution images of high radiometric quality have been used for oil spill detection. Oil spill from ships can also be automatically detected, but some false alarms are expected because natural surface slicks may sometimes be classified as oil slicks at low wind speed. At high wind speeds, it is more difficult to automatically detect oil slicks.

3.27 Ship Wakes and Their Radar Images (224)

Ship wakes in SAR images appear as a dark trailing centreline region, bright V-images aligned at some angle to the ship's path, or as transverse or diverging waves of the Kelvin-wave pattern. The dark region, with low backscatter, is usually associated with a region lacking in short wave components. The bright line features are due to enhanced radar return. The paper presents a survey of remotely sensed wake images, the systems that have collected the wakes, and the theory of Kelvin wakes including examples. Kelvin wakes are the primary source that causes the dark centreline and bright V-images. The paper also presents a survey of the phenomena that causes the dark centreline returns and some predictions of radar reflectivity of these dark centrelines.

3.28 Ship-Sea Contrast Optimization When Using Polarimetric SARS (260)

The experiment presented in the paper is a continuation of the study done in (256). Calibrated polarimetric airborne Convair-580 SAR data collected off the Nova Scotia coast in Canada is used to analyse polarimetric signatures for incidence angles between 45º and 70º. At incidence angles lower than 60º, the TCR is significantly better when full-polarimetric information is used compared to one channel polarized data (HH, VV, or HV). Lower incidence angles and the robustness of the polarimetric discriminators for ship enhancement are investigated for different wind conditions (7, 14, and 20 knots). The information from polarization channel phase difference is also examined, and it is found that the information in the HH-VV channel phase difference is very promising for ship enhancement when dual-polarized SAR is used. The new polarization entropy and anisotropy improve the TCR significantly at operational SAR incidence angles. Rough sea conditions, with 20 knots wind speed, degrade the effectiveness because the sea backscattering becomes very heterogeneous. Cross-polarization (HV,VH) gives the best contrast at steeper incidence angles. The effectiveness of detection using cross-polarization is not degraded at rougher sea conditions.

3.29 Simulation of Polarimetric SAR Vessel Signatures for Satellite Fisheries Monitoring (192)

The paper presents a simulator that is a modified version of the RCS (Radar Cross Section) prediction code, which is developed at the UPC (Universitat Polytècnica de Catalunya). It is used to analyse polarimetric SAR vessel signatures to monitor fisheries activities. In the proposed new version, the characteristics of the chirp radar signal and the orbit of the satellite are taken into account. Commercial computer-aided-design packages with a high degree of detail and fidelity are used to generate the vessel models. The simulator is used to calculate full-polarimetric raw data. Using the simulator and based on polarimetric decomposition, new vessel classification algorithms can be developed. The paper presents the first results with the new proposed SAR simulator. It is shown that the simulator can simulate existing or new sensors to study its limitations and suggest new configurations to improve the usefulness for vessel detection.

3.30 Statistical Modelling of Ocean SAR Images (131)

Statistical modelling of the fully developed backscattering from the ocean surface in SAR images is presented in this paper. A new method is proposed that automatically selects a well-suited distribution of the histogram in a system of parametric distributions. In accordance with the skewness and flatness of its histogram a distribution is selected, and the corresponding intensity distribution is processed called KUBW. This statistic modelling can be used for the design of segmentation, texture analysis or for filtering algorithms.

3.31 Super-Resolution of Polarimetric SAR Images of Ship Targets (210)

Spectral analysis techniques used to analyse polarimetric SAR data are discussed in this paper. The same SAR scene in different polarimetric channels (HH,VV,HV,VH) is used to extract all the information of the same backscattering properties. The classical spectral estimator (Fast Fourier Transform, FFT) is replaced with parametric spectral estimators to obtain super-resolved images. The proposed processing scheme is based on a two-dimensional covariance method for both single channel and polarimetric data. A suitable fusion technique is required to be able to obtain a single super-resolved SAR image. A decentralised fusion strategy and two centralised fusion strategies are proposed for this purpose. The decentralised fusion strategy includes fusion of separately super-resolved images and the centralised fusion strategies include super-resolution of a fused image. The Minimum Mean Square Error (MMSE) strategy is the first centralised fusion strategy, which combines the original images on a pixel-by-pixel basis. The second centralised fusion strategy is the Polarimetric Whitening Filter (PWF), where the fused image is obtained by processing the polarimetric measurement vector through a whitening filter.

SIR-C SAR images are used to test the techniques, and single channel images are compared with multi-polarization images. The total number of identified target scatterers with respect to single channel processing mostly increase, because they are transferred and super-resolved in the output image. A higher TCR is achieved by joint processing of the polarimetric channels compared with single channel images. Thus higher TCR gains are achieved together with greater robustness. The techniques presented in the paper can be directly applied to ship targets. A larger image can be focused in small contiguous patches, and thus parallel processing can be used to speed up the image formation. Future research and applications of these techniques are presented in the end of the paper.

3.32 Synthetic Aperture Radar Imaging of Ship Wakes in the Gulf of Alaska (239)

The paper presents the Gulf of Alaska SAR experiment, which is a study that investigates SAR imaging of narrow-V wakes. The images are taken over a deep mixed layer environment so that surface manifestations of ship-generated internal waves are small. The SAR images were done by five flights over a deep-water region where the mixed layer depth exceeded 100 m. Both range and azimuthally travelling ships were imaged in 4 different sea states. The incidence angle for ships travelling in azimuth direction varied from 24˚ to 53˚. The following results are reported in the paper:

1. The half angles associated with narrow-V wakes are consistent with first-order Bragg surface wave theory.
2. The decay rate along the bright arms of the narrow-V wake is consistent with the combined viscous and radiation decay of short surface waves with the first-order Bragg wavelengths.
3. Narrow-V wakes are observed at incidence angles less than 45˚ in defined sea states. The longest narrow-V wake bright arm observed is 3.3 km.
4. Turbulent wakes (dark band between the bright arms) are observed at incidence angles less than 53˚ in defined sea states. The longest turbulent wake length is 41 km.
5. Bright boundaries along one side of the turbulent wake are observed.

3.33 Synthetic Aperture Radar Imaging of Surface Ship Wakes (189)

The paper presents an overview of ship wake imaging using spaceborne SAR, as well as the ship wakes dependency on environmental conditions and SAR parameters. Various wake phenomena are seen with moving ships in SAR images. Three general categories are used to classify the features: 1) surface waves generated by the ship, 2) turbulent or vortex wakes, and 3) internal waves.

The Bragg wave dispersion mechanism produces <u>narrow</u> wakes, which are only seen in very low wind and under any stratification conditions. It is most strongly observed at L-band, with a look direction perpendicular to the ship track, and at higher ship speeds. <u>Kelvin</u> wakes are visible through the modulation of an existing field of Bragg waves, and are observed under moderate wind conditions, at both L- and X-band, with all look directions. The Kelvin envelope is easiest observed when they are aligned in the azimuth direction, the individual cusp waves when they are range travelling, and the longer stern waves when they are travelling in azimuth direction.

Turbulent wakes appear in moderate winds, under any stratification condition, in any look direction, and in both X- and L-band images. The dark lines are often larger at L-band, while the bright lines at the edge are stronger at X-band. These wakes are the most frequently observed wake signature.

Internal waves are observed under moderate winds, require a strong and shallow density gradient, are larger at L-band than at X-band, and are strongest for a cross-track look direction.

3.34 The Ship Detection Capability of ENVISAT's ASAR (205)

The paper presents a discussion of which of ENVISAT's modes and products that are useful for ship detection. The noise-equivalent values σ_0 and the Equivalent Number of Looks (ENL) are better than what was estimated before the launch of ENVISAT. The Alternating Polarization (AP) mode represents a new and interesting spaceborne capability for routine observations. The Norne oil field, outside the coast of the middle of Norway, was chosen for acquiring data due to the large oil production vessel that is situated there. Results have shown that VV/VH AP data is useful for ship detection. Cross-polarized ocean backscatter is much lower than co-polarized ocean backscatter, especially at steep incidence angles. The radar cross-sections of fishing vessels are more similar at co- and cross-polarized data. Thus, using the cross-polarized channel will make the detection of fishing vessels easier.

The relationship between the length of the ship and the radar cross section (σ_{ship}) is given by:

$$l = \frac{\sigma_{ship}}{0.08R(\theta)} \tag{3.11}$$

To be able to calculate the RCS for the smallest ship that is possible to detect, a threshold value (T) of the average backscattering or noise floor is used:

$$\sigma_{ship}{}^{\min} = \rho_r \rho_a 10^{(\sigma_{sea}+T)/10} \tag{3.12}$$

ρ_r and ρ_a are the resolutions in range and azimuth direction, and σ_{sea} is the RCS from the sea surface. A threshold value of 10 dB over sea, σ_{sea}, is applicable for images with low or moderate resolution.

The relationship can also be expressed in terms of a given intensity level (I_T) and an average intensity value of unity. The minimum detectable vessel cross section can be expressed as:

$$\sigma = I_T \sigma_0 \rho_a \rho_r \tag{3.13}$$

where σ_0 is the ocean's normalised radar backscatter. The minimum vessel size is therefore heavily dependent on the ocean backscatter (σ_0), which varies with radar viewing geometry, polarization, and frequency, as well as with wind speed and direction relative to the radar look direction.

3.35 Evaluation of ENVISAT ASAR for ship detection (In Norwegian) (97)

The report starts with a theory part. It presents polarization theory and polarization in relation to ship detection, ENVISAT, different instruments on board ENVISAT, ASAR instrument, radar reflection, radar cross section, different algorithms used for ship and ship wake detection, and ship detection using ENVISAT.

The report also has a practical part with analysis of ENVISAT's Wide Swath mode and Alternating Polarization (AP) mode. HH-polarization gives lower reflection from the sea surface than VV-polarization under the same sea and wind conditions and the same image resolution, thus resulting in better TCR ratio. The AP mode gives new and unique opportunities to measure radar reflection from the same area at the same time with two different polarizations. It was before launch expected that this mode would be an improvement for ship detection in high sea and within a broader spectre of incidence angles. The opportunities of the ASAR AP mode to detect ships and ship wakes have been explored. The use of different combinations of polarizations (VV/VH, HH/HV and VV/HH) for ships with known shape has been investigated, as well as how they depend on the imaging geometry. The ship detection capacity is better when using cross-polarization for steep incidence angles. The difference is not so evident for larger incidence angles. The TCR for different polarizations, imaging geometries, and sea states have also been investigated. Radar signatures are also analyzed, and it is shown that signatures for cross polarization have prominent structure that can be utilized.

The report summarizes the results in the end, and gives recommendations for use of ENVISAT ASAR for ship detection. The recommendations are partially applicable for new modes on the future RADARSAT-2. HH-polarization is recommended above VV-polarization for ship detection using the Wide Swath mode. An area imaged with steep incidence angles should use the AP mode with co- and cross-polarization. This will give best TCR as well as opportunities for ship wake detection. Choosing the Wide Swath mode or the AP mode will mainly depend on how large area is required to cover. The AP mode with cross- and co-polarization should be used for smaller areas than approximately 100 km × 100 km to be able to get maximum information of the ships.

3.36 Wake Measurements (182)

The paper presents a study that was set up by the Special Group of Experts on Naval Hydrodynamics and Related Problems (SGE (HYDRO)) in 1984 to establish a reliable and accurate wake prediction procedure. The procedure was going to be used in the design of propellers for naval surface ships. RSG4's (Research Study Group on wake measurements) work showed that only limited full-scale data existed, and not enough resources were available to be able to do a full-scale trial. The data that existed had been on unlimited distribution, and thus already been discussed at various international meetings and conferences. ITTC (Information and Instructional Technology Center) provided wake scaling methods for twin-screw ships, while this was not seen as a particular problem by many countries. LDV (Laser Doppler Velocimetry) had been discussed at many international meetings and conferences. There was not enough data and/or interest for RSG4 to make worthwhile progress that had not been already covered.

3.37 Literature

(96) Andersen, T (1992): Detekterbarheten av Utvalgte Fenomener Over Sjø i Digitale ERS-1 Bilder, Thesis, University of Oslo.

(97) Arnesen, T and RB Olsen (2004): Vurdering av ENVISAT ASAR for Skipsdeteksjon, FFI/Rapport-2004/02121, Norwegian Defence Research Establishment, Kjeller, Norway.

(98) Asdornwised, W and S Jitapunkul (2003): Automatic Target Recognition Using Multiple Description Coding Models for Multiple Classifier Systems, Multiple Classifier Systems. Lecture Notes in Computer Science, Vol. 2709, Springer-Verlag, Berlin Heidelberg New York, pp. 336-345.

(99) Avital, E and T Miloh (1994): On the Determination of Density Profiles in Stratified Seas from Kinematical Patterns of Ship-induced Internal Waves, *J of Ship Res*, Vol. 38, No. 4, pp. 308-318.

(100) Axelsson, SRJ (1995): Frequency and Azimuthal Variations of Radar Cross-Section and Their Influence Upon Low-Frequency SAR Imaging, *IEEE Trans on Geosc and Rem Sens*, Vol. 33, No. 5, pp. 1258-1265.

(101) Barkat, M and F Soltani. Cell-Averaging CFAR Detection in Compound Clutter with Spatially Correlated Texture and Speckle, IEE Proc Radar, Sonar and Navig, Vol. 146, No. 6, pp. 279-284.

(102) Berizzi, F and M Diani (1997): Target Angular Motion Effects on ISAR Imaging, IEE Proc Radar, Sonar and Navig, Vol. 144, No. 2, pp. 87-95.

(103) Blacknell D and RG White (1994): Optimum Classification of Non-Gaussian Processing Using Neural Networks, *IEE Proc Vision Image and Signal Proc*, Vol. 141, No. 1, pp. 56-66.

(104) Blacknell, D (1994): Comparison of Parameter Estimators for K-Distribution, IEE Proc Radar, Sonar and Navig, Vol. 141, No. 1, pp. 45-52.

(105) Blacknell, D (1994): K-Distribution, IEE Proc Radar, Sonar and Navig, Vol. 141, No. 1.

(106) Blacknell, D (1994): New Method for the Simulation of Correlated K-Distributed Clutter, IEE Proc Radar, Sonar and Navig, Vol. 141, No. 1, pp. 53-58.

(107) Blacknell, D (1999): Target Detection in Correlated SAR Clutter, IEE Proc Radar, Sonar and Navig, Vol. 147, No. 1, pp. 9-16.

(108) Blacknell, D (2000): Statistical Target Behaviour in SAR Images, IEE Proc Radar, Sonar and Navig, Vol. 147, No. 3, pp. 143-148.

(109) Blacknell, D (2001): Contextual Information in SAR Target Detection, IEE Proc Radar, Sonar and Navig, Vol. 148, No. 1, pp. 41-47.

(110) Blacknell, D and AP Blake (1997): Single Point and Spatial Statistics of Polarimetric SAR Imagery, *Int J Rem Sens*, Vol. 18, No. 3, pp. 629-649.

(111) Boehmsdorff, S and H Essen (1998): Sea Surface and Ship Observation with MEMPHIS, Proc of IGARSS'98, Seattle, USA.

(112) Brown, ED, SB Buchsbaum, RE Hall, JP Penthume, KF Schmitt, KM Watson and DC Watson (1989): Observations of a Nonlinear Solitary Wave Packet in the Kelvin Wake of a Ship, J of Fluid Mech, Vol. 204, pp. 263-293.

(113) Bryant, ML, LL Gostin and M Soumekh (2003): 3-D E-CSAR Imaging of a T-72 Tank and Synthesis of Its SAR Reconstructions, *IEEE Trans on Aerosp and Elect Syst*, Vol. 39, No. 1, pp. 211-227.

(114) Buller, EH and JKE Tunaley (1989): The Effect of the Ship's Screws on the Ship Wake and its Implications for the Radar Image of the Wake, Proc of IGARSS'89, Vol. 1, pp. 362-365, Vancouver, BC, Canada.

(115) Campbell, JWM and PW Vachon (1997): Optimization of the Ocean Features Workstation for Ship Detection, CCRS Internal Report, Canada.

(116) Campbell, JWM, AL Gray, KE Mattar, JH Clarke and MWA van der Kooij (1997): Ocean Surface Feature Detection With the CCRS Along-Track InSAR, *Can J Rem Sens*, Vol. 23. No. 1, pp. 24-37, Canada.

(117) Cao, Y, W Schultz and RF Beck (1992): Inner Angle Wave Packets in an Unsteady Wake, Proc of the 19th ONR Symposium in Naval Hydrodynamics, Seoul, Korea.

(118) Caves, RG, PJ Harley and S Quegan (1995): Clutter Statistics Along Edge Features in Synthetic-Aperture Radar Imagery, *J of Electromag Waves and Appl*, Vol. 9, No. 3, pp. 327-353.

(119) Chellappa, R, QF Zheng, P Burlina, C Shekhar and KB Eom (1997): On the Positioning of Multisensor Imagery for Exploitation and Target Recognition, Proc of the IEEE, Vol. 85, No. 1, pp. 120-138.

(120) Chen, CT, KS Chen and JS Lee (2003): The Use of Fully Polarimetric Information for the Fuzzy Neural Classification of SAR Images, IEEE Trans on Geosc and Rem Sens, Vol. 41, No. 9, pp. 2089-2100.

(121) Christensen, CR (1978): Object Detectability in Speckle Noise, Int Conf on Lasers, pp. 637-645, Orlando, Florida.

(122) Coe, DJ and RG White (1996): Experimental Moving Target Detection Results from a Three-Beam Airborne SAR, Archiv fur Elektronik und Ubertragungstechnik (AEU) - Int J of Electronics and Comm, Vol. 50, No. 2, pp. 157-164.

(123) Cohen, M and GT Toussaint (1977): On the Detection of Structures in Noisy Pictures, Pattern Recognition Letters, Vol. 9, pp. 95-98.

(124) Conte, E, M Lops and G Ricci (1994): Radar Detection in K-Distributed Clutter, IEE Proc Radar, Sonar and Navig, Vol. 141, No. 2, pp. 116-118.

(125) Cowderoy, RI and JG Jones (1991): The Detection of Ship Wakes in Remote Sensed Imagery, Conference, Defence Oceanology Int '91, Brigthon, UK.

(126) Cresswell, G, C Zhou, PC Tildesley and CS Nilsson (1996): SAR Observations of Internal Wave Wakes from Sea Mounts, Marine and Freshwater Res, Vol. 47, No. 3, pp. 489-495.

(127) Curry, GR (1996): A Low-Cost Space-Based Radar System Concept, *IEEE Aerospace and Electronic Systems Magazine*, Vol. 11, No. 9, pp. 21-24.

(128) D'Addio E, S Giannatempo and G Galati (1988): Generation of K-Distributed Random Variables, Trans of the Soc for Computer Simulations, Vol. 5, pp. 159-174.

(129) Daddio, E, M Dibisceglie and S Bottgalico (1994): Detection of Moving-Objects with Airborne SAR, *Signal Proc*, Vol. 36, No. 2, pp. 149-162.

(130) Davies, IOG and NR Bruke (1989): A Proposal for the Simulation of the SAR Imaging of Turbulent Wakes Smith Associayes Technical Proposal, Smith Associates Tech Proposal, TP-89/376.

(131) Delignon, Y, R Garello and A Hillion (1997): Statistical Modelling of Ocean SAR Images, IEE Proc Radar, Sonar and Navig, Vol. 144, No. 6.

(132) Denney, BS and RJP De Figueiredo (2003): Scattering-Based Tomography for HRR and SAR Prediction, *Multidim Systems and Signal Proc*, Vol. 14, No. 1-3, pp. 207-222.

(133) Dias, JMB and PAC Marques (2004): Multiple Moving Target Detection and Trajectory Estimation Using a Single SAR Sensor, *IEEE Trans on Aerosp and Elect Syst*, Vol. 39, No. 2, pp. 604-624.

(134) Dong, Y and B Forster (1996): Understanding of Partial Polarization in Polarimetric SAR Data, *Int J Rem Sens*, Vol. 17, No. 12, pp. 2467-2475.

(135) Dorosinskiy, IG and SI Timoshenko (1993): Target Detection in a Jamming Background in Partially Coherent Synthetic-Aperture Radars, Telecomm and Radio Eng, Vol. 48, No. 8, pp. 74-78.

(136) Douville, PL (2002): Measured and Predicted Synthetic Aperture Radar Target Comparison, *IEEE Trans on Aerosp and Elect Syst*, Vol. 38, No. 1, pp. 25-37.

(137) Du, Y, PW Vachon and JJ van der Sanden (2003): Satellite Image Fusion with Multiscale Wavelet Analysis for Marine Applications: Preserving Spatial Information and Minimizing Artifacts (PSIMA), *Can J Rem Sens*, Vol. 29, No. 1, pp. 14-23, Canada.

(138) Durrani, TS and D Bisset (1984): The Radon Transform and Its Properties, Geophysics, Vol. 49, No. 8, pp. 1180-1187.

(139) Echard, JD (1991): Estimation of Radar Detection and False Alarm Probabilities, *IEEE Trans on Aerosp and Elect Syst*, Vol. 27, No. 2, pp. 255-260.

(140) Elassad, S and I Lakkis (1995): An Approach to Radar Imaging Using the Spherical Projection Density Concept, Annales des Telecommunications-Annals of Telecommunications, Vol. 50, No. 7-8, pp. 695-704.

(141) Eldhuset, K (1998): A New Fourth-Order Processing Algorithm for Spaceborne SAR, *IEEE Trans on Aerosp and Elect Syst*, Vol. 34, No. 3, pp. 824-835.

(142) Eldhuset, K (2004): Ultra High Resolution Spaceborne SAR Processing, *IEEE Trans on Aerosp and Elect Syst*, Vol. 40, No. 1, pp. 370-378.

(143) Ender, JHG (1996): Detection and Estimation of Moving Target Signals by Multi-Channel SAR, Archiv fur Elektronik und Ubertragungstechnik (AEU) - Int J of Electronics and Comm, Vol. 50, No. 2, pp. 150-156.

(144) Evans, DD (1979): A Point Target Model for the Synthetic Aperture Radar Detection Ships and Ice Conditions During a Swell, *IEEE Trans on Antennas and Propagation*, Vol. 27, No. 1, pp. 30-34.

(145) Felli, M and F Di Felice (2004): Analysis of the Propeller-Hull Interaction by LDV Phase Sampling Techniques, *J of Visualization*.

(146) Fotis, A (1988): WAVEAMP: A Program for Computation of Wave Elevations Created by a Ship Travelling at a Constant Speed, Tech Rep No. 88-03, Department of Naval Arch and Marine Eng, University of Michigan, Ann Arbour, Michigan.

(147) Foucher, S, GB Benie and J Boucher (2000): Maximum Likelihood Estimation of the Number of Looks in SAR Images, Mikon, pp. 657-660, Pologne, Wroclaw.

(148) Friedlander, B and B Porat (1997): VSAR: A High Resolution Radar System for Detection of Moving Targets, IEE Proc Radar, Sonar and Navig, Vol. 144, No. 4, pp. 205-218.

(149) Gabriel, AK (2002): A Simple Model for SAR Azimuth Speckle, Focusing, and Interferometric Decorrelation, *IEEE Trans on Geosc and Rem Sens*, Vol. 40, No. 8, pp. 1885-1889.

(150) Gadoś, A, A Gorzelańczyk, A Jarzębska, M Mordzonek, M Smolarczyk, KS Kulpa and B Dawidowicz (2004): First Polish SAR Trials, 5th Conference on Synthetic Aperture Radar, EUSAR 2004, Ulm, Germany.

(151) Gasparovic, RF, DR Thompson and JR Apel (1989): Synthetic Aperture Radar Imaging of Ship-Generated Internal Waves, *Johns Hopkins APL Tech Digest*, Vol. 10, No. 4, pp. 326-331.

(152) Gierull, CH and IC Sikaneta (2002): Estimating the Effective Number of Looks in Interferometric SAR Data, *IEEE Trans on Geosc and Rem Sens*, Vol. 40, No. 8, pp. 1733-1742.

(153) Giuli, D and L Facheris (1991): SAR Application of a Signal Coding Technique for Single-Hit Measurement of the Target Scattering Matrix, European Trans on Telecomm, Vol. 2, No. 6, pp. 675-688.

(154) Godbole, M, PE Dimini and GE Haslam (1999): Instrumented Ship Imaging Using the AN/APS-506 Spotlight SAR System, Proc of the 21st Int Airborne Rem Sens Conf, pp. 550-557, Ottawa, Ont.

(155) Griffin, OM (1988): Ship Wave Modification by a Surface Current Field, *J of Ship Res*, Vol. 32, No. 3, pp. 186-193.

(156) Griffin, OM, HT Wang and GA Meadows (1996): Ship Hull Characteristics from Surface Wake Synthetic Aperture Radar (SAR) Imagery, *Ocean Eng*, Vol. 23, No. 5, pp. 363-383.

(157) Griffin, OM, RD Peltzer, AM Reed and RF Beck (1992): Remote Sensing of Surface Ship Wakes, Naval Eng J, Vol. 104, pp. 245-258.

(158) Grønlien, TR (1998): Deteksjon av Punktmål Ved Hjelp av ScanSAR, Diploma thesis in physics, University of Oslo.

(159) Guo, HW, DN Liang, Y Wang and XT Huang (2003): Detection of Invisible Moving Targets in Foliage Penetration Ultra-Wide-Band Synthetic Aperture Radar Images, *Optical Eng*, Vol. 42, No. 10, pp. 2796-2797.

(160) Hansen, KV and PA Toft. Fast Curve Estimation Using Preconditioned Generalized Radon Transform, IEEE Trans on Image Proc, Vol. 5, No. 12, pp. 1651-1661, Dec 1996.

(161) Hawkins, RK, KP Murnaghan, M Yeremy and M Rey (2001): Ship Detection Using Airborne Polarimetric SAR, CEOS SAR Workshop Proc, pp. 6-15, Tokyo, Japan.

(162) Hennings, I, R Romeiser, W Apers and A Viola (1999): Radar Imaging of Kelvin Arms of Ship Wakes, Int J Rem Sens, Vol. 20, pp. 2519-2543.

(163) Hirosawa, H (1997): Degree of Polarization of Radar Backscatters from a Mixed Target, *IEEE Trans on Geosc and Rem Sens*, Vol. 35, No. 2, pp. 466-470.

(164) Hogan, GG, RD Chapman, G Watson and DR Thompson (1996): Observations of Ship-Generated Internal Waves in SAR Images from Loch Linnhe, Scotland, and Comparison with Theory and In Situ Internal Wave Measurements, *IEEE Trans on Geosc and Rem Sens*, Vol. 34, No. 2, pp. 532-542.

(165) Holcombe, AO, SL Macknik, J Intriligator, AE Seiffert and PU Tse (1999): Wakes and Spokes: New Motion-Induced Brightness Illusions, Perception 28, pp. 1231-1242.

(166) Hou, XY and N Moringa (1989): Detection Performance in K-Distributed and Correlated Rayleigh Clutter, *IEEE Trans on Aerosp and Elect Syst*, Vol. 25, No. 5, pp. 634-641.

(167) Hutt, D, P Chevret and ME Zakharia (2000): Potential of Radar Satellite Remote Sensing for Estimating Underwater Ambient Noise, Proc of the Fifth European Conference on Underwater Acoustics, ECUA 2000, Lyon, France.

(168) Huynen, JR (1978): Phenomenological Theory of Radar Targets, Electromagnetic Scattering, Uslenghi, PL (ed), New York: Academic.

(169) Huynen, JR (1987): Phenomenological Theory of Radar Targets, PhD Thesis, P.Q. Research, Polarimetric Quest, Los Altos Hills, CA, USA.

(170) Illingworth, J and J Kittler (1988): A Survey of the Hough Transform, *Computer Vision, Graphics, and Image Processing*, Vol. 44, No. 1, pp. 87-116.

(171) Ivanov, AY (2004): Ship and Oil Spills Detection with SAR: Experience from the Almaz-1 Mission, 5th Conference on Synthetic Aperture Radar, EUSAR 2004, Ulm, Germany.

(172) Jain, A and I Patel (1992): SAR ISAR Imaging of a Nonuniformly Rotating Object, *IEEE Trans on Aerosp and Elect Syst*, Vol. 28, No. 1, pp. 317-321.

(173) Jakeman, E (1980): On the Statistics of K-Distributed Noise, *J of Phys America: Mathematical and General*, Vol. 13, pp. 31-48.

(174) Jakeman, E (1987): Generalized K Distribution: A Statistical Model for Weak Scattering, *J of Optical. Society of America A: Optics, Image Science, and Vision*, Vol. 4, No. 9, pp. 1764-1772.

(175) Jakowatz, CV and PA Thompson. A New Look at Spotlight Mode Synthetic-Aperture Radar as Tomography - Imaging 3-D Targets, IEEE Trans on Image Proc, Vol. 4, No. 5, pp. 699-703, May 1995.

(176) Jao, JK (2001): Theory of Synthetic Aperture Radar Imaging of a Moving Target, *IEEE Trans on Geosc and Rem Sens*, Vol. 39, No. 9, pp. 1984-1992.

(177) Kaiser, JAC, SE Ramberg, RD Peltzer, MD Andrews and WD Garrett (1988): Wakex 86, A Ship Wake/Films Exploratory Experiment, NRL Memo Report 6270.

(178) Kirscht, M (2003): Detection and Imaging of Arbitrarily Moving Targets with Single-Channel SAR, IEE Proc Radar, Sonar and Navig, Vol. 150, No. 1, pp. 7-11.

(179) Kolev, NZ and CI Alexandrov (2004): ISAR Target Simulation and Matching, 5th Conference on Synthetic Aperture Radar, EUSAR 2004, Ulm, Germany.

(180) Krogstad, HE, O Samset and PW Vachon (1994): Generalizations of the Nonlinear Ocean-SAR Transform and a Simplified SAR Inversion Algorithm, Atmosphere-Ocean, Vol. 32, No. 1, pp. 61-82.

(181) Kuhn, JC (1990): Considerations of Uniqueness in the Inverse Kelvin Wake Problem, SNAME, H-5 Panel, Analytic Ship Wave Relations, Meeting 90, Jersey City, NJ.

(182) Lemche, V et al (1990): Wake Measurements, North Atlantic Treaty Organization Defence Research Group, RSG.4 on Wake Measurements.

(183) Liu, AK, CY Peng and Y-S Chang (1996): Mystery Ship Detected in SAR Image, EOS, Transactions, American Geophysical Union, Vol. 77, No. 3, pp. 17-18.

(184) Liu, AK, DA Berge and SR Borchardt (1984): Surface Signature of Ship-Generated Internal Waves, Rep DT-8311-01, Dyn Technologies, Torrance, CA, USA.

(185) Liu, ZS and J Li (1998): Feature Extraction of SAR Targets Consisting of Trihedral and Dihedral Corner Reflectors, *IEE Proc Radar, Sonar and Navig*, Vol. 145, No. 3, pp. 161-172.

(186) Lyden, JD (1985): Analysis of Seasat Revolution 407 Ship Wake Data, Topic Report 155900-32-T, ERIM, MI.

(187) Lyden, JD, DR Lyzenga and RA Schuman (1988): Synthetic Aperture Radar Detection of Surface Ship Wakes, *J of Geoph Res*, Vol. 93, No. C10, pp. 12,293-12,303.

(188) Lyden, JD, DR Lyzenga, RA Schuman and ES Kasischke (1985): Analysis of Narrow Ship Wakes in the Georgia Strait SAR Data, Topic Report 155900-20-T, ERIM, MI.

(189) Lyden, JD, RR Hammond, DR Lyzenga and RA Schuman (1988): Synthetic Aperture Radar Imaging of Surface Ship Wakes, *J of Geoph Res*, Vol. 93, pp. 12,293-12,303.

(190) Mahafza, BR (1993): 2-Dimensional SAR Imaging Using Linear Arrays with Transverse Motion, J of the Franklin Inst - Eng and Applied Mathematics, Vol. 330, No. 1, pp. 95-102.

(191) Mallorqui, JJ, JM Rius and M Bara (2002): Satellite SAR Simulator for Fishing Vessels Signature Studies, EUSAR 2002, Cologne, Germany.

(192) Mallorqui, JJ, JM Rius and M Bara (2002): Simulation of Polarimetric SAR Vessel Signatures for Satellite Fisheries Monitoring, *IEEE Trans on Geosc and Rem Sens* (IGARSS'02), Vol. 5, pp. 2711-2713, Toronto, Canada.

(193) Margarit, G, P Blanco, J Sanz and JJ Mallorqui (2003): Orbital SAR Simulator of Fishing Vessel Polarimetric Signatures Based on High Frequency Electromagnetic Calculations, IEEE.

(194) Meadows, L and G Meadows (1990): Detailed Analysis of Spaceborne Synthetic Aperture Radar Images of Ship Wakes, The University of Michigan, Ocean Eng Report, OEL-9004-DTRC-0001.

(195) Meyer-Hilberg, J, B Bickert and KP Schmitt (2003): Results of Flight Tests of a Two-Channel Radar System with Real-Time MTI Processing, *IEE Proc Radar, Sonar and Navig*, Vol. 150, No. 1, pp. 23-27.

(196) Milgram, JH (1988): Theory of Radar Backscatter from Short Waves Generated by Ships, with Application to Radar (SAR) Imagery, *J of Ship Res*, Vol. 32, pp. 54-69.

(197) Milgram, JH, RA Skop, RD Peltzer and OM Griffin (1993): Modeling Short Sea Wave Energy-Distributions in the Far Wakes of Ships, *J of Geoph Res - Oceans*, Vol. 98, No. C4, pp. 7115-7124.

(198) Milgram, JH, RD Peltzer and OM Griffin (1993): Suppression of Short Sea Waves in Ship Wakes - Measurements and Observations, *J of Geoph Res - Oceans*, Vol. 98, No. C4, pp. 7103-7114.

(199) Nasr, JM and D Vidalmadjar (1991): Image Simulation of Geometric Targets for Spaceborne Synthetic Aperture Radar, *IEEE Trans on Geosc and Rem Sens*, Vol. 29, No. 6, pp. 986-996.

(200) National Defense Research Committee Division 6 (1946): Physics of Sound in the Sea, Part IV - Acoustic Properties of Wakes, Summary of Tech Report Vol. 8.

(201) Neumann, DG, E Tapio, D Haggard, KE Laws and RW Bland (2001): Observation of Long Waves Generated by Ferries, *Can J Rem Sens*, Vol. 27. No. 4, pp. 361-370, Canada.

(202) Nordland, R (1997): Propageringsfaktorens Betydning for Radar Deteksjon av Mål i Sjøbakgrunn, Kompendium for UNIKF361, Universitetsstudiene på Kjeller

(203) Obi, S and M Murata (2003): Study on Detection of Information on the Sea Surface in SAR Imagery, NEC R&D, Vol. 44, No. 2, pp. 165-169.

(204) Oliver, CJ (1985): Correlated K-Distributed Clutter Models, *Optica Acta*, Vol. 32, No. 12, pp. 1515-1547.

(205) Olsen, RB and T Wahl (2003): The Ship Detection Capability of ENVISAT's ASAR, *IEEE Int Geosc and Rem Sensing Symp* (IGARSS'03), Toulouse, France.

(206) Olsen, RB, T Wahl and K Eldhuset (1988): Ship Detection Using the ASAR Instrument, FFI.

(207) Ouchi, K, M Lehara, K Morimura, S Kumano and I Takami (2002): Nonuniform Azimuth Image Shift Observed in the Radarsat Images of Ships in Motion, *IEEE Trans on Geosc and Rem Sens*, Vol. 40, No. 10, pp. 2188-2195.

(208) Ouchi, K, NR Stapleton and BC Barber (1997): Multi-Frequency SAR Images of Ship-Generated Internal Waves, *Int J Rem Sens*, Vol. 18, No. 18, pp. 3709-3718.

(209) Oumansour, K, Y Wang and J Saillard (1996): Multifrequency SAR Observation of a Ship Wake, *IEE Proc Radar, Sonar and Navig*, Vol. 143, No. 4, pp. 275-280.

(210) Pastina, D, P Lombardo, A Farina and P Daddi (2003): Super-Resolution of Polarimetric SAR Images of Ship Targets, Signal Proc, Vol. 83, No. 8, pp. 1737-1748.

(211) Pavlakis, P, D Tarchi and AJ Sieber (2001): On the Monitoring of Illicit Vessel Discharges Using Spaceborne SAR Remote Sensing - a Reconnaissance Study in the Mediterranean Sea, Annales des Telecommunications-Annals of Telecommunications, Vol. 56, No. 11-12, pp. 700-718.

(212) Peltzer, RD (1984): White-Water Wake Characteristics of Surface Vessels, NRL Memo Report 5335.

(213) Peltzer, RD, JH Milgram, RA Skop, JAC Kaiser, OM Griffin and WR Barger (1990): Hydrodynamics of Ship Wake Surfactant Films, Proc of the 18th Symposium on Naval
Hydrodynamics University of Michigan, Aug 20-23, 1990.

(214) Peltzer, RD, OM Griffin, WR Barger and JAC Kaiser (1992): High-Resolution Measurement of Surface-Active Film Redistribution in Ship Wakes, *J of Geoph Res - Oceans*, Vol. 97, No. C4, pp. 5231-5252.

(215) Peltzer, RD, WD Garrett and P Smith (1987): A Remote Sensing Study of a Surface Ship Wake, *Int J Rem Sens*, Vol. 8, No. 5, pp. 689-704.

(216) Pentini, FA, A Farina and F Zirilli (1992): Radar Detection of Targets Located in a Coherent K Distributed Clutter Background, *IEEE Proc for Radar and Signal Processing*, Vol. 139, No. 3, pp. 239-245.

(217) Perceival, RC, OM Griffin, RD Peltzer, AM Reed and RF Beck (1992): Remote-Sensing of Surface Ship Wakes, Naval Eng J, Vol. 104, No. 4, pp. 122-123.

(218) Peregrine, DH (1971): A Ship's Wave and Its Wake, *J of Fluid Mech*, Vol. 49, pp. 353-360.

(219) Perry, PP, RC Dipietro and RL Fante (1999): SAR Imaging and Moving Targets, *IEEE Trans on Aerosp and Elect Syst*, Vol. 35, No. 1.

(220) Pettersson, MI (2001): Extraction of Moving Ground Targets by a Bistatic Ultra-Wideband SAR, *IEE Proc Radar, Sonar and Navig*, Vol. 148, No. 1, pp. 35-40.

(221) Porch, WM, CYJ Kao and RG Kelley (1990): Ship Trails and Ship Induced Cloud Dynamics, Atmospheric Environment Part A - General Topics, Vol. 24, No. 5, pp. 1051-1059.

(222) Radford, SF, RL Gran and RV Miller (1994): Detection of Whale Wakes with Synthetic-Aperture Radar, *Marine and Tech Soc J*, Vol. 28, No. 2, pp. 46-52.

(223) Raney, RK (1971): Synthetic Aperture Imaging Radar and Moving Targets, *IEEE Trans on Aerosp and Elect Syst*, Vol. 7, pp. 499-505.

(224) Reed, AM and JH Milgram (2002): Ship Wakes and Their Radar Images, Annual Review of Fluid Mechanics, Vol. 34, pp. 469-502.

(225) Reed, AM, RF Beck, OM Griffin and RD Peltzer (1990): Hydrodynamics of Remotly Sensed Surface Ship Wakes, SNAME Trans., Vol. 98, pp. 319-363.

(226) Rees, WG and MJF Satchell (1997): The Effect of Median Filtering on Synthetic Aperture Radar Images, *Int J Rem Sens*, Vol. 18, No. 13, pp. 2887-2893.

(227) Rey, M, RK Hawkins, M Yeremy, B Noise, B Bayer and K Murnaghan (2000): Preliminary Results from Polarimetric SAR in the Crusade-2000 Experiment on Ship Detection, Ship Detection in Coastal Waters Workshop, poster presentation, Nova Scotia, Canada, May 31-June 1, 2000.

(228) Rignot, E and R Kwok (1993): Characterization of a Spatial Statistics of Distributed Targets in SAR Data, *Int J Rem Sens*, Vol. 14, No. 2, pp. 345-363.

(229) Rihaczek, AW. Radar Resolution of Moving Targets, IEEE Trans on Information Theory, Vol. 13, pp. 51-56, Jan 1967.

(230) Ringrose, R and N Harris (1999): Ship Detection Using Polarimetric SAR Data, Proc of the CEOS SAR workshop, ESASP-450.

(231) Robertson, N, P Bird and C Brownsword (2000): Ship Surveillance Using RADARSAT ScanSAR Images.

(232) Russel, LM, JH Seinfeld, RC Flagan, RJ Ferek, DA Hegg, PV Hobbs, W Wobrock, AI Flossmann, CD O'Dowd, KE Nielsen and PA Durkee (1999): Aerosol Dynamics in Ship Tracks, *J of Geoph Res*, Vol. 104, No. 24, pp. 31,077-31,095.

(233) Rye, AJ, FG Sawyer and R Sothinathan (1989): A Workstation for the Fast Detection of Ships, Proc of IGARSS'90, pp. 2263-2266, Vancouver, Canada.

(234) Santalla, V and YMM Antar (2002): A Comparison Between Different Polarimetric Measurement Schemes, *IEEE Trans on Geosc and Rem Sens*, Vol. 40, No. 5, pp. 1007-1017.

(235) Sarabandi, K (1994): Calibration of a Polarimetric Synthetic-Aperture Radar Using a Known Distributed Target, *IEEE Trans on Geosc and Rem Sens*, Vol. 32, No. 3, pp. 575-582.

(236) Sarabandi, K, LE Pierce, MC Dobson, FT Ulaby, JM Stiles, TC Chiu, R Deroo, R Hartikka, A Zambetti and A Freeman (1995): Polarimetric Calibration of SIR-C Using Point and Distributed Targets, *IEEE Trans on Geosc and Rem Sens*, Vol. 33, No. 4, pp. 858-866.

(237) Schuman, RA, ES Kasischke, DR Lyzenga and A Klooster (1983): SAR Ship Wake Signatures, Topic Report 157700-1-X, ERIM, MI.

(238) Shemdin, OH (1987): SAR Imaging of Ship Wakes in the Gulf of Alaska, Report, JPL/Ocean Res and Eng, Pasadena, CA, USA.

(239) Shemdin, OH (1990): Synthetic Aperture Radar Imaging of Ship Wakes in the Gulf of Alaska, *J of Geoph Res*, Vol. 95, No. C9, pp. 16,319-16,338.

(240) Shemer, L, L Kagan and G Zilman (1996): Simulation of Ship Wakes Image by an Along-Track Interferometric SAR, *Int J Rem Sens*, Vol. 17, No. 18, pp. 3577-3597.

(241) Shen, L, C Zhang and DKP Yue (2002): Free-Surface Turbulent Wake Behind Towed Ship Models: Experimental Measurements, Stability Analyses and Direct Numerical Simulations, J of Fluid Mech, Vol. 469, pp. 89-120.

(242) Shurman, SR (1989): Radar Characterization of Ship Wake Signatures of Ambient Ocean Clutter Features, IEEE Proc of the National Radar Conference, pp. 3-8, Dallas, Texas, USA.

(243) Simard, M, G DeGrandi, KPB Thomson and GB Beniev (1998): Analysis of Speckle Noise Contribution on Wavelet Decomposition of SAR Images, *IEEE Trans on Geosc and Rem Sens*, Vol. 36, No. 6, pp. 1953-1962.

(244) Simoes, MVS (2001): Ship Detection Performance Predictions for Next Generation Spaceborne Synthetic Aperture Radars, Thesis Naval Postgraduate School, Monterey, CA, USA.

(245) Skolnik, MI (1973): An Empirical Formula for the Radar Cross Section of Ships at Grazing Incidence, *IEEE Trans on Aerosp and Elect Syst*, Vol. 10.

(246) Skøelv, Å and T Wahl (1990): SAR Imaging of Vortex Ship Wakes. Vol. III: An Overview of the Pre-ERS-1 Observations and Models, FFI/Notat-90/7055, Norwegian Defence Research Establishment, Kjeller, Norway.

(247) Skøelv, Å, T Wahl and SS Eriksen (1988): SAR Imaging of Vortex Ship Wakes. Vol. I: Basic Theory and Simulation in L-band Using Bragg Model, FFI/Notat-88/9001, Norwegian Defence Research Establishment, Kjeller, Norway.

(248) Skøelv, Å, T Wahl and SS Eriksen (1990): SAR Imaging of Vortex Ship Wakes. Vol. II: Simulation in L- and C-Band Comparing the Bragg and HSW Imaging Models, FFI/Notat-88/9001, Norwegian Defence Research Establishment, Kjeller, Norway.

(249) Souyris, JC, C Henry and F Adragna (2003): On the Use of Complex SAR Image Spectral Analysis for Target Detection: Assessment of Polarimetry, *IEEE Trans on Geosc and Rem Sens*, Vol. 41, No. 12, pp. 2725-2734.

(250) Stapleton, NR (1997): Ship Wakes in Radar Imagery, *Int J Rem Sens*, Vol. 18, No. 6, pp. 1381-1386, 1997.

(251) Suzuki, T (1998): Radar Beamwidth Reduction Techniques, IEEE Aerospace and Electronic Systems Magazine, Vol. 13, No. 5, pp. 43-48.

(252) Swanson, CF (1984): Radar Observability of Ship Wakes, Cortana Corporation Report. Falls Church, VA, USA.

(253) Swean, TF Jr (1987): Numerical Simulation of the Wake Downstream of a Twin-Screw Destroyer Model, Naval Res Lab Memorandum Report 6131, 41 pp.

(254) Teti, JG Jr. and HN Kritikos (1992): SAR Ocean Image Decomposition Using the Gabor Expansion, *IEEE Trans on Geosc and Rem Sens*, Vol. 30, No. 1, pp. 192-196.

(255) Touzi, R (1992): Extraction of Point Target Response Characteristics from Complex SAR Data, *IEEE Trans on Geosc and Rem Sens*, Vol. 30, pp. 1158–1161.

(256) Touzi, R (1999): On the Use of Polarimetric SAR Data for Ship Detection, Proc of IGARSS'99, 3p, Hamburg, Germany, June 28-July 2 1999.

(257) Touzi, R (2004): Reconsideration of Coherency Matrix Parameters for Target Scattering Characterization, 5th Conference on Synthetic Aperture Radar, EUSAR 2004, Ulm, Germany.

(258) Touzi, R and F Charbonneau (2002): Characterization of Target Symmetric Scattering Using Polarimetric SARs, *IEEE Trans on Geosc and Rem Sens*, Vol. 40.

(259) Touzi, R and K Raney (1994): Effect of Doppler Centroid Mis-Tracking on the Parameter Estimation of Point Target Complex Signals, *IEEE Trans on Geosc and Rem Sens* (IGARSS'94), Pasadena, California, USA.

(260) Touzi, R, F Charbonneau, RK Hawkins, K Murnaghan and X Kavoun (2001): Ship-Sea Contrast Optimization When Using Polarimetric SARS, Proc of IGARSS'01, Australia.

(261) Trask, J, M Henschel and B Eid (1994): Analysis of Marine Radar Image Spectra Collected During the Grand-Banks ERS-1 SAR Wave Experiment, Atmosphere-Ocean, Vol. 32, No. 1, pp. 215-236.

(262) Tuck, EO, JL Collins and WH Wells (1971): On Ship Wave Pattern and Their Spectra, *J of Ship Res*, Vol. 15, pp.11-21.

(263) Tunaley, JKE, EH Buller, KH Wu and MT Rey (1991): The Simulation of the SAR Image of a Ship Wake, *IEEE Trans on Geosc and Rem Sens*, Vol. 29, No. 1, pp. 149-156.

(264) Tunaley, KE, JR Dubois and JBA Mitchell (1989): The Radar Image of the Turbulent Wake Generated by a Moving Ship, Proc of IGARSS'89.

(265) Uberoi, MS and P Freymuth (1970): Turbulent Energy Balance and Spectra of the Axisymmetric Wake, *Physics of Fluids*, Vol. 13, No. 9, pp. 2205-2210.

(266) Ulug, B, SC Ahalt, RA Mitchell (1997): Efficient ATR Using Compression, *IEEE Trans on Aerosp and Elect Syst*, Vol. 33, No. 4, pp. 1199-1211.

(267) Ursell, F (1960): On Kelvin's Ship Wave Pattern, *J of Fluid Mech*, Vol. 8, pp. 418-432.

(268) Venkatraman, M, H Kwon and NM Nasrabadi (2000): Object-Based SAR Image Compression Using Vector Quantization, *IEEE Trans on Aerosp and Elect Syst*, Vol. 36, No. 4, pp. 1036-1046.

(269) Wahl, T, K Eldhuset and K Asknes (1986): SAR Detection of Ships and Ship Wakes, SAR Applications Workshop (ESA Special Publication SP-264), p. 61, Paris, France.

(270) Wahl, T, K Eldhuset and Å Skøelv (1992): Ship Traffic Monitoring Using the ERS-1 SAR, Proc of the 1st ERS-1 Symp, pp. 823-828, Cannes, France.

(271) Wang, GY, XG Xia and VC Chen (2001): Three-Dimensional ISAR Imaging of Maneuvering Targets Using Three Receivers, IEEE Trans on Image Proc, Vol. 10, No.35, pp. 436-447.

(272) Wang, HT, OM Griffin and GA Meadows (1994): Hull Characteristics from SAR Images of Ship Wakes, *IEEE Trans on Geosc and Rem Sens* (IGARSS '94), "Surface and Atmospheric Remote Sensing: Technologies, Data Analysis and Interpretation", Vol. 3, pp. 1278-1280.

(273) Ward, KD (1992): Low-Grazing Angle Radar Measurements of Ship Generated Internal Waves in Scotland 1989-1991, Memorandum 4589, Defence Research Agency, Malvern, UK.

(274) Ward, KD, RJ Tough amd B Haywood (1990): Hybrid SAR-ISAR Imaging of Ships, Record of the IEEE 1990 National Radar Conf, pp.64-69, Arlington, VA.

(275) Watson, G, RD Chapman and JR Apel (1992): Measurements of the Internal Wave Wake of a Ship in a Highly Stratified Sea Loch, *J of Geoph Res - Oceans*, Vol. 97, No. C6, pp. 9689-9703.

(276) Watts, S (1987): Radar Detection Prediction in K-Distributed Sea Clutter and Thermal Noise, *IEEE Trans on Aerosp and Elect Syst*, Vol. 28, No. 1.

(277) Waxman, AM, MC Seibert, A Gove, DA Fay, AM Bernardon, C Lazott, WR Steele and RK Cunningham (1995): Neural Processing of Targets in Visible Multispectral IR and SAR Imagery, *Neural Networks*, Vol. 8, No. 7-8, pp. 1029-1051, 1995.

(278) Waymont, DK and IOG Davies (1990): Functional and Software Specification for a Model of the SAR Igamging of Turbulent Wakes, Smith Associates Tech Proposal, TR-90/173/1.0.

(279) Waymont, DK and IOG Davies (1999): An Appraisal of Literature on the Simulation of the SAR Imaging of Turbulent Ship Wakes, Tech Note-90/515/1.0, Smith Associates, Guilford, UK.

(280) Wilmut, MJ and RF MacKinnon (1986): Detection of Wake-Like Signals in SAR Images: Model and Methods, DREP Technical Memorandum, No. 86-10.

(281) Witting, JM and R Vaglio-Laurin (1985): Mechanisms and Models of Narrow-V Wakes, ORI Inc Tech Report 2529, 120 p.

(282) Waastad, H (1996): RCS Studier av Skip og Sjø ved Bruk av RADARSAT, Internal paper, SATOV-project, FFI/E.

(283) Xu, JY, J Yang, YN Peng, C Wang and YA Liou (2002): Using Similarity Parameters for Supervised Polarimetric SAR Image Classification, *IEEE Trans on Comm*, Vol E85B, No. 12, pp. 2934-2942.

(284) Yamashita, S and G Hornhof (1995): Assessing the Feasibility of a Vessel Monitoring System in the Western Pacific Pelagic Longline Fishery, Draft Report forwarded by Robert Harman, NMFS, Honolulu, HI.

(285) Yeang, CP, CY Cho and JH Shapiro (2003): Toward Target Recognition from Synthetic Aperture Radar Imagery Using Electromagnetics-Based Signatures, *Optical Eng*, Vol. 42, No. 7, pp. 2129-2149.

(286) Yeremy, M, JWM Campbell, K Mattar and T Potter (2001): Ocean Surveillance with Polarimetric SAR, *Can J Rem Sens*, Vol. 27. No. 4, pp. 328-344, Canada.

(287) Yeremy, ML, G Geling and M Rey (2002): Results from the Crusade Ship Detection Trial: Polarimetric SAR, *IEEE Trans on Geosc and Rem Sens* (IGARSS 02), Vol. 2, pp. 711-713.

(288) Zheng, QN, P Clemente-Colón, XH Yan, WT Liu and NE Huang (2004): Satellite Synthetic Aperture Radar Detection of Delaware Bay Plumes: Jet-Like Feature Analysis, *J of Geoph Res - Oceans*, Vol. 109, No. C3, pp. 953-967.

(289) Zilman, G and T Miloh (2001): Kelvin and V-like Ship Wakes Affected by Surfactants, *J of Ship Res*, Vol. 45, No. 2, pp. 150-163.

(290) Zink, M (2002): Derivation of RCS and σ^0 from ASAR products. ESA. ASAR Calibration Review. ESTEC, the Netherlands.

(291) Zou, N and A Nehorai (2000): Detection of Ship Wakes Using an Airborne Magnetic Transducer, *IEEE Trans on Geosc and Rem Sens*, Vol. 38, No. 1, pp. 532-539.

4 TARGET AND WAKE DETECTION

4.1 Overview

The following table gives an overview of publications on the theme “Target and Wake Detection” sorted after publication year. The papers include descriptions of approaches for detecting ships and wake-like features in SAR images. Summaries of a selection of some of the most important and available papers are given following the table.

YEAR	TITLE	AUTHOR	PUBLISHED
2000	Automatic Moving Target Detection Using a Rule-Based System: Comparison Between Different Study Cases	Ferrara, MN and A Torre	IEEE.
1998	A New Fourth-Order Processing Algorithm for Spaceborne SAR	Eldhuset, K	IEEE Trans on Aerosp and Elect Syst, Vol. 34, No. 3, pp. 824-835.
1998	Ship Detection in RADARSAT SAR Imagery	Jiang, QS, D Ziou, GB Bénié, A El Zaart, M Rey and M Henschel	Proc of IEEE SMC'98, San Diego..
1997	Ship and Ship Wake Detection in the ERS SAR Imagery Using Computer-Based Algorithm	Lin, I-I, LK Kwoh, YC Lin and V Khoo	IEEE Trans on Geosc and Rem Sens, GARSS'97, pp. 151-153.
1997	Computer-Based Algorithm for Ship Detection from ERS SAR Imagery	Lin, I-I and V Khoo	Proc 3rd ERS Symp (ESA SP-414), pp. 1411-1416, Florence.
1996	An Automatic Ship and Ship Wake Detection System for Spaceborne SAR Images in Coastal Regions	Eldhuset, K	IEEE Trans on Geosc and Rem Sens Symp, Vol. 34. No. 4, pp. 1009-1019.
1992	Interferometric Ocean Surface Mapping and Moving Object Relocation with a Norden Systems Ku-Band SAR	Orwig, LP and DN Held	Proc of IGARSS'92, pp. 1598-1600, Houston, Texas, May 26-29, 1992.
1992	Automatic Ship Detection in SAR Images	Argentini, F, G Benelli, A Garzelli and A Mecocci	Proc of the Int Conf Radar'92, Brighton, England, Vol. 365, pp. 465-468.
1991	Modelling Spatially Correlated K-Distributed Clutter	Armstrong, BC and HD Griffiths	Elect Letters, Vol. 27, pp.1355-1366.
1989	Principles and Performance of an Automated Ship detection System for SAR Images	Eldhuset, K	Proc of IGARSS'89, pp. 358-361, Vancouver, Canada.

1988	Automatic Ship and Ship Wake Detection in Spaceborne SAR Images from Coastal Regions	Eldhuset, K	IEEE Proc of IGARSS'88, pp. 1529-1533, Edinburg, Scotland, 1988.
1987	SAR Detection of Ships and Ship Wakes. Vol.1: Executive Summary, Vol.2: Main Volume	Aksnes, K, K Eldhuset and T Wahl	ESA Contract Report No. 6.507/85/F/FL., Norwegian Defence Research Establishment, Kjeller, Norway.
1970	Detection of Vessels and Mesoschale Oceanographic Features in Synthetic Aperture Radar Imagery off the West Coast of Canada	Borstad, GA, D Hill, L Armstrong and R Kerr	Borstad Associates, Contract Report to Institute of Ocean Sciences, DFO.

4.2 An Automatic Ship and Ship Wake Detection System for Spaceborne SAR Images in Coastal Regions (298)

The paper describes and automatic ship and ship wake detection system for space borne SAR images over coastal regions, which include eddies, fronts, waves and swells. It uses a variation of the N-sigma approach, which is the simplest of three methods to define the threshold. It sets the threshold intensity, I_T, to n standard deviations, σ, above the image mean, $<I>$:

$$I_T = <I> + n\sigma \qquad (4.1)$$

Digital terrain models are used to mask out land areas from the images. A search for ship targets, both stationary and moving, is performed. In addition, a wake search around the detected ships is done along a line in the azimuth direction, drawn through the vessel candidate. For each position along this line, a set of scan lines sampled at fixed angular intervals, are used to extract profiles of pixel values. Each profile is averaged to one value, and then a scan curve emerges, which consists of relative intensity as a function of angle around the search point. A polynomial fit is done to the curve to produce a smoothed curve, which is offset several deviations to form upper and lower thresholds (see Figure 4.1). Peaks and valleys are then examined further to filter out possible ships and ship wakes, by using least square method together with Chebyshev polynomials up to a certain order.

The complete method is illustrated in Figure 4.2. Window B is used to calculate pixel statistics, while window A is used for actual target search.

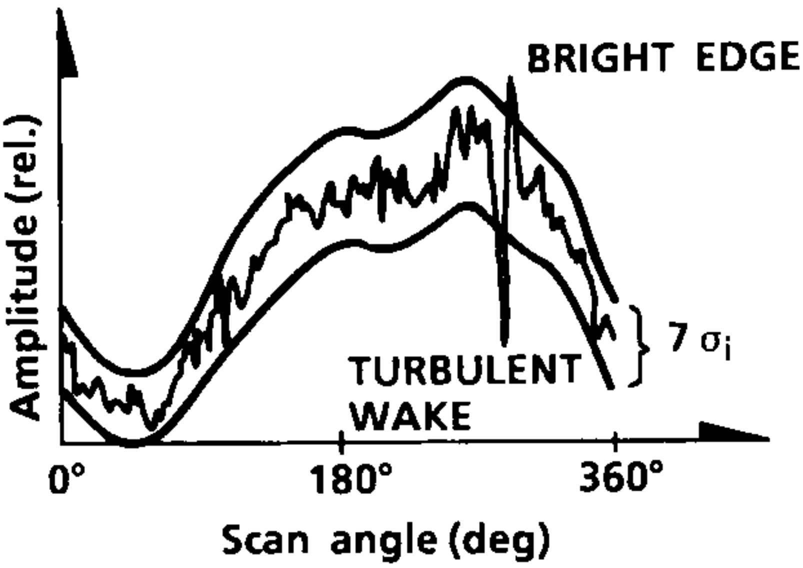

Figure 4.1 *Scan curve including features corresponding to a turbulent wake.*

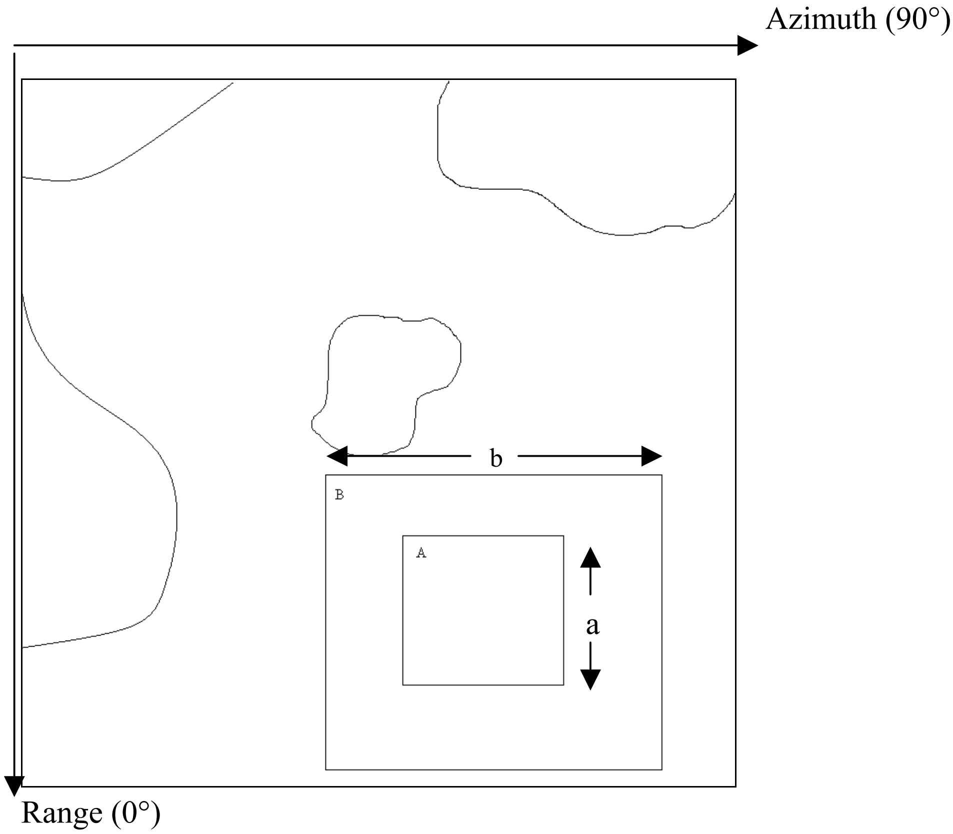

Figure 4.2 *Shows the principal for a simple method for ship detection. b is 20 pixels, while a is 10 pixels.*

All the image pixels are compared to a threshold, which is defined by $q\sigma_B$. q is normally 5.0. σ_B is for amplitude images given by:

$$\sigma_B = \mu_B \sqrt{\frac{\left(\frac{4}{\pi} - 1\right)}{N}} \tag{4.2}$$

and for intensity images:

$$\sigma_B = \frac{\mu_B}{\sqrt{N}} \tag{4.3}$$

If neighbouring pixels above the threshold are found, then they are grouped together, and each group is a potential ship.

Performing homogeneity and scan curve tests, wake behaviour test, and ship-to sea condition test reduce the number of false alarms. ERS-1 images are used to demonstrate the system, while both ERS-1 and Seasat images are used to assess the system. To test the system, visual evaluation is compared with the test results. Results showed that there were no false ships detected. The percentage of lost ships was 7-8 % for both ERS-1 and Seasat. The ERS-1 images had a higher percentage of lost and false ship wakes (14.8 %) than the images from Seasat-A (7.4 %). Other parameters and thresholds were used to show that the number of lost ships can be reduced, but an adverse effect is that the number of false ships increases heavily. Many of the detected ERS-1 wakes were vague, and they were difficult to detect visually. The automatic detection performance is very good, taken into account that some of the selected images had extremely strong variations in the sea state. The project also showed that it is possible to analyse a 3-look ERS-1 scene in less than eight minutes. The strong sensitivity of sea backscatter with increasing wind for short radar wavelength and small incidence angles (like ERS-1) is a big limitation to the use of the described detection system. Ships shorter than 50 m disappear with wind speeds greater than 4 m/s, while ships less than 100 m disappear in wind speeds greater than 10 m/s.

4.3 Automatic Moving Target Detection Using a Rule-Based System: Comparison Between Different Study Cases (299)

The paper describes a method for SAR data analysis and Automatic Target Detection and Recognition (ATD&R) that was developed at the Space Division at Alenia Aerospazio in Rome, Italy. A rule-based system is used for target detection. The rules are parameterised based on the image resolution and the size of searched target. The method is following the steps:

- The demonstrator first reads the data file and gets input from the screen.
- The image is enhanced and a speckle filter image is produced.
- Coastline detection is performed.
- A region of interest is chosen and CFAR is performed.
- Target pixels are extracted, and the target detection module is performed followed by the wake detection module.

- The output gives a list of moving targets, the direction of motion, information about wake properties, and the wake's dependence on the Doppler shift.

The method is tested on a collection of images with different statistical properties and resolution. The results of the testing phase are presented in the paper. The method is well suited for modelling and parameterisation of the coastline and linear feature detection. The model shows some weakness in detection of ship pixels. Ship pixels are not always simple to detect at low resolution where the intensity of the ship pixels might be low, and the CFAR threshold is not able to detect it. Improving the image quality can decrease the false detection rate. Pre-processing the image by applying a non-linear technique to reduce the power of the side lobes can improve the image quality. The results confirm the versatility of the algorithm to different images and resolution.

4.4 Automatic Ship and Ship Wake Detection in Spaceborne SAR Images from Coastal Regions (296)

The paper presents methods for automatic detection of ships and ship wakes in SAR images. The SAR processor, CESAR, has been developed at FFI for processing of ERS-1 data. Digital maps together with accurate pixel location algorithms are used to distinguish sea from land. Using a Wiener filter and a high pass filter enhances potential ship targets. All visible ships are detected using an appropriate choice of threshold. In addition more rapid working filters have been developed using statistics. The various types of wakes may be detected with high probability by analysing the statistics of the backscatter scan around each ship candidate. It is also possible to detect weak wakes using this method.

4.5 Automatic Ship Detection in SAR Images (293)

The paper presents an analysis of the problem of using fully automatic ship detection algorithms. This paper proposes a processing chain that first detects possible targets by searching through the image in parallel for bright spots and elongated wakes. Then the wakes are cross-validated against the bright spots to reject false alarms. The system detects bright spots and wakes, and afterwards associates a degree of goodness to each possible ship. The degree of goodness is based on suitable fuzzification functions set up during the system training.

The system has been implemented and tested on a MicroVax II sequential machine and on hypercube architecture of IMS T800 transputers. 42 Seasat SAR 4-views images have been used to test the processing chain. Suitable threshold values necessary for the p-tile filtering is computed on the basis of the histogram of the analysed image. The threshold values are not fixed, which allows good adaptation capabilities. Every ship belongs to the same subclass, and this demonstrates the algorithm's robustness. Considering the information from wakes, the false alarms in seacoast scenes and in very noisy images can be reduced. For the ship-wake couples correctly identified, a high coefficient of confidence has been obtained. The algorithm presented in this paper has the following advantages compared to the classical methods using the Hough transform:

- Accurate localization of the whole wake and not only its direction
- Detection of an arbitrary number of wakes
- Low processing time due to the use of binarized images and morphological operators

4.6 Computer-Based Algorithm for Ship Detection from ERS SAR Imagery (301)

The paper describes ERS SAR imagery used for detection of ships and ship wakes in Singapore waters. Since the SAR processor assumes the target to be stationary, the target position is shifted azimuthally from its actual position if the ship is moving. This information can be used to find the ship’s speed and heading. It is desirable to develop computer-based algorithms to perform the routine task ship monitoring of ship traffic. An algorithm based on the Radon transform is introduced in the paper and results from testing are described. The Radon transform is used to detect the location of turbulent wakes. The basic steps of the algorithm are as follows. An individual ship is being identified in the input image. The determination of the ship’s centre and orientation for each ship is done. The region of the Radon transform is defined, and the Radon transform for wake detection is done. If the wake is a dark turbulent wake, the minimum is chosen and the ship’s velocity is calculated. If the wake is a bright turbulent wake, the ship pixel is replaced with the background, the maximum is chosen, and the ship’s velocity is calculated.

4.7 Principles and Performance of an Automated Ship detection System for SAR Images (297)

The paper presents an automated ship detection system for SAR images that has been developed on an Apollo DN 10000 workstation. The model can be parallel computed, and it may work with 4 computers. The system is very promising because it uses short time and has a low false alarm rate. Accurate pixel location algorithms, digital terrain models, and sea depth models are used to distinguish land from sea. The potential ship targets are extracted by using an adaptive point detector, and searches for wakes are performed around the ship target. The detected ships and ship wakes may be natural phenomena like fronts, eddies or internal waves. Thus, a homogeneity test and a detailed wake analysis are done to reduce false alarms.

4.8 Ship and Ship Wake Detection in the ERS SAR Imagery Using Computer-Based Algorithm (302)

This paper presents a computer-based algorithm for ship and ship wake detection, which is developed to monitor ship traffic near Singapore waters. The algorithm is a modified version of the CRISP (Centre for Remote Imaging, Sensing and Processing) ship detection algorithm. ERS SAR PRI images have been used to test the algorithm. The images are made up of 8000 pixels x 8200 pixels, equivalent to 1000 km by 102.5 km. Geographical registration and land masking are performed. A 500 pixels x 500 pixels working window is defined, and the pixel intensity is calibrated for the working window to NCRS (Normalised Radar Cross Section). The ship detection is done by thresholding to identify possible ship pixels. A morphological filter is used to eliminate false ship pixels. Next, ship pixels are clustered into individual ships using neighbour clustering criterion. Afterwards, the ship's centre and coordinates are determined. A Radon transform is defined on the ship centre to be able to detect ship wakes. The ship pixels are replaced with background, and half-Radon transforms are done to detect possible wake candidates. For each ship wake, wake extension test, wake orientation test and wake vs. background test are done. Calculation of azimuth displacement, ship speed and heading are done. The algorithm is repeated until the end of the PRI image. The next working window has 30 pixels x 30 pixels overlap with the current window. It is more difficult to accurately detect ship wakes than ships, because the ship wakes are often weak. To reject false ship wakes, it is necessary to use several wake criterion tests. The proposed algorithm does not perform successfully under rough sea conditions.

4.9 Ship Detection in RADARSAT SAR Imagery (300)

Statistical methods, Radon transform, and other image processing techniques have been used to develop an automatic model for ship detection in RADARSAT-1 images. The algorithm uses the K-distribution to describe the PDF of the intensity in RADARSAT-1 SAR images. Then two threshold values, I_1 and I_2, are calculated based on required significance levels (η_1, η_2, where $\eta_1 < \eta_2$). The threshold value, I_1, is used to identify possible pixels, and a morphological filter is used to eliminate false ship pixels. If more than seven pixels are possible ship pixels, the centre pixel is considered a true ship pixel.

A second part of the algorithm is used to refine some ship targets, by using simple thresholding and Radon transform techniques. First, some pixels are identified that have intensities between the two threshold values, and then for each ship candidate, a Radon region is defined at the ship's centre to be able to detect possible ship wakes. Then the targets are rewritten in the image, and a new output image is made.

Further development is needed to improve the applicability of the model, to reduce the computational time, and to reduce false alarms. It is shown that the K-distribution does not always give a good fit. In future work, it is recommended that other statistical models are used describe the distribution of SAR image intensities. A Probabilistic Neural Networks (PNN) statistical model is a good method because it gives an excellent fit for the intensity of SAR imagery.

4.10 Literature

(292) Aksnes, K, K Eldhuset and T Wahl (1987): SAR Detection of Ships and Ship Wakes. Vol.1: Executive Summary, Vol.2: Main Volume, ESA Contract Report No. 6.507/85/F/FL., Norwegian Defence Research Establishment, Kjeller, Norway.

(293) Argentini, F, G Benelli, A Garzelli and A Mecocci (1992): Automatic Ship Detection in SAR Images, Proc of the Int Conf Radar'92, Brighton, England, Vol. 365, pp. 465-468.

(294) Armstrong, BC and HD Griffiths (1991): Modelling Spatially Correlated K-Distributed Clutter, *Elect Letters*, Vol. 27, pp.1355-1366.

(295) Borstad, GA, D Hill, L Armstrong and R Kerr (1970): Detection of Vessels and Mesoschale Oceanographic Features in Synthetic Aperture Radar Imagery off the West Coast of Canada, Borstad Associates, Contract Report to Institute of Ocean Sciences, DFO.

(296) Eldhuset, K (1988): Automatic Ship and Ship Wake Detection in Spaceborne SAR Images from Coastal Regions, IEEE Proc of IGARSS'88, pp. 1529-1533, Edinburg, Scotland, 1988.

(297) Eldhuset, K (1989): Principles and Performance of an Automated Ship detection System for SAR Images, Proc of IGARSS'89, pp. 358-361, Vancouver, Canada.

(298) Eldhuset, K (1996): An Automatic Ship and Ship Wake Detection System for Spaceborne SAR Images in Coastal Regions, *IEEE Trans on Geosc and Rem Sens* Symp, Vol. 34. No. 4, pp. 1009-1019.

(299) Ferrara, MN and A Torre (2000): Automatic Moving Target Detection Using a Rule-Based System: Comparison Between Different Study Cases, IEEE.

(300) Jiang, QS, D Ziou, GB Bénié, A El Zaart, M Rey and M Henschel (1998): Ship Detection in RADARSAT SAR Imagery, Proc of IEEE SMC'98, San Diego.

(301) Lin, I-I and V Khoo (1997): Computer-Based Algorithm for Ship Detection from ERS SAR Imagery, Proc 3rd ERS Symp (ESA SP-414), pp. 1411-1416, Florence.

(302) Lin, I-I, LK Kwoh, YC Lin and V Khoo (1997): Ship and Ship Wake Detection in the ERS SAR Imagery Using Computer-Based Algorithm, *IEEE Trans on Geosc and Rem Sens*, GARSS'97, pp. 151-153.

(303) Orwig, LP and DN Held (1992): Interferometric Ocean Surface Mapping and Moving Object Relocation with a Norden Systems Ku-Band SAR, Proc of IGARSS'92, pp. 1598-1600, Houston, Texas, May 26-29, 1992.

5 WAKE DETECTION PAPERS

5.1 Overview

The following table gives an overview of publications on the theme “Wake Detection” sorted after publication year. The papers primarily include descriptions of approaches to detect wake-like features in SAR images. Summaries of a selection of some of the most important and available papers are given following the table.

YEAR	TITLE	AUTHOR	PUBLISHED
2004	Detection of Linear Features in Synthetic-Aperture Radar Images by Use of the Localized Radon Transform and Prior Information	Onana, V, E Trouve, G Mauris, JP Rudant and E Tonye	Applied Optics, Vol. 43, No. 2, pp. 264-273.
2003	The Application of Wavelets Correlator for Ship Wake Detection in SAR Images	Kuo, JM and KS Chen	IEEE Trans on Geosc and Rem Sens, Vol. 41, No. 6, pp. 1506-1511.
2003	Multichannel ATI-SAR With Application to the Adaptive Doppler Filtering of Ocean Swell Waves	Barber, BC	IEE Proc Radar, Sonar and Navig, Vol. 150, No. 6, pp. 403-410.
2002	Ship Wake Detection in Synthetic Aperture Radar Images Using a Combination of a Wavelet Correlator and Radon Transform	Kuo, JM and KS Chen	Optical Eng, Vol. 41, No. 3, pp. 686-696.
2000	An Algorithm for Ship Wake Detection from the Synthetic Aperture Radar Images Using the Radon Transform and Morphological Image Processing	Jin, YQ and SQ Wang	Imaging Science J, Vol. 48, No. 4, pp. 159-163.
1999	Gap Winds and Wakes: SAR Observations and Numerical Simulations	Pan, FF and RB Smith	J of Atm Sciences, Vol. 56, No. 7, pp. 905-923.
1999	Pattern Recognition by Means of the Radon Transform and the Continuous Wavelet Transform	Magli, E, G Olmo and LL Presti	Signal Proc, Vol. 73, No. 3, pp. 277-289.
1999	Intelligent Pattern Detection and Compression. An Application to Very Low Bit Rate Transmission of Ship Wake Aerial Images	Magli, E and G Olmo	Pattern Recognition Letters, Vol. 20, No. 2, pp. 215-220.

1999	Optimal Edge Detection and Edge Localization in Complex SAR Images with Correlated Speckle	Fjørtoft, R, A Lopes, J Bruniquel and P Marthon	IEEE Trans on Geosc and Rem Sens, Vol. 37, No. 5, pp. 2272-2281.
1998	Bragg-Wave Scattering and the Narrow-Vee Wake	Balser, M, C Harkless, W Mclaren and S Schurmann	IEEE Trans on Geosc and Rem Sens, Vol. 36, No. 2, pp. 576-588.
1998	On the Radar Imaging Mechanism of Kelvin Arms of Ship Wakes	Alpers, W, R Romeiser and I Hennings	Proc of IGARSS'98, Seattle, Washington, 6-10 July, 1998.
1997	Wake Detection Leading to Fuzzy Localisation of Ships	Burdsall, B	Rapport de Stage. Mastere Image et Intelligence Artificielle. 1997
1997	Model-Based Enhancement of Internal Wave Images	Candy, JV and DH Chambers	IEEE J of Oceanic Eng, Vol. 22, No. 1, pp. 1-8.
1995	Localized Radon Transform-Based Detection of Ship Wakes in SAR Images	Copeland, AC, G Ravichandran and MM Trivedi	IEEE Trans on Geosc and Rem Sens, Vol. 33, pp. 35-45.
1995	Detection of Ship Wakes in SAR Images Using Morphological Operators	Garzelli, A	Computers & Geosciences, Vol. 21, No. 10, pp. 1201-1203.
1994	On Narrow V-Like Ship Wakes	Gu, DF and OM Phillips	J of Fluid Mech, Vol. 275, pp. 301-321.
1993	Use of the Dempster-Shafer Algorithm for the Detection of SAR Ship Wakes	Rey, M, JKE Tunalcy and T Sibbald	IEEE Trans on Geosc and Rem Sens, Vol. 31, No. 5.
1993	Synthetic-Aperture Radar Interferometry Applied to Ship-Generated Internal Waves in the 1989 Loch-Linnhe Experiment	Thompson, DR and JR Jensen	J of Geoph Res - Oceans, Vol. 98, No. C6, pp. 10259-10269.
1991	Ship Wake-Detection Procedure Using Conjugate Gradient Trained Artificial Neural Networks.	Fitch, JP, SK Lehmann, FU Dowla, SY Lu, EM Johansson and DM Goodman	IEEE Trans on Geosc and Rem Sens, Vol. 29, No. 5, pp. 718-726.
1991	Shipwake Detection Using Conjugate Gradient Trained Artificial Neural Networks	Fitch, JP, SK Lehman and FU Dowla	IEEE Trans on Geosc and Rem Sens, Vol. 29, No. 5, pp. 718-726.
1990	Modification of Directional Wave Number Spectra by Currents in the Wake of a Surface Ship	Skop, RA, OM Griffin and Y Leipold	J of Ship Res, Vol. 34, pp. 69-78.
1990	Use of the Hough Transform in Automated Lineament Detection	Wang, J and PJ Howart	IEEE Trans on Geosc and Rem Sens, Vol. 28, pp. 561-566, 1990.
1990	Application of Radon Transform Techniques to Wake Detection in Seasat-A SAR Images	Rey, MT, JK Tunaley, JT Folinsbee, PA Jahans, JA Dixon and MR Vant	IEEE Trans on Geosc and Rem Sens, Vol. 28, No. 4, pp. 553-560.
1990	Simulation of SAR Imaging of Ship Wakes, Comparing Different Wind Growth Rate Models	Skøelv, Å	FFI/Notat-90/7054, Norwegian Defence Research Establishment, Kjeller, Norway.
1989	Analysis of Two-Pass Modified Hough Transform	Wilmut, MJ and RF MacKinnon	Tech Mem No. 89-3. Defence Res Establishmment Pacific.

	Technique for the Detection of Wave-Like Signals		
1989	Modification of Wave Spectra by Currents in the Wake of a Surface Ship	Skop, RA, OM Griffin, KR Nicolas and TF Swean Jr	Naval Res Lab Memorandum Report 6336, 37 p.
1988	Automated Linear Feature Detection and Its Application to Curve Location in Synthetic Aperture Radar Imagery	Hendry, A, J Skingley and AJ Rye	Proc of IGARSS'88.
1988	Simulation of SAR Imaging of Ship Wakes	Skøelv, A, T Wahl and S Eriksen	IEEE Trans on Geosc and Rem Sens (IGARSS'88), pp. 1525-1528, Edinburgh, UK.
1988	Analysis of Ship-Generated Surface Waves Using a Method Based Upon the Local Fourier Transform	Wyatt, DC and RE Hall	J of Geoph Res, Vol. 93, No. 14, pp. 133-164.
1987	The Hough Transform Applied to SAR Images for Thin Line Detection	Skingley, J and AJ Rye	Pattern Recognition Letters, Vol. 6, No. 1, pp.61-67, The Netherlands.
1987	A Model for the Short Wavelength Portion of the Surface Wave Wake of a Ship and Comparison with Observation	Hall, RE, D Loeser and DC Wyatt	Science Appl Int Coperation, SAIC-87/1794.
1986	Linear Feature Detection and Enhancement in Noisy Images Via the Radon Transform	Murphey, LM	Pattern Recognition Letters, Vol. 4, No. 4, pp. 279-284.
1986	Detection of Wake-Like Signals in SAR Images: Model and Methods	Wilmut, MJ and RF MacKinnon	DREP Technical Memorandum, No. 86-10.
1985	Using Ship Wake Patterns to Evaluate SAR Ocean Wave Imaging Mechanisms	Hammond, RR, RR Buntzen and EE Floren	Tech Report No. 978, Nav Ocean Syst Center, San Diego, CA.
1985	SAR Detection of Ship Generated Turbulent and Vortex Wakes	Lyden, JD, DR Lyzenga, RA Schuman and CV Swanson	Tech Mem, Env Res Inst of Michigan.
1984	Use of Ship Wake Patterns in the Evaluations of SAR Ocean Wave Imaging Mechanisms	Hammond, RRR, RR Buntzen and EE Floren	NOSC Interim Report, San Diego, CA, USA.
1982	Use of the Hough Transformation to Detect Lines and Curves in Pictures	Duda, RO and PE Hart	Comm of the ACM, Vol.15, pp.11-15.
	Use of a Priori Knowledge and the Modified Hough Transform for the Detection of Wake-Like Signals	Wilmut, MJ and RF MacKinnon	
	Ship Wake Detection Using Radon Transforms of Filtered SAR Imagery	Sherbakov, A, R Hansen, G Vosselman and R Feron	SPIE, Vol. 2958, pp. 96-106.

5.2 An algorithm for Ship Wake Detection from the Synthetic Aperture Radar Images Using the Radon Transform and Morphological Image Processing (319)

The paper describes the algorithm Ship Wake Detection based on Radon transform and Morphological image processing (SWDRM). The algorithm is used to detect ship wakes in SAR images, and contains the following four steps:

1. The ocean is classified, and median filtering over the entire image is done to reduce single speckle noise in the pre-image process.
2. The image is divided into many sub images by moving a working window over the image. This step may reduce the mosaic pattern for reconstruction of the grey-level image.
3. Two threshold values are set for the peaks and troughs, and the Radon transform is applied to the sub images. The pixels with values between the two peaks are defined as zero. Single peaks are eliminated using the morphological image process (erosion and dilation operations).
4. The grey-level image is obtained by performing the inverse Radon transform.

Moving the working window over the entire image, and repeating the four steps described above, construct an inverted grey-level image. A binary image can also be obtained. The linear texture of a ship wake in an oceanic clutter background can easily be detected, because it is manipulated in the Radon space to invert grey-level and binary images. The algorithm is not so sensitive to the threshold parameter and the working window size, and is very robust in a noisy background. Seasat images have been used to test the algorithm.

5.3 Application of Radon Transform Techniques to Wake Detection in Seasat-A SAR Images (328)

The paper describes research using the Radon transform for automatic ship wake detection. The research's two main objectives were to automatically detect ships and to be able to differentiate ship wakes from other ocean linear features. The Automatic Detection Algorithm (ADA) was developed and tested on Seasat imagery.

The Radon is given in the continuous domain by:

$$f(r,v) = \iint_A p(x,y)\delta(r - x\cos v - y\sin v) \qquad (5.1)$$

where A is the image plane, $p(x,y)$ is the pixel value at position (x,y), r and v are the range and orientation coordinates of a straight line, and δ is the Dirac delta function. The Radon transform results in a surface with strong maxima and minima for significant bright and dark lines, and therefore acts as a detector. When strong features have been detected in the radon transform space, hypotheses based on feature shapes and separations are tested to determine whether they can be associated with a wake feature, a natural feature, or neither. The Radon transform is performed on the image, and bright and dark peaks are detected in the image. The Radon transform integrates the image intensity along every straight line in the image, thus each integral becomes one element in transform space. The result is a probability estimate, which can be combined with information about the hard target, as well as *a priori* to give a total estimated probability that the identified candidate in fact is a vessel. Targets below an operator-specified threshold are eliminated from the list.

The TCR is greater in the transform domain compared to the image plane. The integration process averages out the intensity fluctuations due to noise, and the TCR of the feature of interest increases. To be able to improve the PD (Probability of Detection) and reduce the PFA (Probability of False Alarm) other processing methods were developed and tested. An ADA, which uses a high-pass filter followed by a normalized Radon transform and a Wiener filter, has shown that it is able to distinguish wake peaks from false alarms. The high-pass filtering alone is capable of doubling the TCR. It is shown that wake features are easily detected by the Radon transform for ideal Rayleigh-distributed sea background. The false alarms are partly caused by the departure of sea clutter statistics.

5.4 Linear Feature Detection and Enhancement in Noisy Images Via the Radon Transform (324)

The paper presents an approach to the problem of detecting linear features. The approach is based on the Radon transform, which increases the computational efficiency compared to the similar Hough transform. The efficiency is achieved by using an algorithm based on the Fourier Slice Theorem. The transformation from image space to feature space is made via the frequency domain, thus a repeated application of an efficient Fast Fourier transform routine can do most of the computation. The algorithm can be implemented on a machine with parallel processing capability. The algorithm can be tested on a noisy SAR image. The Radon transformation increases the TCR, and thus it is easier to detect lines against a noisy background. It is shown that the method is not reliable to detect short linear features.

5.5 Localized Radon Transform-Based Detection of Ship Wakes in SAR Images (309)

The paper describes a localized Radon transform-based approach for detection of ship wakes in SAR images. A ship wake is more distinct and larger than the ship itself, and thus it might be easier to locate the ship’s true location using information from the ship wake. Instead of performing the intensity integration across the entire image, it is performed over short line segments. This Radon transform is utilized, and the Feature Space Line Detection (FSLD) algorithm is developed. Then the transform space is processed, which isolates and locates the response of linear features and decreases the false alarm rate. The algorithm is tested on actual SAR images including ship wakes. In addition synthetic images corrupted by various levels of Weibull multiplicative noise are also used. The tests showed that the algorithm is robust and in the presence of noise and the ability to detect and localize linear features that are significantly shorter than the image dimensions. The algorithm is most appropriate for steep radar depressions where the wake feature edges are not obscured by shadowing.

5.6 Ship Wake Detection in Synthetic Aperture Radar Images Using a Combination of a Wavelet Correlator and Radon Transform (320)

Detection of a moving ship's wake behind in a Synthetic Aperture Radar (SAR) image can give useful information about the ship's size, direction, and speed of movement. One type of ship wake is a characteristic linear V-shaped pattern. It is associated with high sea clutter, which causes the deterioration of detection performance. The paper presents a hybrid method using a combination of a wavelet correlator and Radon transform to detect ship wakes.

First, a wavelet technique is applied to generate a set of multiscale images. Three high-pass images, in horizontal, vertical, and diagonal direction, are generated for each resolution scale. Then a process is done to be able to correlate among the modules of different scale images formed from the three high-pass images. The process' output is highly representative at the ship's wake edges. Using this method, the wakes can be detected and in addition their V-shaped pattern is well preserved. The Radon transform technique is then used to be able to estimate the wake's V-opening angle. The proposed scheme in this paper is demonstrated to be much more effective, robust and reliable in noisy background compared to a direct Radon transform. Using only a Radon transform, the opening angle is shown to be very fuzzy, and can barely be determined.

5.7 The Application of Wavelets Correlator for Ship Wake Detection in SAR Images (321)

A ship-generated wake can give information about the ship's size, direction, and velocity. Wakes in SAR images are associated with high sea clutter, thus deterioration will be caused in the detection performance. Thus, a wavelet correlator is adopted, based on an orthogonal basis function (320). Using this method, the wakes can be detected, and in addition their V-shaped pattern is well preserved. The Radon transform technique is then used to be able to estimate the wake's V-opening angle. Ship-generated wakes will be enhanced in the reconstructed data, because they are found to be the local maxima in the wavelet transform method of several adjacent scales. The algorithm was tested on a real SAR image acquired by the airborne CV-580 SAR off the west coast of Taiwan in November 1993. The background noise is reduced significantly, using the method described, and the process spatial correlation is found to be critical. The proposed scheme in this paper is demonstrated to be much more effective, robust and reliable in noisy background compared to a direct Radon transform. Using only a Radon transform, the opening angle is shown to be very fuzzy, and can barely be determined.

5.8 Use of the Dempster-Shafer Algorithm for the Detection of SAR Ship Wakes (327)

The paper presents an Automatic Detection Algorithm (ADA) for detection of ship wakes in SAR images. It is based on the Dempster-Shafer algorithm. The Dempster-Shafer method is designed for data fusion to combine evidence from multiple sensors or pieces of evidence from one sensor. It uses probabilities based on belief functions instead of statistics. These estimates of belief “can be applied to decisions about the truth of a hypothesis”. Ignorance is treated in a quantitative manner, and thus they are more general than standard statistical techniques. Heuristic methods are acceptable for the Dempster-Shafer algorithm. The peaks detected by the Wiener filter belongs to one of the following hypotheses:

1. There exists a linear feature, which belongs to a ship wake.
2. There exists a linear feature, which does not belong to a ship wake.

The third possible conclusion is uncertainty of which of the two hypotheses the peak belongs to. The Dempster-Shafer method is applied to the problem of ship detection. Analysis of several peaks from the output of the Wiener filter is done, and the probabilities for the three possible conclusions are labeled pd1, pd2, and pd3. A second sensor might give new probabilities and uncertainty p1, p2, and p3. A “mass” is computed for each possible conclusion by the Dempster-Shafer rule of combination, as given in Table 5.1.

	pd1	**pd2**	**pd3**
p1	p1pd1	k	p1pd3
p2	k	p2pd2	p2pd3
p3	p3pd1	p3pd2	p3pd3

Table 5.1 The Dempster-Shafer rule of combination.

k is used to identify contradictory hypotheses. The masses of the three hypotheses are given by:

$$\text{m1} = \text{p1pd1} + \text{p1pd3} + \text{p3pd1 (wake feature)}$$

$$\text{m2} = \text{p2pd2} + \text{p2pd3} + \text{p3pd2 (natural feature)} \quad (5.2)$$

$$\text{m3} = \text{p3pd3 (uncertainty)}$$

The masses are normalized, and new updated probability values are obtained for the hypotheses.

A large set of SEASAT images are used to test the algorithm's limitations. The images included multiple SAR ship wakes, short or faint wake features, striated ocean background, and/or the presence of other naturally occurring linear ocean features. The algorithm usually classified the wakes correctly. The misclassifications were due to very short or faint linear features, inadequate number of detected peaks, or SAR processing errors. It performed very well in areas where the wake features were competing with naturally occurring linear ocean structure and in striated ocean regions. The ADA including the Dempster-Shafer algorithm is called the Complete ADA (CADA). Even though the possible presence of land features was not removed, and that there was no attempt done to adjust the CADA to differing background ocean statistics, 86 of 93 ships and 21 of 24 sea scenes were classified correctly.

5.9 Literature

(304) Alpers, W, R Romeiser and I Hennings (1998): On the Radar Imaging Mechanism of Kelvin Arms of Ship Wakes, Proc of IGARSS'98, Seattle, Washington, 6-10 July, 1998.

(305) Balser, M, C Harkless, W Mclaren and S Schurmann (1998): Bragg-Wave Scattering and the Narrow-Vee Wake, *IEEE Trans on Geosc and Rem Sens*, Vol. 36, No. 2, pp. 576-588.

(306) Barber, BC (2003): Multichannel ATI-SAR With Application to the Adaptive Doppler Filtering of Ocean Swell Waves, IEE Proc Radar, Sonar and Navig, Vol. 150, No. 6, pp. 403-410.

(307) Burdsall, B (1997): Wake Detection Leading to Fuzzy Localisation of Ships, Rapport de Stage. Mastere Image et Intelligence Artificielle.

(308) Candy, JV and DH Chambers (1997): Model-Based Enhancement of Internal Wave Images, *IEEE J of Oceanic Eng*, Vol. 22, No. 1, pp. 1-8.

(309) Copeland, AC, G Ravichandran and MM Trivedi (1995): Localized Radon Transform-Based Detection of Ship Wakes in SAR Images, *IEEE Trans on Geosc and Rem Sens*, Vol. 33, pp. 35-45.

(310) Duda, RO and PE Hart (1982): Use of the Hough Transformation to Detect Lines and Curves in Pictures, Comm of the ACM, Vol.15, pp.11-15.

(311) Fitch, JP, SK Lehman and FU Dowla (1991): Shipwake Detection Using Conjugate Gradient Trained Artificial Neural Networks, *IEEE Trans on Geosc and Rem Sens*, Vol. 29, No. 5, pp. 718-726.

(312) Fitch, JP, SK Lehmann, FU Dowla, SY Lu, EM Johansson and DM Goodman (1991): Ship Wake-Detection Procedure Using Conjugate Gradient Trained Artificial Neural Networks., *IEEE Trans on Geosc and Rem Sens*, Vol. 29, No. 5, pp. 718-726.

(313) Fjørtoft, R, A Lopes, J Bruniquel and P Marthon (1999): Optimal Edge Detection and Edge Localization in Complex SAR Images with Correlated Speckle, *IEEE Trans on Geosc and Rem Sens*, Vol. 37, No. 5, pp. 2272-2281.

(314) Garzelli, A (1995): Detection of Ship Wakes in SAR Images Using Morphological Operators, *Computers & Geosciences*, Vol. 21, No. 10, pp. 1201-1203.

(315) Gu, DF and OM Phillips (1994): On Narrow V-Like Ship Wakes, *J of Fluid Mech*, Vol. 275, pp. 301-321.

(316) Hall, RE, D Loeser and DC Wyatt (1987): A Model for the Short Wavelength Portion of the Surface Wave Wake of a Ship and Comparison with Observation, Science Appl Int Coperation, SAIC-87/1794.

(317) Hammond, RR, RR Buntzen and EE Floren (1985): Using Ship Wake Patterns to Evaluate SAR Ocean Wave Imaging Mechanisms, Tech Report No. 978, Nav Ocean Syst Center, San Diego, CA.

(318) Hendry, A, J Skingley and AJ Rye (1988): Automated Linear Feature Detection and Its Application to Curve Location in Synthetic Aperture Radar Imagery, Proc of IGARSS'88.

(319) Jin, YQ and SQ Wang (2000): An Algorithm for Ship Wake Detection from the Synthetic Aperture Radar Images Using the Radon Transform and Morphological Image Processing, *Imaging Science J*, Vol. 48, No. 4, pp. 159-163.

(320) Kuo, JM and KS Chen (2002): Ship Wake Detection in Synthetic Aperture Radar Images Using a Combination of a Wavelet Correlator and Radon Transform, Optical Eng, Vol. 41, No. 3, pp. 686-696.

(321) Kuo, JM and KS Chen (2003): The Application of Wavelets Correlator for Ship Wake Detection in SAR Images, *IEEE Trans on Geosc and Rem Sens*, Vol. 41, No. 6, pp. 1506-1511.

(322) Lyden, JD, DR Lyzenga, RA Schuman and CV Swanson (1985): SAR Detection of Ship Generated Turbulent and Vortex Wakes, Tech Mem, Env Res Inst of Michigan.

(323) Magli, E, G Olmo and LL Presti (1999): Pattern Recognition by Means of the Radon Transform and the Continuous Wavelet Transform, *Signal Proc*, Vol. 73, No. 3, pp. 277-289.

(324) Murphey, LM (1986): Linear Feature Detection and Enhancement in Noisy Images Via the Radon Transform, *Pattern Recognition Letters*, Vol. 4, No. 4, pp. 279-284.

(325) Onana, V, E Trouve, G Mauris, JP Rudant and E Tonye (2004): Detection of Linear Features in Synthetic-Aperture Radar Images by Use of the Localized Radon Transform and Prior Information, *Applied Optics*, Vol. 43, No. 2, pp. 264-273.

(326) Pan, FF and RB Smith (1999): Gap Winds and Wakes: SAR Observations and Numerical Simulations, *J of Atm Sciences*, Vol. 56, No. 7, pp. 905-923.

(327) Rey, M, JKE Tunalcy and T Sibbald (1993): Use of the Dempster-Shafer Algorithm for the Detection of SAR Ship Wakes, *IEEE Trans on Geosc and Rem Sens*, Vol. 31, No. 5.

(328) Rey, MT, JK Tunaley, JT Folinsbee, PA Jahans, JA Dixon and MR Vant (1990): Application of Radon Transform Techniques to Wake Detection in Seasat-A SAR Images, *IEEE Trans on Geosc and Rem Sens*, Vol. 28, No. 4, pp. 553-560.

(329) Sherbakov, A, R Hansen, G Vosselman and R Feron: Ship Wake Detection Using Radon Transforms of Filtered SAR Imagery, SPIE, Vol. 2958, pp. 96-106.

(330) Skingley, J and AJ Rye (1987): The Hough Transform Applied to SAR Images for Thin Line Detection, *Pattern Recognition Letters,* Vol. 6, No. 1, pp.61-67, The Netherlands.

(331) Skop, RA, OM Griffin and Y Leipold (1990): Modification of Directional Wave Number Spectra by Currents in the Wake of a Surface Ship, *J of Ship Res*, Vol. 34, pp. 69-78.

(332) Skop, RA, OM Griffin, KR Nicolas and TF Swean Jr (1989): Modification of Wave Spectra by Currents in the Wake of a Surface Ship, Naval Res Lab Memorandum Report 6336, 37 p.

(333) Skøelv, A, T Wahl and S Eriksen (1988): Simulation of SAR Imaging of Ship Wakes, *IEEE Trans on Geosc and Rem Sens* (IGARSS'88), pp. 1525-1528, Edinburgh, UK.

(334) Skøelv, Å (1990): Simulation of SAR Imaging of Ship Wakes, Comparing Different Wind Growth Rate Models, FFI/Notat-90/7054, Norwegian Defence Research Establishment, Kjeller, Norway.

(335) Thompson, DR and JR Jensen (1993): Synthetic-Aperture Radar Interferometry Applied to Ship-Generated Internal Waves in the 1989 Loch-Linnhe Experiment, *J of Geoph Res - Oceans*, Vol. 98, No. C6, pp. 10259-10269.

(336) Wang, J and PJ Howart (1990): Use of the Hough Transform in Automated Lineament Detection, *IEEE Trans on Geosc and Rem Sens*, Vol. 28, pp. 561-566, 1990.

(337) Wilmut, MJ and RF MacKinnon (1986): Ship Wake Detection in Speckle Noise Using a Modified Hough Transform, Proc of the Tenth Canadian Symp on Rem Sens, Edmonton, Alberta.

(338) Wilmut, MJ and RF MacKinnon (1989): Analysis of Two-Pass Modified Hough Transform Technique for the Detection of Wave-Like Signals, Tech Mem No. 89-3. Defence Res Establishmment Pacific.

(339) Wilmut, MJ and RF MacKinnon: Use of a Priori Knowledge and the Modified Hough Transform for the Detection of Wake-Like Signals.

(340) Wyatt, DC and RE Hall (1988): Analysis of Ship-Generated Surface Waves Using a Method Based Upon the Local Fourier Transform, *J of Geoph Res*, Vol. 93, No. 14, pp. 133-164.

6 TARGET DETECTION

6.1 Overview

The following table gives an overview of publications on the theme “Target Detection” sorted after publication year. The papers primarly include descriptions of different algorithms for target detection. Summaries of a selection of some of the most important and available papers are given following the table.

YEAR	TITLE	AUTHOR	PUBLISHED
2004	Ship and Oil Spills Detection with SAR: Experience from the Almaz-1 Mission	Ivanov, AY	5th Conference on Synthetic Aperture Radar, EUSAR 2004, Ulm, Germany.
2004	A New X-band Experimental Airborne Radar for SAR and GMTI	Damini, A, G Haslam, B Balaji and M Goulding	5th Conference on Synthetic Aperture Radar, EUSAR 2004, Ulm, Germany.
2003	The Changeable Sampling-Rate Processing Technology with Application to SAR-MTD	Sun, HB, SL Wang, GS Liu and JL Ni	Int J Rem Sens, Vol. 24, No. 15, pp. 3033-3047.
2003	Manoeuvring Target Detection in Over-the-Horizon Radar Using Adaptive Clutter Rejection and Adaptive Chirplet Transform	Wang, G, XG Xia, BT Root, VC Chen, Y Zhang and M Amin	IEE Proc Radar, Sonar and Navig, Vol. 150, No. 4, pp. 292-298.
2003	Target-Centered Models and Information-Theoretic Segmentation for Automatic Target Recognition	DeVore, MD and JA O'Sullivan	Multidim Systems and Signal Proc, Vol. 14, No. 1-3, pp. 139-159.
2003	Application of Frequency Correlation Function to Radar Target Detection	El-Rouby, AE, AY Nashashibi and FT Ulaby	IEEE Trans on Aerosp and Elect Syst, Vol. 39, No. 1, pp. 125-139.
2003	Synthetic Aperture Radar Target Acquisition Model Based on a National Imagery Interpretability Rating Scale to Probability of Discrimination Conversion	Driggers, RG and JA Ratches, JC Leachtenauer and RW Kistner	Optical Eng, Vol. 42, No. 7, pp. 2104-2112.
2003	Structure-Context Based Fuzzy Neural Network Approach for Automatic Target Detection	Jishuang, Q, W Chao and W Zhengzhi	IEEE Int Geosc and Rem Sensing Symp (IGARSS'03), Toulouse, France.
2003	Moving Target Detection in Over-the-Horizon Radar Using Adaptive Chirplet Transform	Wang GY, XG Xia, BT Root and VC Chen	Radio Science, Vol. 38, No. 4 (Art.no. 1062).

2003	PAMIR - a Wideband Phased Array SAR/MTI System	Ender, JHG and AR Brenner	IEE Proc Radar, Sonar and Navig, Vol. 150, No. 3, pp. 165-172.
2003	A Domain-Independent Window Approach to Multiclass Object Detection Using Genetic Programming	Zhang, MJ, VB Ciesielski and P Andreae	EURIASP, J on Signal Processing, Special Issue on Genetic and Evolutionary Computation for Signal Processing and Image Analysis, Vol. 8, pp. 841–859.
2003	Automatic Target Recognition Using Multiple Description Coding Models for Multiple Classifier Systems	Asdornwised, W and S Jitapunkul	Multiple Classifier Systems. Lecture Notes in Computer Science, Vol. 2709, Springer-Verlag, Berlin Heidelberg New York, pp. 336-345.
2003	Genetic Algorithm Based Feature Selection for Target Detection in SAR Images	Bhanu, B and YQ Lin	Image and Vision Computing, Vol. 21, No. 7, pp. 591-608.
2003	Physics-Based Detection of Targets in SAR Imagery Using Support Vector Machines	Krishnapuram, B, J Sichina and L Carin	IEEE Sensors J, Vol. 3, No. 2, pp. 147-157 .
2003	SAR Observations of Typical Phenomena in the Black Sea Shore Area	Lavrova, OY, TY Bocharova and MI Mityagina	IEEE Int Geosc and Rem Sensing Symp (IGARSS'03), Toulouse, France.
2003	An Automatic Ship Detection System Using ERS SAR Images	Liu, Y, M Fang, Q Feng and L Wang	IEEE.
2002	Increasing the Discrimination of Synthetic Aperture Radar Recognition Models	Bhanu, B and G Jones	Optical Eng, Vol. 41, No. 12, pp. 3298-3306.
2002	Comments on "Non-Iterative Quality Phase-Gradient Autofocus (QPGA) Algorithm for Spotlight SAR Imagery"	Chan, HL and TS Yeo	IEEE Trans on Geosc and Rem Sens, Vol. 40, No. 11, pp. 2517-2517.
2002	Application of the Fractional Fourier Transform to Moving Target Detection in Airborne SAR	Sun, H, GS Liu, H Gu and WM Su	IEEE Trans on Aerosp and Elect Syst, Vol. 38, No. 4, pp. 1416-1424.
2002	Exploiting the Polarimetric Information for the Detection of Ship Targets in Non-Homogeneous SAR Images	Sciotti, M, D Pastina and P Lombardo	IEEE.
2002	Expectation-Maximization Approach to Target Model Generation from Multiple Synthetic Aperture Radar Images	Richards, JA, AS Willsky and JW Fisher	Optical Eng, Vol. 41, No. 1, pp. 150-166.
2002	A Two-Scale Model to Predict C-band VV and HH Normalized Radar Cross Section Values Over the Ocean	Wackerman, CC, P Clemente-Col?n, WG Pichel and XF Li	Can J Rem Sens, Vol. 28, No. 3, pp. 367 - 384, Canada.
2002	Model-Based Recognition of Articulated Objects	Ahn, JS and B Bhanu	Pattern Recognition Letters, Vol. 23, No. 8, pp. 1019-1029.
2002	Performance Complexity Study of Several Approaches to Automatic Target Recognition from SAR Images	DeVore, MD and JA O'Sullivan	IEEE Trans on Aerosp and Elect Syst, Vol. 38, No. 2, pp. 632-648.
2002	Detection System for Ship Targets in SAR Imagery	Jiang, Q	PhD Thesis, Université de Sherbrooke, Canada.
2002	An Improved Minimum Entropy Method for Refocusing the	Jin, YQ and Y Chen	Imaging Science J, Vol. 50, No. 3, pp. 591-608.

	Moving Target Image in Synthetic Aperture Radar Observations		
2002	An Airborne Synthetic Aperture Radar (SAR) Experiment to Support RADARSAT-2 Ground Moving Target Indication (GMTI)	Livingstone, CE, I Sikaneta, CH Gierull, S Chiu, A Beaudoin, J Campbell, J Beaudoin, S Gong and TA Knight	Can J Rem Sens, Vol. 28, No. 6, pp. 794 - 813, Canada.
2002	A SAR Target Classifier Using Radon Transforms and Hidden Markov Models	Nilubol, C, RM Mersereau and MJT Smith	Digital Signal Processing, Vol. 12, No. 2-3, pp. 274-283.
2001	Automatic Detection of Ships in RADARSAT-1 SAR Imagery	Wackerman, CC, KS Friedman, WG Pichel, P Clemente-Col?n and X Li	Can J Rem Sens, Vol. 27. No. 4, pp. 371-378, Canada.
2001	A Reverse-SAR (R-SAR) Algorithm for the Detection of Targets Buried in Ground Clutter	Yoo, JC and YS Kim	Microwave and Optical Tech Letters, Vol. 28, No. 2, pp. 121-126.
2001	Improved SAR Target Detection Via Extended Fractal Features	Kaplan, LMi	IEEE Trans on Aerosp and Elect Syst, Vol. 37, No. 2, pp. 436-451.
2001	Predicting an Upper Bound on SAR ATR Performance	Boshra, M and Bhanu	IEEE Trans on Aerosp and Elect Syst, Vol. 37, No. 3, pp. 876-888.
2001	Unbiased Coherence Estimator for SAR Interferometry with Application to Moving Target Detection	Gierull, CH	Elect Letters, Vol. 37, No. 14, pp. 913-915.
2001	Computational RCS Analysis and Technique for Precise Location of the Hot Spots on the Concept Ship ALSC	Kashyap, S and A Louie	Defence Research Establishment Ottawa Technical Note # 2001-03, DREO, Ottawa, ON.
2001	Multi-Aspect Target Detection for SAR Imagery Using Hidden Markov Models	Runkle, P, LH Nguyen, JH McClellan and L Carin	IEEE Trans on Geosc and Rem Sens, Vol. 39, No. 1, pp. 46-55.
2001	Context-Based Target Detection with Multi-Pass RADARSAT-1 Data – Application to Coastal Surveillance	Jouan, A and Y Marcoz	ASAR 2001 Workshop, Canadian Space Centre, Québec, Canada.
2001	Support Vector Machines for SAR Automatic Target Recognition	Zhao, Q and JC Principe	IEEE Trans on Aerosp and Elect Syst, Vol. 37, No. 2, pp. 643-654.
2001	Robust Autofocus Algorithm for ISAR Imaging of Moving Targets	Li, J, RB Wu and VC Chen	IEEE Trans on Aerosp and Elect Syst, Vol. 37, No. 3, pp. 1056-1069.
2001	Detecting Moving Targets in SAR Imagery by Focusing	Fienup, JR	IEEE Trans on Aerosp and Elect Syst, Vol. 37, No. 3, pp. 794-809.
2001	Segmentation-Based Technique for Ship Detection in SAR Images	Lombardo, P and M Sciotti	IEE Proc Radar, Sonar and Navig (Special Issue), Vol. 148, No. 3, pp. 147-159.
2001	Detection of Ships Using Cross-Correlation of Split-Look SAR	Iehara, M, K Ouchi, I Takami, K	IEEE Trans on Geosc and Rem Sens Symp (IGARSS

	Images	Morimura and S Kumano	'01), Vol. 4, pp. 1807-1809, Sydney, Australia.
2001	SAR ATR Performance Using a Conditionally Gaussian Model	O'Sullivan, JA, MD DeVore, V Kedia and MI Milleri	IEEE Trans on Aerosp and Elect Syst, Vol. 37, No. 1, pp. 91-108.
2000	Probabilistic Winner-Take-All Segmentation of Images with Application to Ship Detection	Osman, H and SD Blostein	IEEE Trans on Systems Man and Cybernetics Part B-Cybernetics, Vol. 30, No. 3, pp. 485-490.
2000	Ship Detection in ERS-1 and RADARSAT SAR Images Using a Self-Organising Neural Network	Foulkes, SB	AMRS Ship Detection Workshop, 31 May - 2 June, 2000.
2000	An Automatic Approach to Ship Detection in Spaceborne Synthetic Aperture Radar Imagery: An Assessment of Ship Detection Capability Using RADARSAT	Askari, F and B Zerr	NATO Saclant Undersea Research Centre Report, Saclantcen Report, Serial no: SR-338.
2000	Recognizing Target Variants and Articulations in Synthetic Aperture Radar Images	Bhanu, B and G Jones	Optical Eng, Vol. 39, No. 3, pp. 712-723.
2000	Automatic Target Recognition of Time Critical Moving Targets Using 1D high Range Resolution (HRR) Radar	Williams, R, J Westerkamp, D Gross and A Palomino	IEEE Aerospace and Electronic Systems Magazine, Vol. 15, No. 4, pp. 37-43.
2000	Synthetic Aperture Radar Automatic Target Recognition with Three Strategies of Learning and Representation	Zhao, Q, JC Principe, VL Brennan, DX Xu and Z Wang	Optical Eng, Vol. 39, No. 5, pp. 1230-1244.
2000	LADAR Target Detection Using Morphological Shared-Weight Neural Networks	Khabou, MA, PD Gader and JM Keller	Machine Vision and Appl, Vol. 11, No. 6, pp. 300-305.
2000	Adaptive Target Recognition	Bhanu, B, YQ Lin, G Jones and J Peng	Machine Vision and Appl, Vol. 11, No. 6, pp. 289-299.
2000	A Quasi-Parametric Algorithm for Synthetic Aperture Radar Target Feature Extraction and Imaging with Angle Diversity	Man, JZ, GQ Liu, J Li and R Williams	Circuits and Signal Processing, Vol. 19, No. 4, pp. 301-319.
2000	Moving Target Feature Extraction with Polarisation Diversity in the Presence of Arbitrary Range Migration and Phase Errors	Liu, G, H Li and J Li	IEE Proc Radar, Sonar and Navig, Vol. 147, No. 4, pp. 208-216.
2000	Target Recognition Based on Directional Filter Banks and Higher-Order Neural Networks	Park, SI, MJT Smith and RM Mersereau	Digital Signal Processing, Vol. 10, No. 4, pp. 297-308.
1999	Automatic Detection for Ship Targets in RADARSAT SAR Images from Coastal Regions	Jiang, Q, S Wang, D Ziou and A El Zaart	Vision Interface '99, Trois-Rivieres, Canada.
1999	Automated Target Recognition Using Enhanched Resolution SAR Data	Novak, LM, GJ Owirka and AL Weaver	IEEE Trans on Aerosp and Elect Syst, Vol. 35, No. 1, pp. 157-174.
1999	Target Detection in SAR Imagery by Genetic Programming	Howard, D, SC Roberts, and R Brankin	Advances in Engineering Software, Vol. 30, No. (5), pp. 303 - 311.
1999	Complex ISAR Imaging of Maneuvering Targets Via the Capon Estimator	Liu, ZS, RB Wu and J Li	IEEE Trans on Signal Proc, Vol. 47, No. 5, pp. 1262-1271.

1999	A New Fast Method for the Reconstruction of 2-D Microwave Images of Rotating Objects	Berizzi, F and G Corsini	IEEE Trans on Image Proc, Vol. 8, No. 5, pp. 679-687, May 1999.
1999	Coherent Spatial Filtering for SAR Detection of Stationary Targets	Jao, JK, CF Lee and S Ayasli	IEEE Trans on Aerosp and Elect Syst, Vol. 35, No. 2, pp. 614-626.
1999	Adaptive Target Detection in Foliage-Penetrating SAR Images Using Alpha-Stable Models	Banerjee, A, P Burlina and R Chellappa	IEEE Trans on Image Proc, Vol. 8, No. 12, pp. 1823-1831, Dec 1999.
1999	Multiscale Models for Target Detection and Background Discrimination in Synthetic Aperture Radar Imagery	Howard, D and J Schroeder	Digital Signal Processing, Vol. 9, No. 3, pp. 149-161.
1999	Evolution of Ship Detectors for Satellite SAR Imagery	Howard, D, SC Roberts and R Brankin	Genetic Programming Lecture Notes in Comp Science 1598, pp. 135-148,.
1999	Optimal Target Detection Using One Channel SAR. Complex Imagery: Application to Ship Detection	Lopès, A, J Bruniquel, F Sery, J-C Souyris and F Adragna	Proc of IGARSS'98, Seattle, WA, USA.
1999	Entropy Optimized Morphological Shared-Weight Neural Networks	Khabou, MA, PD Gader and HC Shi	Optical Eng, Vol. 38, No. 2, pp. 263-273.
1998	Comparison of Probability Statistics for Automated Ship Detection in SAR Imagery	Henschel, MD, MT Rey, JWM Campbell and D Petrovic	Proc of the Int Conf on Appl of Photonic Technology (ICAPT'98), Int Society for Optical Eng, Bellingham, Washington.
1998	Automatic Detection for Ship Targets in SAR Imagery Using PNN-model	Jiang, Q, E Aitnouri, S Wang and D Ziou	ADRO Symposium'98 in Montreal, Canada.
1998	Application of Angular Correlation Function of Clutter Scattering and Correlation Imaging in Target Detection	Zhang, GF and L Tsang	IEEE Trans on Geosc and Rem Sens, Vol. 36, No. 5, pp. 1485-1493.
1998	Function Approximation Framework for Region of Interest Determination in Synthetic Aperture Radar Images	Kothari, R and D Ensley	Optical Eng, Vol. 37, No. 10, pp. 2817-2825.
1998	Target Prescreening Based on a Quadratic Gamma Discriminator	Principe, JC, A Radisavljevic, J Fisher, M Hiett and LM Novak	IEEE Trans on Aerosp and Elect Syst, Vol. 34, No. 3, pp. 706-715.
1998	Target Discrimination in Synthetic Aperture Radar Using Artificial Neural Networks	Principe, JC, M Kim and JW Fisher	IEEE Trans on Image Proc, Vol. 7, No. 8, pp. 1136-1149, Aug 1998.
1998	High-Performance Automatic Target Recognition Through Data-Specific VLSI	Chia, KN, HJ Kim, S Lansing, WH Mangione-Smith and J Villasenor	IEEE Trans on Very Large Scale Integration Systems, Vol. 6, No. 3, pp. 364-371.
1998	Numerical Studies of the Detection of Targets Embedded in Clutter by Using Angular Correlation Function and Angular Correlation Imaging	Zhang, GF, L Tsang, and Y Kuga	Microwave and Optical Tech Letters, Vol. 17, No. 2, pp. 82-86.
1997	A Review of Target Decomposition Theorems in Radar	Cloude, SR and E Pottier	IEEE Trans on Geosc and Rem Sens, Vol. 35, No. 2,

	Polarimetry		pp. 498-518.
1997	Report on Automatic Identification System Installed at VTS Tofino	Penney, R	Department of Fisheries and Oceans, DFO/5513.
1997	Results from the Ocean Monitoring Workstation (OMW) Dark Feature Detection Algorithm	Thomas, SJ, PW Vachon and J Cranton	
1997	Effects of Polarization and Resolution on SAR ATR	Novak, LM, SD Halversen, GJ Owirka and M Hiett	IEEE Trans on Aerosp and Elect Syst, Vol. 33, No. 1, pp. 102-116.
1997	Model-Based Neural Network for Target Detection in SAR Images	Perlovsky, LI, WH Schoendorf, BJ Burdick and DM Tye	IEEE Trans on Image Proc, Vol. 6, No. 1, pp. 203-216, Jan 1997.
1997	3-D Target Feature Extraction Via Interferometric SAR	Li, J, ZS Liu and P Stoica	IEE Proc Radar, Sonar and Navig, Vol. 144, No. 2, pp. 71-80.
1997	Some Issues in Inverse Synthetic Aperture Radar Image Reconstruction	Borden, B	Inverse Problems, Vol. 13, No. 3, pp. 571-584.
1997	Efficient ATR Using Compression	Ulug, B, SC Ahalt, RA Mitchell	IEEE Trans on Aerosp and Elect Syst, Vol. 33, No. 4, pp. 1199-1211.
1997	A Multiresolution Approach to Discrimination in SAR imagery	Irving, WW, LM Novak and AS Willsky	IEEE Trans on Aerosp and Elect Syst, Vol. 33, No. 4, pp. 1157-1169.
1997	Use of Curvilinear SAR for Three-Dimensional Target Feature Extraction	Li, J, Z Bi, ZS Liu and K Knaell	IEE Proc Radar, Sonar and Navig, Vol. 144, No. 5, pp. 275-283.
1997	Ship Detection by the RADARSAT SAR: Validation of Detection Model Predictions	Vachon, PW, JWM Campbell, CA Bjerklund, FW Dobson and MT Rey	Can J Rem Sens, Vol. 23. No. 1, pp. 48-59, Canada.
1996	Ship Detection by the RADARSAT SAR: Validation of Detection Model Predictions	Vachon PW, JW Campbell, C Bjerkelund, FW Dobson and MT Rey	Proc of the Pacific Ocean Rem Sens Conf (PORSEC'96), Victoria, BC, Canada.
1996	A Search Procedure for Ships in RADARSAT Imagery	Rey, MT, A Drosopoulos and D Petrovic	Tech Report No. 35, Defence Research Establishment Ottawa, Ottawa, Canada.
1996	Feature-Based Target Recognition with a Bayesian Network	Liu, J and KC Chang	Optical Eng, Vol. 35, No. 3, pp. 701-707.
1996	Effects of Polarization and Resolution on the Performance of a SAR Automatic Target Recognition System	Novak, LM, SD Halversen, GJ Owirka and M Hiett	Archiv fur Elektronik und Ubertragungstechnik (AEU) - Int J of Electronics and Comm, Vol. 50, No. 2, pp. 92-99.
1996	Target Detection with Synthetic Aperture Radar	Li, JA and EG Zelnio	IEEE Trans on Aerosp and Elect Syst, Vol. 32, No. 2, pp. 613-627.

1995	Development of an Automatic Target Detection and Characterisation System in Polarimetric SAR Images	Yongjian, Y, H Shun-Ji and A Torre	Proc of IGARRS'95, Florence.
1995	Cueing, Feature Discovery, and One-Class Learning for Synthetic Aperture Radar Automatic Target Recognition	Koch, MW, MM Moya, LD Hostetler and RJ Fogler	Neural Networks, Vol. 8, No. 7-8, pp. 1081-1102.
1995	A Neural System for Automatic Target Learning and Recognition Applied to Bare and Camouflaged SAR Target	Bernardon, AM and JE Carrick	Neural Networks, Vol. 8, No. 7-8, pp. 1103-1108.
1995	A New MTI-SAR Approach Using the Reflectivity Displacement Method	Moreira, JR and W Keydel	IEEE Trans on Geosc and Rem Sens, Vol. 33, No. 5, pp. 1238-1244.
1995	Nonlinear Techniques in Optical Synthetic-Aperture Radar Image Generation and Target Recognition	Weaver, S and K Wagner	Applied Optics, Vol. 34, No. 20, pp. 3981-3996.
1994	Complete Processing System that Uses Fuzzy-Logic for Ship Detection in SAR Images	Benelli, G, A Garzelli and A Mecocci	IEE Proc Radar, Sonar and Navig, Vol. 141, No. 4.
1994	Joint Spatial-Polarimetric Whitening Filter to Improve SAR Targets Detection Performance for Spatially Distributed Targets	Larson, V, L Novak and C Stewart	Proc of the Algorithm for Synthetic Aperture Radar Imagery, Vol. 22, No. 30, pp.285-301.
1994	Radar Target Identification Using Spatial Matched-Filters	Novak, LM, GJ Owirka and CM Netishen	Pattern Recognition Letters, Vol. 27, No. 4, pp. 607-617.
1993	Automatic Ship Detection In Satellite Multispectral Imagery	Burgess, DW	Photogrammetric Eng and Rem Sens, Vol. 59, No. 2, pp. 229-237.
1993	Optimal Polarimetric Processing for Enhanced Target Detection	Novak, LM, MC Burl and WW Irving	IEEE Trans on Aerosp and Elect Syst, Vol. 29, No. 1, pp. 234-244.
1992	Automatic Detection of Targets Against Cluttered Backgrounds Using a Fractal-Oriented Statistical-Analysis and Radon-Transform	Berenyi, HM, VF Leavers and RE Burge	Pattern Recognition Letters, Vol. 13, No. 12, pp. 869-877.
1992	Target Motion Compensation by Spectrum Shifting in Synthetic Aperture Radar	Chen, HC and CD McGillem	IEEE Trans on Aerosp and Elect Syst, Vol. 28, No. 3, pp. 895-901.
1991	A Fuzzy Complete SAR Processing Chain for Ship detection and Velocity Estimation	Alparone, L, F Argenti and G Benelli	European Trans on Telecomm and Related Tech, Vol. 2, No. 6, pp. 689-693, Italy.
1991	Adaptive Airborne MTI with 2-Dimensional Motion Compensation	Klemm R (	IEE Proc Radar and Signal Processing, Vol. 138, No. 6, pp. 551-558.
1990	Moving Target Imaging Algorithm for SAR Data	Werness, S, W Carrara, L Joyce and D Franczak	IEEE Trans on Aerosp and Elect Syst, Vol. 26, No. 1, pp. 57-67.
1982	Enhancement and Detection of Convex Objects Using Regression Models	Rewo, L	Computer Vision, Graphics, and Image Processing Vol. 25, pp. 257-269.

1960	A Statistical Theory of Target detection By Pulsed Radar	Marcum, JI	IRE Trans, Vol. IT-6, pp. 59-267.
	A System for Ship Detection from SAR Imagery Using Different PDF Models	Jiang, Q, S Wang and	Workshop for Ship Detection in Coastal Waters, Halifax, May 31-June 2.
	A Neural-Network-Fusion Architecture for Automatic Extraction of Oceanographic Features from Satellite Remote Sensing Imagery	Askari, F and B Zerr	SACLANTCEN SR-306.
	Automatic Target Recognition Using Sequences of High Resolution Radar Range-Profiles	Jacobs, SP and JA O'Sullivan	IEEE Transactions on Aerospace and Electronic Systems, Vol. 36, No. 2, pp. 364-382.
	High-Resolution Radar Models for Joint Tracking and Recognition	Jacobs, SP and JA O'Sullivan	Automatic Target Recognition VII (Proc of SPIE), Vol. 3069, pp. 94-105.
	Automatic Target Recognition Using High Resolution Radar Range-Profiles	Jacobs, SP	Ph.D. Dissertation, Washington University, St. Louis, MO, May 1997.
	Statistical Modelling in Ship Target Detection	Jiang, Q	PhD Thesis, Université de Sherbrooke, Canada.
	Statistical Analysis of SAR Images and Its Application in Ship Detection	Qingshan, J	PhD Thesis, Université de Sherbrooke, Canada.

6.2 A Neural System for Automatic Target Learning and Recognition Applied to Bare and Camouflaged SAR Targets (350)

The paper describes the use of a neural system for automatic target learning and detection. Both camouflaged and uncamouflaged military vehicles can be recognized using the ART-2A (Adaptive Resonance Theory) neural network. Different radar views and depression angles are used and both spotlight and stripmap radar collection modes are used. A confidence measure reflecting the goodness of match is also reported, which successfully eliminates a high percentage of clutter. Since the algorithm is computationally simple, real-time target recognition is possible.

ISAR (Inverse Synthetic Aperture Radar) turntable data and ADTS (Advanced Detection Technology Sensor) SAR data were used for the experiments. Even some camouflaged targets can be recognized using the proposed algorithm.

6.3 A Search Procedure for Ships in RADARSAT Imagery (427)

The report describes how the Constant False Alarm Rate (CFAR) procedure, based on the K-distributed sea clutter model, is applied to the Ocean Features Workstation (OFW). This approach is attractive because it provides a theoretical basis for selecting a CFAR. The objective is to improve the ship detection performance. Scenes from ERS-1 and RADARSAT-1 are examined. Visual and standard statistical tests are used to examine the data. The goodness-of-fit of the K-distribution model is investigated.

Histogram, cumulative distribution function matching, Pearson diagrams, standard χ^2 test and Kolmogorov-Smirnov test are performed as visual criteria. All tests, except the χ^2 test, show good fit between the model and experimental data. The report explains the poor performance of the χ^2, and why it is unsuitable for long-tailed models. The approximation between the χ^2 statistics and the probability function becomes poorer for data bins with few elements. Direct comparison of goodness-of-fit results cannot be performed, because the number of degrees of freedom is not constant. Another problem with this test is that the results are heavily dependent on the main body of the distribution. Thus it is difficult to accurately determine the shape parameter.

The K-distribution model can successfully model the sea clutter, and is for a radar signal X given by (3.10). v is an order parameter for the distribution that defines the skewness and shape of the tail. It is important to obtain a good estimate for this parameter to set a proper threshold. Above this threshold, detected pixels will be expected to belong to a different population with a given probability.

The different pixels in an image are from different ocean surface conditions and wind regimes. Thus, to be able to successfully determining the appropriate *v*, it is necessary to define an appropriate sample size (window) that can be used in the estimation. The window should be large enough to provide a stable estimate and small enough to be regarded as homogenous. Choosing a too small window, it is possible that the presence of a large enough vessel could influence the statistics to such an extent that it would not exceed the resulting threshold limit. It is important to make the calculation time as little as possible. Many different methods to determine *v* have been proposed in the literature. Methods based on moment estimates are discussed in (105). The ML approach provides the optimum parameter estimates. The ML approach is computationally very intensive and impractical to use. The solution must therefore be obtained numerically or by developing an alternative estimation scheme.

After determined a suitable PDF and *v*, one may set a threshold that supports detection with a CFAR. The threshold intensity, I_T, is determined by integrating the PDF, $p_X(I)$:

$$\eta_T = \int_0^{I_T} p(x)dx \tag{6.1}$$

where η_T is the specified probability of false alarm, e.g. ($1/10^{-7}$). With this value, for a typical ENVISAT ASAR image with 8500 x 7000 pixels, we would expect approximately 6 pixels to be wrong classified as vessels. The required false alarm rate is:

$$CFAR = 1 - \int_0^{I_T} p(x)dx \tag{6.2}$$

It is important that the CFAR threshold value is adaptive to how the ocean backscatter changes with incidence angle and with different ocean regions. Thus, it is important to choose appropriate sub swath width to minimize the change in mean backscatter from the ocean across the sub swath. A rule of thumb is that homogeneity in the ocean can not be assumed in more than 10 km x 10 km of the ocean. Non-stationarity can occur in smaller areas, for example in coastal areas. Thus, care must be taken when parameter estimation of “goodness of fit” relative to choice of sample size is carried out. A test must be done to determine the goodness of fit of the sample probability distribution to see if the estimated theoretical probability distribution fit. Two examples of goodness-of-fit estimators are the χ^2 test and the Kolmogorov-Smirnov (KS) test. The χ^2 statistics is given by:

$$\chi^2 = \sum_{t=1}^{N} \frac{(O_i - E_i)^2}{E_i} \tag{6.3}$$

N is the number of histogram bins, ($N > 1$), $E_1,\ldots,E_N$ are the expected frequency values in each bin, and $O_1,\ldots,O_N$ are the observed frequencies. The test is used to see how close the observed frequencies are to the expected frequencies, based on a theoretical probability distribution. If the fit is good, the numerator is small, and the test will be low, and vice versa. In contrast with the χ^2 test, which uses the nominal statistical relationships between the sampled and theoretical distributions, the KS test uses ordinal relationships on unbinned data. The maximum difference between the sampled and theoretical cumulative distributions is estimated with the KS test:

$$D = \max_{-\infty < x < \infty} \left| P(x) - S_M(x) \right| \tag{6.4}$$

Compared with the previously implemented model of the OFW, improved performance of ship targets is observed. Only a small number of preliminary RADARSAT-1 images were examined. A more general and simpler model may be more appropriate for tasks that will be performed by the OFW in the future.

6.4 An Automatic Approach to Ship Detection in Spaceborne Synthetic Aperture Radar Imagery: An Assessment of Ship Detection Capability using RADARSAT (344)

Precise and rapid reconnaissance of ships in coastal areas is vital for shipboard self-defence systems, ASW (Anti-Submarine Warfare), mine-hunting, and clearing systems. The paper examines the ship detection capability using various RADARSAT-1 SAR imaging modes. In addition, an automated procedure for ship and ship wake detection in SAR images is presented. Three approaches are examined for ship detection: 1) The combined Neural-Network-Dempster-Shafer (NNDS) morphology, 2) a statistical approach utilizing the K-distribution, and 3) Mathematical Morphology (MM). The multi-stage procedure can be used depending on requirements, computational resources, and scene composition. The methods differ in complexity and computational efficiency. The localized K-distribution can be used for scene segmentation and identification of scenes with possible ship targets. The coupled NNDS detection system is used to analyse the scene in more detail and for accountability of probabilities of occurrence of targets in conjunction with other oceanic features. The NNDS algorithm is the most computationally efficient. Compared with visual interpretations, the NNDS algorithm detects 97 % of the ships. The MM algorithm incorporates neighbouring information and signal amplitudes for target detection, and thus it is better suited for SAR imagery with low signal-to-clutter ratios. The algorithm is simple and computationally efficient, and is better than the NNDS algorithm to detect hard targets in clipped or thresholded imagery. It is recommended to use the K-distribution for scene-segmentation to identify regions, which have high possibility of including targets. Then the NNDS can be used to get the more precise location of the ship.

RADARSAT-1 images with different imaging geometry and beam modes were used to test the proposed methods. The Standard beam is much better for ship detection than the ScanSAR-narrow beam (due to poor radiometric resolution). At higher incidence angle the Standard beam S6 is recommended due to low clutter levels and high spatial-radiometric resolution. It is shown that it is possible to determine the ship's localization and extract the ship size and heading. The ship size tends to be overestimated by at least a factor of 2 for ScanSAR and 1.4 for Standard imagery. This depends on the azimuth viewing angle.

6.5 An Automatic Ship Detection System Using ERS SAR Images (404)

This paper presents the main algorithms in an Automatic Ship Detection (ASD) system. The system is mainly composed of a ship detector and a wake detector. The morphological filter in the post-processing procedures improves the detection accuracy and decreases the false target detection. The scan line based seed cluster algorithm is used to identify ships. The wake detection procedure is done much more quickly in the ASD by using the localized Hough transform compared to the conventional Hough transform.

Two ships can be mis-identified as one ship in the ASD if the distance between the two ships is less than three pixels. Estimation of ship parameters like the ship's length, direction, position, orientation and speed are also done. The results are considered reasonable.

6.6 Automatic Detection for Ship Targets in RADARSAT SAR Images from Coastal Regions (384)

The paper describes and assesses an automatic ship detection model using RADARSAT-1 SAR images. The program has been developed in the C programming language and UNIX operating system. It uses a moving window for ship detection. The algorithm first discriminates the land regions in a coastal image. A 19 pixels by 19 pixels moving window is used. An assumed land pixel is placed in the centre, and a filter examines the 360 neighbouring pixels. The centre pixel is considered a true land pixel if more than 47 neighbouring pixels are possible land pixels. A morphological filter (5 pixels by 5 pixels moving window) is used to extend the land region. If more than 5 neighbouring pixels of the 24 pixels around the centre pixel are possible land pixels, then all pixels in the window are considered land pixels. When sea and land have been separated, the next step in the algorithm is to detect ships in the sea region. The main problem of detecting ships in the sea region is to determine an analytical solution of the threshold value I_T. The threshold value is determined by integrating (3.10) to obtain (6.1). A morphological filter (7 pixels by 7 pixels moving window) is applied to eliminate the false ship pixels. Each image pixel examined is placed in the filter centre, and then the filter examines the 48 neighbouring pixels. The centre pixel is considered a ship pixel if more than 7 neighbouring pixels are possible ship pixels. SAR images with 16 bits were used to test the model.

6.7 Automatic Detection for Ship Targets in SAR Imagery Using PNN-model (382)

This paper describes the current process made on an automatic model for detection of ship targets. Using an image processing technique and a statistical method developed the model. It is an efficient method for data classification. The statistical Probabilistic Neural Networks (PNN) model is based on a non-parametric approach to estimate the Probability Density Function (PDF). The function is based on more statistical descriptions without using fixed parameters. It gives a good fit for gray-level image histograms of SAR images and smoothed estimated PDF. Thus, it is an efficient method for data classification, and it gives a good fit for gray-level image histograms of SAR images. Thus, the PNN-model is chosen for ship detection in SAR images instead of other statistical models like K-distribution and Gamma distribution. The algorithm is divided into three steps (see Figure 6.1):

- Estimating parameters
- Determining the threshold level
- Identifying ship targets

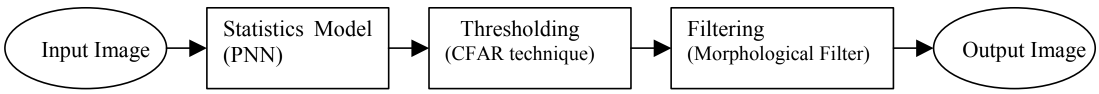

Figure 6.1 The ship detection algorithm

The PNN model has its roots in the Parzen window model. The Parzen window model is a class of kernel-based techniques for estimation of PDF. It suggests superposing a kernel function, on each data point, which occupies a fixed volume. The Parzen model uses the Gaussian distribution as a weight function, which is centred on each point of the training. The Parzen's window PDF is a linear combination of *N* Gaussians given by:

$$p(x) = \frac{1}{N}\sum_{n=1}^{N} G(x_n,\sigma)(x) \tag{6.5}$$

σ is the width of each Gaussian, and

$$G(x_n,\sigma)(x) = \frac{1}{\sqrt{2\pi\sigma}} e^{-\frac{(x-x_n)^2}{2\sigma^2}} \tag{6.6}$$

How to estimate σ is not easy, and the computational complexity is another disadvantage. The PNN architecture for one class of data is illustrated in Figure 6.2. Each data point is entering the network through the input layer. The learning set, which corresponds to many random points from the original image, is stored in the pattern layer. The values of the pattern layer are summed in the output layer.

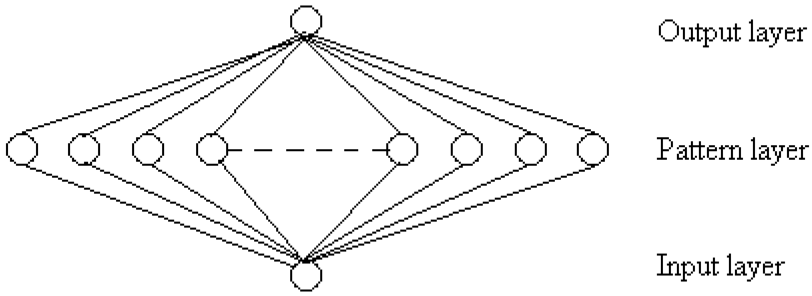

Figure 6.2 PNN model for one class of data.

The image is divided in small windows of size p x l (typical values of p and l are 3). The learning set is chosen randomly from the p x l window. A learning histogram can be constituted with the selected pixels, and the comparison data is chosen to be a median value of the resting pixels of the window (obtained using a median filter). The learning set is used to train the PNN, which results in a "learn historgram" (H_l). The learning procedure is done for each half value of σ, σ = 0.5, 1, 1.5,…, 9.5. H_l is compared to the "test histogram" (comparison data) for each value of σ. The σ-value, which gives the best minimum error, E_p, is chosen:

$$E_p = E_q + \eta \Delta H_l \tag{6.7}$$

where E_q is the quadratic error given by:

$$E_q = \sqrt{\frac{1}{2}\sum_{n=1}^{N}(H_t(n) - H_l(n))^2} \tag{6.8}$$

The Constant False Alarm Rate (CFAR) technique is based on the PNN-model. The CFAR detector makes target-in-clutter decision in high-resolution SAR images, and it is used to improve the ship target detection performance. Compared to the widely used K-distribution model, the PNN-model has given promising results in terms of processor and computation time. The research in this paper is a development of the research in (193).

6.8 Automatic Detection of Ships in RADARSAR-1 SAR Imagery (437)

The Alaska SAR Demonstration Program that was initiated by NOAA/NESDIS has the goal of "demonstrating the utility of RADARSAT-1 C-band SAR imagery to provide useful, timely environmental and resource management information to users in Alaska". The paper describes the algorithm developed to generate one of the products that is generated under the program, which is a list of ship locations. The algorithm uses changes in the local statistics to automatically detect ships. A local window is moved through the image, which determines statistically different regions. The algorithm is based on the CFAR approach. The mean over a small region is calculated as well as the mean and the standard deviation over an enclosing background region. If the signal mean is statistically different than the background, the mean values are compared.

Ships longer than 35-41 m can be detected using low-resolution imagery (100 m sample spacing) with threshold of 5.0. There were 105 ships out of a total of 272 in the test set longer than 35-41 m. This limit is dominated by the sample spacing. The false alarm rate was 0.01 % for a single detection. Using high-resolution imagery (50 m sample spacing) makes it possible to detect ships longer than 32 m (124 ships out of a the 272). In this case, the false alarm rate was 0.002 % for a single detection. It takes approximately 10 minutes to run the completely automated algorithm on a ScanSAR Wide B Mode image. The algorithm uses a threshold of 5.0 for the detection statistics.

6.9 Comparison of Probability Statistics for Automated Ship Detection in SAR Imagery (371)

The OMW is a commercial software suite. It is essentially a Constant False Alarm Rate (CFAR) filter, which provides modules for automated vessel detection, oil spill monitoring, and environmental monitoring. The paper presents the Ocean Monitoring Workstation's (OMW) ship detection algorithm applied to SAR data and the choice of probability distribution and methodologies for calculating scene specific statistics. The goal in the project has been to fine-tune the OMW algorithms. Focus has also been on false alarm rate of each algorithm. The results are compared using a 1-look, k-distribution function with various parameter choices and estimation methods. Two methods, which are used to fit the k-distribution to empirical data, are compared and contrasted:

- Estimates based on Mean and Variance (MV) of the data
- Estimates based on Mean of the data and Mean of the Log (MML)

The application of a χ^2-distribution is discussed as a special case of sea clutter statistics. The MML algorithm usually produces more false targets than the MV algorithm (at a CFAR of 10^{-8}). The χ^2 algorithm produces most false targets. The MML algorithm detects most of the targets that were visually detected by a trained military operator. Thus, the MML algorithm is the best compromise between detecting all significant targets and rejecting false targets. The SAR data used are collected with RADARSAT-1 during the Maritime Command Operation Training (MARCOT) exercise in Atlantic Canadian Waters in June 1998. Previously collected statistics are also taken into account.

6.10 Context-Based Target Detection with Multi-Pass RADARSAT-1 Data – Application to Coastal Surveillance (388)

This paper presents a data fusion simulation test bed. It demonstrates the fusion of target related features obtained when processing SAR imagery and information provided by other non-imaging sensors. The test bed's objective is to examine which conditions give the most complete description of the scene and the most precise identification of the surrounding targets. These projects were used to demonstrate how the incorporation contextual information could be used to improve the Target Detection/Target Recognition (TD/TR) algorithms.

Based on the results from the data fusion projects, the paper proposes to develop a methodology for change monitoring based on the fusion of contextual features extracted from multi-pass imagery. The main aspects and results obtained by the proposed approach are described. The data is collected over the Stephenville Bay Arena in Newfoundland.

6.11 Detection of Ships Using Cross-Correlation of Split-Look SAR Images (375)

This paper focuses on the problem of the presence of sea clutter in coherent imagery. The traditional approach is to utilize the difference of pixel intensity between ship and sea clutter, but these methods are not efficient in high sea states. A new technique, which is based on cross-correlating split-look SAR images, is proposed in the paper to solve this problem. The degree of mutual correlation increases if the inter-look images consist of the correlated images of a ship and clutter. The ships can be identified from the difference in correlation. Using this method, it is possible to detect ships without using the pixel intensities. This method was applied on RADARSAT-1 images (Standard mode, 30 m resolution) in fairly calm sea state (ships could be identified with the naked eye), and the minimum detectable ship length was 62.6 m. Further study is required in high sea states.

6.12 Exploiting the Polarimetric Information for the Detection of Ship Targets in Non-Homogeneous SAR Images (430)

The paper presents an approach for ship detection in polarimetric SAR images of non-homogenous ocean areas. It is necessary to extract the image structure and the impact of non-homogenous sea features on the False Alarm Rate. The paper also gives a description on how false alarms can be controlled by polarimetric segmentation procedures that cooperate with high-resolution polarimetric detection features. Real data is used to test polarimetric segmentation-plus-detection procedures to see if the method used in the project is satisfactory to utilize the polarimetric information in the SAR imagery. Testing the described approach indicated improved ship detection capabilities.

6.13 Model-Based Neural Network for Target Detection in SAR Images (422)

This paper discussed mathematical difficulties of combining *a priority* with adaptivity encountered in the past. A novel mathematical technique of neural-based neural network is introduced. The adaptive model combines *a priori* knowledge of the physical laws of electromagnetic scattering with adaptation to the actual environment. The combination is achieved with linear computational complexity without considering multiple combinations of models and parameters.

Applications of this model for target detection in Synthetic Aperture Radar (SAR) images are discussed. The model has successfully detected small, low-signature targets in heavy clutter environments. The model was also successful demonstrated in single-pixel detection of resolved multi-pixel targets. By combining adaptivity and *a priori* knowledge, multi-pixel models can be developed.

The principles of SAR are briefly described, relatively simple physics-based models of SAR signals are derived, and finally model-based neural networks that utilize these models are described. Examples of real-world applications are presented.

6.14 Optimal Target Detection Using One Channel SAR. Complex Imagery: Application to Ship Detection (408)

Point targets often have higher radar reflectivity than the cluttered background. Due to the speckle, the backscattered signal has high variability, especially with one-look, and point targets may be confused with high speckle peaks. The paper presents a proposed solution to this problem; optimal target detection based on radiometric criteria. The LRT (Likelihood Ratio Test) permits to choose between two hypotheses, and can be used if the target can be modelled by a Gaussian circular signal. This leads to a radiometric criterion algorithm. Optimal radiometric estimation by means of Spatial Whitening Filter (SWF), which also takes spatial correlation into account, can be used in complex images to optimise the estimation of the radiometry. The paper presents an example of a complex fine mode RADARSAT-1 image used for ship detection that was acquired over the coastal town Toulon, France on September 2nd, 1997. The sea state was very calm and the wind was low. Some targets are easily recognized, while others are more difficult to detect. Thresholding makes the detection easier.

6.15 Probabilistic Winner-Take-All Segmentation of Images with Application to Ship Detection (418)

The paper presents the neural clustering scheme “Probabilistic Winner-Take-All” (PWTA). It is applied to image segmentation, and the desired properties for image segmentation is examined. The PWTA adapts the form of cluster-conditional probability density function while clustering proceeds, and thus avoids under-utilization of clusters. The probability of being adapted for an input vector that is sufficiently far from its mean decreases if a cluster gets adapted frequently. To be able to utilize the spatial continuity of image regions and improve the PWTA segmentation performance a modification to PWTA is introduced. The spatial continuity of image regions is utilized through the inclusion of *a priori* probabilities. The probabilities depend on the input feature space, and are estimated for each image pixel. Segmentation of airborne SAR images is used to demonstrate the effectiveness of PWTA for ship detection. An approach is proposed to find the suitable number of clusters required for ship detection. 87.5 % of the ships are being detected using the PWTA. The scheme gives significantly better results than four other segmentation techniques, 1) K-means, 2) Maximum Likelihood (ML), 3) Back Propagation Network (BPN), and 4) histogram thresholding.

6.16 Results from the Ocean Monitoring Workstation (OMW) Dark Feature Detection Algorithm (433)

The Ocean Monitoring Workstation (OMW) extracts marine information from RADARSAT-1 SAR ocean images. Examples of applications are ship detection, calculation of two-dimensional wave spectra, extraction of wind vector information, classification of ocean features, and detection of dark features such as oil spill and natural biological slicks. Before the exercise, described in this paper, the ship detection configuration parameters were tuned as a function of the CDPF (Canadian Data Processing Facility) product and beam mode (115). This paper presents a similar exercise to define a set of parameters for the dark feature detection algorithm as well as to make recommendations to improve the algorithms. Results from the wind retrieval algorithm are also presented. The following conclusions and recommendations are given in the paper (as written in the paper):

1. A routine to merge fragmented slicks based on a proximity flag and distance parameter should be implemented to reduce the number of small slicks detected and to provide a more accurate account of the slick size.
2. Imagery should be processed through the OMW wind retrieval algorithm together with the dark feature detection algorithm. Oil slick results should be interpreted in the context of the wind products and vice versa.
3. The dark feature algorithm has limited reliability. The incorporation of other slick and edge detectors, such as texture and wavelet-based algorithms, as well as the used of classification techniques, should improve the utility of the algorithm.
4. The configuration parameters suggested above provide a general starting point for operation of the algorithm. Several of the parameters (in particular the minimum and the maximum areas and the target threshold) may need to be iteratively modified on a case by case basis, especially if ancillary oil slick data and wind speed information are available.

5. The OWM configuration routines for dark feature detection should be redesigned so that the **Threshold Win Wd** and **Threshold Win Ht** parameters are specified in distance, not pixels. This will avoid the necessity of dynamically changing these parameters based on CDPF product type and beam mode.
6. We suggest that the dark feature detection algorithm **Minimum Area** and **Maximum Area** configuration parameters, as well as the area of the dark features output in the products, be specified in km^2 rather than m^2.
7. The wind retrieval algorithm calculates wind vector information for the pre-set frames of the $25km^2$ in size. A “frame size” parameters should be included in the configuration parameters set so that the value can be modified based on CDPF product type and beam mode.
8. The maximum wind speed which can be calculated by the wind retrieval algorithm is currently hardwired to 15 m/s. This hardlimit should be removed.

6.17 SAR ATR Performance Using a Conditionally Gaussian Model (419)

The paper presents a family of conditionally Gaussian signal models for SAR images. These models are an extension of a class of models developed for high-resolution radar range profiles. The target type and the relative orientations of the sensor, target, and ground plane parameterize the model. Algorithms that estimate both the target type and pose are developed based on this model. The direct extension of the conditionally Gaussian model used successfully to model high resolution radar range profiles (377)-(379) is given by:

$$l(\vec{r} \mid \Theta, a) = \sum_i \left[-\ln(K_{i,i}(\Theta, a) + N_0) - \frac{|r_i|^2}{K_{i,i}(\Theta, a) + N_0} \right] \tag{6.9}$$

K is the diagonal covariance matrix, $l(\vec{r} \mid \Theta, a)$ is the log-likelihood function, a is the target type, and $K_{i,i}(\Theta, a)$ is the covariance matrix.

Results of performance on data from the MSTAR (Moving and Stationary Target Acquisition) program for target pose estimation and target recognition are presented. The recognition rates are over 97 % for a ten class problem under standard operating conditions, while the rates are 81 % for a four class problem under configuration operating conditions, and 79 % for a four class problem under version variation extended operating conditions. The configuration and version variants can be incorporated into one model. This model gives good ATR (Automatic Target Recognition) performance for the test data.

6.18 Segmentation-Based Technique for Ship Detection in SAR Images (407)

The paper describes a segmentation-based ship detection scheme in SAR images. It also deals with the typical features of sea clutter. It is shown that it is not possible to adequate control the false-alarm rate for non-homogeneity and non-gaussianity characteristics of backscattering from the sea by applying the standard 2D-CFAR schemes on low- and high-resolution SAR images. An appropriate first segmentation stage is proposed as an alternative, which allows standard CFAR techniques to be applied inside homogenous areas. The detection threshold can be set to achieve the desired false alarm rate by using the derived approximate CFAR techniques against non-gaussian clutter. A set of low-resolution quick-look ERS SAR images and a set of high-resolution single-look X-SAR/SIR-C images are used to test the scheme. Both sets show that the scheme gives very high probability for ship detection and that the false alarm rate is low.

6.19 Ship Detection by the RADARSAT SAR: Validation of Detection Model Predictions (435)

A well-known problem for ship detection is the sea background clutter. The sea clutter increases and the ship detection probability decreases with increased wind speeds and decreasing incidence angle. To improve ship detection probability, larger incidence angles should be used. Analyses of the use of ERS-1 SAR data for ship detection have shown considerable success. The approach of first using the ship signature as the primary ship indicator, and the ship wake as the secondary indicator, has been used in Norway. Analyses of the ship wake may give additional information about the ship and its velocity. This approach is attractive because it provides a theoretical basis for selecting a CFAR.

RADARSAT-1 operates in the C-band with HH-polarization. The paper describes a statistical approach for analyses of ship detection performance in a clutter background of the RADARSAT-1 SAR, as well as it compares the different beam modes of RADARSAT-1 SAR. The RADARSAT-1 SAR model includes ocean clutter, image PDF, and ship cross-section elements. To be able to detect smaller ships, low wind is necessary, high-resolution image, as well as large incidence angles. The ScanSAR Narrow Far mode is a good compromise between the spatial coverage and detection probability. Data has been collected during a RADARSAT-1 SAR ship detection/validation field program held off the coast of Halifax, Nova Scotia in March/April 1996. The data was used to validate the RADARSAT-1 SAR ship detection model, and the results are excellent. It was shown that the:

- Hybrid C-band HH-polarization cross-section model is excellent for the conditions encountered.
- K-distribution is a suitable PDF for RADARSAT-1 ocean images.
- Simple model for ship cross-section is within the correct order of magnitude.

- Model tends to underestimate the ship cross section especially at larger incidence angles.

A Figure of Merit (FOM) has been defined in for a minimum detectable vessel size as a function of incidence angle, for a wind speed of 10 m/s and a radar look direction opposite to the wind direction. Using the FOM, it is possible to do a relative comparison of the available RADARSAT-1 beam modes. In addition it is possible to select the optimal RADARSAT-1 beam modes based on surveillance requirements

6.20 Literature

(341) Ahn, JS and B Bhanu (2002): Model-Based Recognition of Articulated Objects, Pattern Recognition Letters, Vol. 23, No. 8, pp. 1019-1029.

(342) Alparone, L, F Argenti and G Benelli (1991): A Fuzzy Complete SAR Processing Chain for Ship detection and Velocity Estimation, European Trans on Telecomm and Related Tech, Vol. 2, No. 6, pp. 689-693, Italy.

(343) Asdornwised, W and S Jitapunkul (2003): Automatic Target Recognition Using Multiple Description Coding Models for Multiple Classifier Systems, Multiple Classifier Systems. Lecture Notes in Computer Science, Vol. 2709, Springer-Verlag, Berlin Heidelberg New York, pp. 336-345.

(344) Askari, F and B Zerr (2000): An Automatic Approach to Ship Detection in Spaceborne Synthetic Aperture Radar Imagery: An Assessment of Ship Detection Capability Using RADARSAT, NATO Saclant Undersea Research Centre Report, Saclantcen Report, Serial no: SR-338.

(345) Askari, F and B Zerr: A Neural-Network-Fusion Architecture for Automatic Extraction of Oceanographic Features from Satellite Remote Sensing Imagery, SACLANTCEN SR-306.

(346) Banerjee, A, P Burlina and R Chellappa. Adaptive Target Detection in Foliage-Penetrating SAR Images Using Alpha-Stable Models, IEEE Trans on Image Proc, Vol. 8, No. 12, pp. 1823-1831, Dec 1999.

(347) Benelli, G, A Garzelli and A Mecocci (1994): Complete Processing System that Uses Fuzzy-Logic for Ship Detection in SAR Images, IEE Proc Radar, Sonar and Navig, Vol. 141, No. 4.

(348) Berenyi, HM, VF Leavers and RE Burge (1992): Automatic Detection of Targets Against Cluttered Backgrounds Using a Fractal-Oriented Statistical-

Analysis and Radon-Transform, *Pattern Recognition Letters*, Vol. 13, No. 12, pp. 869-877.

(349) Berizzi, F and G Corsini. A New Fast Method for the Reconstruction of 2-D Microwave Images of Rotating Objects, IEEE Trans on Image Proc, Vol. 8, No. 5, pp. 679-687, May 1999.

(350) Bernardon, AM and JE Carrick (1995): A Neural System for Automatic Target Learning and Recognition Applied to Bare and Camouflaged SAR Target, *Neural Networks*, Vol. 8, No. 7-8, pp. 1103-1108.

(351) Bhanu, B and G Jones (2000): Recognizing Target Variants and Articulations in Synthetic Aperture Radar Images, Optical Eng, Vol. 39, No. 3, pp. 712-723.

(352) Bhanu, B and G Jones (2002): Increasing the Discrimination of Synthetic Aperture Radar Recognition Models, *Optical Eng*, Vol. 41, No. 12, pp. 3298-3306.

(353) Bhanu, B and YQ Lin (2003): Genetic Algorithm Based Feature Selection for Target Detection in SAR Images, *Image and Vision Computing*, Vol. 21, No. 7, pp. 591-608.

(354) Bhanu, B, YQ Lin, G Jones and J Peng (2000): Adaptive Target Recognition, Machine Vision and Appl, Vol. 11, No. 6, pp. 289-299.

(355) Borden, B (1997): Some Issues in Inverse Synthetic Aperture Radar Image Reconstruction, Inverse Problems, Vol. 13, No. 3, pp. 571-584.

(356) Boshra, M and Bhanu (2001): Predicting an Upper Bound on SAR ATR Performance, *IEEE Trans on Aerosp and Elect Syst*, Vol. 37, No. 3, pp. 876-888.

(357) Burgess, DW (1993): Automatic Ship Detection In Satellite Multispectral Imagery, *Photogrammetric Eng and Rem Sens*, Vol. 59, No. 2, pp. 229-237.

(358) Chan, HL and TS Yeo (2002): Comments on "Non-Iterative Quality Phase-Gradient Autofocus (QPGA) Algorithm for Spotlight SAR Imagery", *IEEE Trans on Geosc and Rem Sens*, Vol. 40, No. 11, pp. 2517-2517.

(359) Chen, HC and CD McGillem (1992): Target Motion Compensation by Spectrum Shifting in Synthetic Aperture Radar, *IEEE Trans on Aerosp and Elect Syst*, Vol. 28, No. 3, pp. 895-901.

(360) Chia, KN, HJ Kim, S Lansing, WH Mangione-Smith and J Villasenor (1998): High-Performance Automatic Target Recognition Through Data-Specific VLSI, *IEEE Trans on Very Large Scale Integration Systems*, Vol. 6, No. 3, pp. 364-371.

(361) Cloude, SR and E Pottier (1997): A Review of Target Decomposition Theorems in Radar Polarimetry, *IEEE Trans on Geosc and Rem Sens*, Vol. 35, No. 2, pp. 498-518.

(362) Damini, A, G Haslam, B Balaji and M Goulding (2004): A New X-band Experimental Airborne Radar for SAR and GMTI, 5th Conference on Synthetic Aperture Radar, EUSAR 2004, Ulm, Germany.

(363) DeVore, MD and JA O'Sullivan (2002): Performance Complexity Study of Several Approaches to Automatic Target Recognition from SAR Images, *IEEE Trans on Aerosp and Elect Syst*, Vol. 38, No. 2, pp. 632-648.

(364) DeVore, MD and JA O'Sullivan (2003): Target-Centered Models and Information-Theoretic Segmentation for Automatic Target Recognition, *Multidim Systems and Signal Proc*, Vol. 14, No. 1-3, pp. 139-159.

(365) Driggers, RG and JA Ratches, JC Leachtenauer and RW Kistner (2003): Synthetic Aperture Radar Target Acquisition Model Based on a National Imagery Interpretability Rating Scale to Probability of Discrimination Conversion, *Optical Eng*, Vol. 42, No. 7, pp. 2104-2112.

(366) El-Rouby, AE, AY Nashashibi and FT Ulaby (2003): Application of Frequency Correlation Function to Radar Target Detection, *IEEE Trans on Aerosp and Elect Syst*, Vol. 39, No. 1, pp. 125-139.

(367) Ender, JHG and AR Brenner (2003): PAMIR - a Wideband Phased Array SAR/MTI System, IEE Proc Radar, Sonar and Navig, Vol. 150, No. 3, pp. 165-172.

(368) Fienup, JR (2001): Detecting Moving Targets in SAR Imagery by Focusing, IEEE Tans on Aerosp and Elect Syst, Vol. 37, No. 3, pp. 794-809.

(369) Foulkes, SB (2000): Ship Detection in ERS-1 and RADARSAT SAR Images Using a Self-Organising Neural Network, AMRS Ship Detection Workshop, 31 May - 2 June, 2000.

(370) Gierull, CH (2001): Unbiased Coherence Estimator for SAR Interferometry with Application to Moving Target Detection, *Elect Letters*, Vol. 37, No. 14, pp. 913-915.

(371) Henschel, MD, MT Rey, JWM Campbell and D Petrovic (1998): Comparison of Probability Statistics for Automated Ship Detection in SAR Imagery, Proc of the Int Conf on Appl of Photonic Technology (ICAPT'98), Int Society for *Optical Eng*, Bellingham, Washington.

(372) Howard, D and J Schroeder (1999): Multiscale Models for Target Detection and Background Discrimination in Synthetic Aperture Radar Imagery, *Digital Signal Processing*, Vol. 9, No. 3, pp. 149-161.

(373) Howard, D, SC Roberts and R Brankin (1999): Evolution of Ship Detectors for Satellite SAR Imagery, Genetic Programming Lecture Notes in Comp Science 1598, pp. 135-148.

(374) Howard, D, SC Roberts, and R Brankin (1999): Target Detection in SAR Imagery by Genetic Programming, Advances in Engineering Software, Vol. 30, No. (5), pp. 303 - 311.

(375) Iehara, M, K Ouchi, I Takami, K Morimura and S Kumano (2001): Detection of Ships Using Cross-Correlation of Split-Look SAR Images, *IEEE Trans on Geosc and Rem Sens* Symp (IGARSS '01), Vol. 4, pp. 1807-1809, Sydney, Australia.

(376) Irving, WW, LM Novak and AS Willsky (1997): A Multiresolution Approach to Discrimination in SAR imagery, *IEEE Trans on Aerosp and Elect Syst*, Vol. 33, No. 4, pp. 1157-1169.

(377) Jacobs, SP (1997): Automatic Target Recognition Using High Resolution Radar Range-Profiles, Ph.D. Dissertation, Washington University, St. Louis, MO, May 1997.

(378) Jacobs, SP and JA O'Sullivan (1997): Automatic Target Recognition Using Sequences of High Resolution Radar Range-Profiles, IEEE Transactions on Aerospace and Electronic Systems, Vol. 36, No. 2, pp. 364-382.

(379) Jacobs, SP and JA O'Sullivan (1997): High-Resolution Radar Models for Joint Tracking and Recognition, Automatic Target Recognition VII (Proc of SPIE), Vol. 3069, pp. 94-105.

(380) Jao, JK, CF Lee and S Ayasli (1999): Coherent Spatial Filtering for SAR Detection of Stationary Targets, *IEEE Trans on Aerosp and Elect Syst*, Vol. 35, No. 2, pp. 614-626.

(381) Jiang, Q (2002): Detection System for Ship Targets in SAR Imagery, PhD Thesis, Université de Sherbrooke, Canada.

(382) Jiang, Q, E Aitnouri, S Wang and D Ziou (1998): Automatic Detection for Ship Targets in SAR Imagery Using PNN-model, ADRO Symposium'98 in Montreal, Canada.

(383) Jiang, Q, S Wang and D Ziou: A System for Ship Detection from SAR Imagery Using Different PDF Models, Workshop for Ship Detection in Coastal Waters, Halifax, May 31-June 2.

(384) Jiang, Q, S Wang, D Ziou and A El Zaart (1999): Automatic Detection for Ship Targets in RADARSAT SAR Images from Coastal Regions, Vision Interface '99, Trois-Rivieres, Canada.

(385) Jiang, Q: Statistical Modelling in Ship Target Detection, PhD Thesis, Université de Sherbrooke, Canada.

(386) Jin, YQ and Y Chen (2002): An Improved Minimum Entropy Method for Refocusing the Moving Target Image in Synthetic Aperture Radar Observations, *Imaging Science J*, Vol. 50, No. 3, pp. 591-608.

(387) Jishuang, Q, W Chao and W Zhengzhi (2003): Structure-Context Based Fuzzy Neural Network Approach for Automatic Target Detection, *IEEE Int Geosc and Rem Sensing Symp* (IGARSS'03), Toulouse, France.

(388) Jouan, A and Y Marcoz (2001): Context-Based Target Detection with Multi-Pass RADARSAT-1 Data – Application to Coastal Surveillance, ASAR 2001 Workshop, Canadian Space Centre, Québec, Canada.

(389) Kaplan, LMi (2001): Improved SAR Target Detection Via Extended Fractal Features, *IEEE Trans on Aerosp and Elect Syst*, Vol. 37, No. 2, pp. 436-451.

(390) Kashyap, S and A Louie (2001): Computational RCS Analysis and Technique for Precise Location of the Hot Spots on the Concept Ship ALSC, Defence Research Establishment Ottawa Technical Note # 2001-03, DREO, Ottawa, ON.

(391) Khabou, MA, PD Gader and HC Shi (1999): Entropy Optimized Morphological Shared-Weight Neural Networks, *Optical Eng,* Vol. 38, No. 2, pp. 263-273.

(392) Khabou, MA, PD Gader and JM Keller (2000): LADAR Target Detection Using Morphological Shared-Weight Neural Networks, *Machine Vision and Appl*, Vol. 11, No. 6, pp. 300-305.

(393) Klemm R (19951): Adaptive Airborne MTI with 2-Dimensional Motion Compensation, *IEE Proc Radar and Signal Processing*, Vol. 138, No. 6, pp. 551-558.

(394) Koch, MW, MM Moya, LD Hostetler and RJ Fogler (1995): Cueing, Feature Discovery, and One-Class Learning for Synthetic Aperture Radar Automatic Target Recognition, *Neural Networks*, Vol. 8, No. 7-8, pp. 1081-1102.

(395) Kothari, R and D Ensley (1998): Function Approximation Framework for Region of Interest Determination in Synthetic Aperture Radar Images, Optical Eng, Vol. 37, No. 10, pp. 2817-2825.

(396) Krishnapuram, B, J Sichina and L Carin (2003): Physics-Based Detection of Targets in SAR Imagery Using Support Vector Machines, IEEE Sensors J, Vol. 3, No. 2, pp. 147-157.

(397) Larson, V, L Novak and C Stewart (1994): Joint Spatial-Polarimetric Whitening Filter to Improve SAR Targets Detection Performance for Spatially Distributed Targets, Proc of the Algorithm for Synthetic Aperture Radar Imagery, Vol. 22, No. 30, pp.285-301.

(398) Li, J, RB Wu and VC Chen (2001): Robust Autofocus Algorithm for ISAR Imaging of Moving Targets, *IEEE Trans on Aerosp and Elect Syst*, Vol. 37, No. 3, pp. 1056-1069.

(399) Li, J, Z Bi, ZS Liu and K Knaell (1995): Use of Curvilinear SAR for Three-Dimensional Target Feature Extraction, *IEE Proc Radar, Sonar and Navig*, Vol. 144, No. 5, pp. 275-283.

(400) Li, J, ZS Liu and P Stoica (1997): 3-D Target Feature Extraction Via Interferometric SAR, *IEE Proc Radar, Sonar and Navig*, Vol. 144, No. 2, pp. 71-80.

(401) Li, JA and EG Zelnio (1996): Target Detection with Synthetic Aperture Radar, *IEEE Trans on Aerosp and Elect Syst*, Vol. 32, No. 2, pp. 613-627.

(402) Liu, G, H Li and J Li (2000): Moving Target Feature Extraction with Polarisation Diversity in the Presence of Arbitrary Range Migration and Phase Errors, *IEE Proc Radar, Sonar and Navig*, Vol. 147, No. 4, pp. 208-216.

(403) Liu, J and KC Chang (1996): Feature-Based Target Recognition with a Bayesian Network, Optical Eng, Vol. 35, No. 3, pp. 701-707.

(404) Liu, Y, M Fang, Q Feng and L Wang (2003): An Automatic Ship Detection System Using ERS SAR Images, IEEE.

(405) Liu, ZS, RB Wu and J Li (1999): Complex ISAR Imaging of Maneuvering Targets Via the Capon Estimator, *IEEE Trans on Signal Proc*, Vol. 47, No. 5, pp. 1262-1271.

(406) Livingstone, CE, I Sikaneta, CH Gierull, S Chiu, A Beaudoin, J Campbell, J Beaudoin, S Gong and TA Knight (2002): An Airborne Synthetic Aperture Radar (SAR) Experiment to Support RADARSAT-2 Ground Moving Target Indication (GMTI), *Can J Rem Sens*, Vol. 28, No. 6, pp. 794 - 813, Canada.

(407) Lombardo, P and M Sciotti (2001): Segmentation-Based Technique for Ship Detection in SAR Images, *IEE Proc Radar, Sonar and Navig* (Special Issue), Vol. 148, No. 3, pp. 147-159.

(408) Lopès, A, J Bruniquel, F Sery, J-C Souyris and F Adragna (1998): Optimal Target Detection Using One Channel SAR. Complex Imagery: Application to Ship Detection, Proc of IGARSS'98, Seattle, WA, USA.

(409) Man, JZ, GQ Liu, J Li and R Williams (2000): A Quasi-Parametric Algorithm for Synthetic Aperture Radar Target Feature Extraction and Imaging with Angle Diversity, *Circuits and Signal Processing*, Vol. 19, No. 4, pp. 301-319.

(410) Marcum, JI (1960): A Statistical Theory of Target detection By Pulsed Radar, IRE Trans, Vol. IT-6, pp. 59-267.

(411) Moreira, JR and W Keydel (1995): A New MTI-SAR Approach Using the Reflectivity Displacement Method, *IEEE Trans on Geosc and Rem Sens*, Vol. 33, No. 5, pp. 1238-1244.

(412) Nilubol, C, RM Mersereau and MJT Smith (2002): A SAR Target Classifier Using Radon Transforms and Hidden Markov Models, Digital Signal Processing, Vol. 12, No. 2-3, pp. 274-283.

(413) Novak, LM, GJ Owirka and AL Weaver (1999): Automated Target Recognition Using Enhanched Resolution SAR Data, *IEEE Trans on Aerosp and Elect Syst*, Vol. 35, No. 1, pp. 157-174.

(414) Novak, LM, GJ Owirka and CM Netishen (1994): Radar Target Identification Using Spatial Matched-Filters, *Pattern Recognition Letters*, Vol. 27, No. 4, pp. 607-617.

(415) Novak, LM, MC Burl and WW Irving (1993): Optimal Polarimetric Processing for Enhanced Target Detection, *IEEE Trans on Aerosp and Elect Syst*, Vol. 29, No. 1, pp. 234-244.

(416) Novak, LM, SD Halversen, GJ Owirka and M Hiett (1996): Effects of Polarization and Resolution on the Performance of a SAR Automatic Target Recognition System, Archiv fur Elektronik und Ubertragungstechnik (AEU) - Int J of Electronics and Comm, Vol. 50, No. 2, pp. 92-99.

(417) Novak, LM, SD Halversen, GJ Owirka and M Hiett (1997): Effects of Polarization and Resolution on SAR ATR, *IEEE Trans on Aerosp and Elect Syst*, Vol. 33, No. 1, pp. 102-116.

(418) Osman, H and SD Blostein (2000): Probabilistic Winner-Take-All Segmentation of Images with Application to Ship Detection, *IEEE Trans on Systems Man and Cybernetics Part B-Cybernetics*, Vol. 30, No. 3, pp. 485-490.

(419) O'Sullivan, JA, MD DeVore, V Kedia and MI Milleri (2001): SAR ATR Performance Using a Conditionally Gaussian Model, *IEEE Trans on Aerosp and Elect Syst*, Vol. 37, No. 1, pp. 91-108.

(420) Park, SI, MJT Smith and RM Mersereau (2000): Target Recognition Based on Directional Filter Banks and Higher-Order Neural Networks, Digital Signal Processing, Vol. 10, No. 4, pp. 297-308.

(421) Penney, R (1997): Report on Automatic Identification System Installed at VTS Tofino, Department of Fisheries and Oceans, DFO/5513.

(422) Perlovsky, LI, WH Schoendorf, BJ Burdick and DM Tye. Model-Based Neural Network for Target Detection in SAR Images, IEEE Trans on Image Proc, Vol. 6, No. 1, pp. 203-216, Jan 1997.

(423) Principe, JC, A Radisavljevic, J Fisher, M Hiett and LM Novak (1998): Target Prescreening Based on a Quadratic Gamma Discriminator, *IEEE Trans on Aerosp and Elect Syst*, Vol. 34, No. 3, pp. 706-715.

(424) Principe, JC, M Kim and JW Fisher. Target Discrimination in Synthetic Aperture Radar Using Artificial Neural Networks, IEEE Trans on Image Proc, Vol. 7, No. 8, pp. 1136-1149, Aug 1998.

(425) Qingshan, J: Statistical Analysis of SAR Images and Its Application in Ship Detection, PhD Thesis, Université de Sherbrooke, Canada.

(426) Rewo, L (1984): Enhancement and Detection of Convex Objects Using Regression Models, *Computer Vision, Graphics, and Image Processing* Vol. 25, pp. 257-269.

(427) Rey, MT, A Drosopoulos and D Petrovic (1996): A Search Procedure for Ships in RADARSAT Imagery, Tech Report No. 35, Defence Research Establishment Ottawa, Ottawa, Canada.

(428) Richards, JA, AS Willsky and JW Fisher (2002): Expectation-Maximization Approach to Target Model Generation from Multiple Synthetic Aperture Radar Images, *Optical Eng*, Vol. 41, No. 1, pp. 150-166.

(429) Runkle, P, LH Nguyen, JH McClellan and L Carin (2001): Multi-Aspect Target Detection for SAR Imagery Using Hidden Markov Models, *IEEE Trans on Geosc and Rem Sens*, Vol. 39, No. 1, pp. 46-55.

(430) Sciotti, M, D Pastina and P Lombardo (2002): Exploiting the Polarimetric Information for the Detection of Ship Targets in Non-Homogeneous SAR Images, IEEE.

(431) Sun, H, GS Liu, H Gu and WM Su (2002): Application of the Fractional Fourier Transform to Moving Target Detection in Airborne SAR, *IEEE Trans on Aerosp and Elect Syst*, Vol. 38, No. 4, pp. 1416-1424.

(432) Sun, HB, SL Wang, GS Liu and JL Ni (2003): The Changeable Sampling-Rate Processing Technology with Application to SAR-MTD, *Int J Rem Sens*, Vol. 24, No. 15, pp. 3033-3047.

(433) Thomas, SJ, PW Vachon and J Cranton (1997): Results from the Ocean Monitoring Workstation (OMW) Dark Feature Detection Algorithm.

(434) Ulug, B, SC Ahalt, RA Mitchell (1997): Efficient ATR Using Compression, *IEEE Trans on Aerosp and Elect Syst*, Vol. 33, No. 4, pp. 1199-1211.

(435) Vachon PW, JW Campbell, C Bjerkelund, FW Dobson and MT Rey (1996): Ship Detection by the RADARSAT SAR: Validation of Detection Model Predictions, Proc of the Pacific Ocean Rem Sens Conf (PORSEC'96), Victoria, BC, Canada.

(436) Vachon, PW, JWM Campbell, CA Bjerklund, FW Dobson and MT Rey (1997): Ship Detection by the RADARSAT SAR: Validation of Detection Model Predictions, *Can J Rem Sens*, Vol. 23. No. 1, pp. 48-59, Canada.

(437) Wackerman, CC, KS Friedman, WG Pichel, P Clemente-Colón and X Li (2001): Automatic Detection of Ships in RADARSAT-1 SAR Imagery, *Can J Rem Sens*, Vol. 27. No. 4, pp. 371-378, Canada.

(438) Wackerman, CC, P Clemente-Colón, WG Pichel and XF Li (2002): A Two-Scale Model to Predict C-band VV and HH Normalized Radar Cross Section Values Over the Ocean, *Can J Rem Sens*, Vol. 28, No. 3, pp. 367 - 384, Canada.

(439) Wang GY, XG Xia, BT Root and VC Chen (2003): Moving Target Detection in Over-the-Horizon Radar Using Adaptive Chirplet Transform, Radio Science, Vol. 38, No. 4
(Art.no. 1062).

(440) Wang, G, XG Xia, BT Root, VC Chen, Y Zhang and M Amin (1991): Manoeuvring Target Detection in Over-the-Horizon Radar Using Adaptive Clutter Rejection and Adaptive Chirplet Transform, *IEE Proc Radar, Sonar and Navig*, Vol. 150, No. 4, pp. 292-298.

(441) Weaver, S and K Wagner (1995): Nonlinear Techniques in Optical Synthetic-Aperture Radar Image Generation and Target Recognition, *Applied Optics*, Vol. 34, No. 20, pp. 3981-3996.

(442) Werness, S, W Carrara, L Joyce and D Franczak (1990): Moving Target Imaging Algorithm for SAR Data, *IEEE Trans on Aerosp and Elect Syst*, Vol. 26, No. 1, pp. 57-67.

(443) Williams, R, J Westerkamp, D Gross and A Palomino (2000): Automatic Target Recognition of Time Critical Moving Targets Using 1D high Range Resolution (HRR) Radar, IEEE Aerospace and Electronic Systems Magazine, Vol. 15, No. 4, pp. 37-43.

(444) Yongjian, Y, H Shun-Ji and A Torre (1995): Development of an Automatic Target Detection and Characterisation System in Polarimetric SAR Images, Proc of IGARRS'95, Florence.

(445) Yoo, JC and YS Kim (2001): A Reverse-SAR (R-SAR) Algorithm for the Detection of Targets Buried in Ground Clutter, *Microwave and Optical Tech Letters*, Vol. 28, No. 2, pp. 121-126.

(446) Zhang, GF and L Tsang (1998): Application of Angular Correlation Function of Clutter Scattering and Correlation Imaging in Target Detection, *IEEE Trans on Geosc and Rem Sens*, Vol. 36, No. 5, pp. 1485-1493.

(447) Zhang, GF, L Tsang, and Y Kuga (1998): Numerical Studies of the Detection of Targets Embedded in Clutter by Using Angular Correlation Function and Angular Correlation Imaging, *Microwave and Optical Tech Letters*, Vol. 17, No. 2, pp. 82-86.

(448) Zhang, MJ, VB Ciesielski and P Andreae (2003): A Domain-Independent Window Approach to Multiclass Object Detection Using Genetic Programming, EURIASP, J on Signal Processing, Special Issue on Genetic and Evolutionary Computation for Signal Processing and Image Analysis, Vol. 8, pp. 841–859.

(449) Zhao, Q and JC Principe (2001): Support Vector Machines for SAR Automatic Target Recognition, *IEEE Trans on Aerosp and Elect Syst*, Vol. 37, No. 2, pp. 643-654.

(450) Zhao, Q, JC Principe, VL Brennan, DX Xu and Z Wang (2000): Synthetic Aperture Radar Automatic Target Recognition with Three Strategies of Learning and Representation, *Optical Eng*, Vol. 39, No. 5, pp. 1230-1244.

7 CLASSIFICATION

7.1 Overview

The following table gives an overview of publications on the theme “Classification” sorted after publication year. The reports are primarily about exploitation of target signatures for determination of classes of various ships. Summaries of a selection of some of the most important and available papers are given following the table.

YEAR	TITLE	AUTHOR	PUBLISHED
2003	Impact of ScanSAR Images’ Radiometric Calibration on Vessels and Identificatio	Aresu, E and G Schwartz	IEEE Int Geosc and Rem Sensing Symp (IGARSS'03), Toulouse, France.
2003	The SSCM for Ship Characterization Using Polarimetric SAR	Touzi, R and F Charbonneau	IEEE Int Geosc and Rem Sensing Symp (IGARSS'03), Toulouse, France.
2002	Composite Filters for Inverse Synthetic Aperture Radar Classification of Small Ships	Yuan, C and D Casasent	Optical Eng, Vol. 41, No. 1, pp. 94-104.
2002	Improved Target Classification Using Optimum Polarimetric SAR Signatures	Sadjadi, F	IEEE Trans on Aerosp and Elect Syst, Vol. 38, No. 1, pp. 38-49.
2000	Performance of 10-and 20-target MSE Classifiers	Novak, LM, GJ Owirka and WS Broweri	IEEE Trans on Aerosp and Elect Syst, Vol. 36, No. 4, pp. 1279-1289.
1999	Vehicle Detection and Recognition in Multi-Source Reconnaissance Imagery	Booth, D, PK Kent, AR Herminston, A Horne and S Foulkes	Proc of the Fourth Int Airborne Rem Sens Conf And Ex, pp. 1812-1820, Environmental Research Inst of Michigan, Ann Arbour, Michigan.
1998	Investigation of Computational Vision and Principal Component Analysis with Application to Target Classification	Jacobs, EL and G O'Brien	Optical Eng, Vol. 37, No. 7, pp. 2022-2028.
1997	Vessel Classification as Part of an Automated Vessel Traffic Monitoring System Using SAR Data	Morse, AJ and MA Protheroe	Int J Rem Sens, Vol. 18, No. 13, pp. 2709-2712.
1997	Polarimetric Fusion for Synthetic Aperture Radar Target Classification	Hauter, A, KC Chang and S Karp	Pattern Recognition Letters, Vol. 30, No. 5, pp. 769-775.

1997	Feature Space Trajectory for Distorted-Object Classification and Pose Estimation in Synthetic Aperture Radar	Casasent, D and R Shenoy	Optical Eng, Vol. 36, No. 10, pp. 2719-2728.
1997	Synthetic Aperture Radar Detection, Recognition, and Clutter Rejection with New Minimum Noise and Correlation Energy Filters	Casasent, D and S Ashizawa	Optical Eng, Vol. 36, No. 10, pp. 2729-2736.
1996	Target Indexing in SAR Images Using Scattering Centers and the Hausdorff Distance	Yi, JH, B Bhanu and M Li	Pattern Recognition Letters, Vol. 17, No. 11, pp. 1191-1198.
1992	Estimation of a Moving Ship's Hull Shape from Its Wave Spectra	Meadows, GA and Z Wu	IEEE Trans on Geosc and Rem Sens, Special IGARSS'92 issue, Vol. 2, pp.1321-1324, Houston, TX, USA.
1991	Classification of SAR Ship Images with the Aid of a Syntactic Pattern Recognition Algorithm	Klepko, R	Tech Note 91-10, Defence Research Establishment Ottawa.
1991	Overview of Automated Ship Classification Work Within the Airborne Radar Section at DREO	Klepko, R	DREO Report in Review.
1990	Klassifisering av Skip i SAR-bilder	Christoffersen, T	FFI/Notat-91/7046, Norwegian Defence Research Establishment, Kjeller, Norway.

7.2 Composite Filters for Inverse Synthetic Aperture Radar Classification of Small Ships (466)

The paper discusses pattern recognition of small ships in Inverse Synthetic Aperture Radar (ISAR) images, which is a distortion-invariant pattern recognition problem. New range alignment (weighted correlation range) and new motion compensation (weighted multiple scatterers) of standard image formation steps were developed and used. An algorithm was developed to find out if the satellite image was useful for ISAR ship detection. Three different types of filters were considered:

1. An average filter (average of training images).
2. The Standard Discriminant Function (SDF) filter
3. The standard Minance filter

New concepts were provided:

- Use of a validation set is vital, and should be more widely used.
- A goodness measure to select filter parameters and to determine the advance if the filter is expected to perform well.
- Use of a new output criteria where a filter in a bank of filters is best for class determination.
- Rejection of decisions on some poor test input images
- Use of voting over a time sequence of test inputs

The initial results from ISAR ship detection using distortion-invariant (composite) filters are presented. The average filter performs best for the initial data used. Normalized correlation data is used to be able to utilise the largest correlation output for classification with average filters.

7.3 Classification of ships in SAR images (In Norwegian) (455)

The thesis focuses on classification of ships in SAR images, and it is a development of the work done by Eldhuset at FFI (298). Seasat images over part of the Oslofjord and an ocean area outside the French-Belgian coast are used. The input to the algorithm is a small segment of a SAR image (50 pixels x 50 pixels) and an angle that state the direction of the ship. The segment only contains one ship, and covers an area of 825 m x 825 m. The algorithm has the following steps:

- Masking out land in the image.
- Ship detection is done.
- Ship wake detection is done.
- Estimation of the ship’s speed and direction is performed.
- Classification of the ship is carried out.
- The results are printed out.

The classification depends on knowledge of the ocean and the ship. The filtering and threshold of the picture are based on the ocean and the ship's distributions. The filtering is done because of the speckle to be able to even out the ocean background as much as possible. The sigma-filter gives good results for this purpose. The threshold, which is used to remove the sea pixels, is based on an average value of the sea (should be calculated locally). The threshold removes all sea pixels, but also some of the weakest ship pixels. The ship is split into three regions, which can have weak or strong reflection, and this gives seven different ship classes. Warships have largest reflection in the middle, a tanker largest reflection in the back, while an ore-carrier has largest reflection in the back and the front. The template matching for each ship is implemented in the program, and then it is possible to separate all seven different ship types. The parameterisation has been mentioned theoretically, and it is described how it can be implemented.

7.4 The SSCM for Ship Characterization Using Polarimetric SAR (464)

The Symmetric Scattering Characterization Method (SSCM) that was introduced in (258) is used to characterize ships. The results indicate that the SSCM method is very promising for characterization of ships. It is possible to identify the ship elemental targets of significant maximized symmetric scattering component, and thus providing a ship specific distribution of "permanent" scattering targets. This information can be used to identify ships at different wind and sea conditions. It is possible to obtain accurate ASP's (Anne S Pierce) pitch angle under these wind and sea conditions by identifying such ship targets with significant symmetric scattering. The SSCM strongly depends on the signal phase of the peak signal, and it is very sensitive to the system focus setting and Doppler centroid shift. Before applying the SSCM, these errors should be removed.

7.5 Vessel Classification as Part of an Automated Vessel Traffic Monitoring System Using SAR Data (461)

The paper presents research that has been done to investigate the feasibility of an automated Vessel Traffic Monitoring System (VTMS) using spaceborne SAR data collected over the Dover Strait. The automated VTMS has two primary goals. The first one is to "develop a system for the surveillance of vessels carrying hazardous cargo around the coastline of the British Isles", while the secondary goal is to "monitor fishing vessels around the British shores". The VTMS gives the users information about location, speed, heading, length, width and class of vessel. The algorithm development is separated into detection and classification. The vessel pixels are separated from the background sea clutter and land regions in the detection part. The actual vessel pixels are analysed in the classification part to provide information on the type and structure of the ship.

7.6 Literature

(451) Aresu, E and G Schwartz. Impact of ScanSAR Images' Radiometric Calibration on Vessels and Identification, *IEEE Int Geosc and Rem Sensing Symp* (IGARSS'03), Toulouse, France.

(452) Booth, D, PK Kent, AR Herminston, A Horne and S Foulkes (1999): Vehicle Detection and Recognition in Multi-Source Reconnaissance Imagery, Proc of the Fourth Int Airborne Rem Sens Conf And Ex, pp. 1812-1820, Environmental Research Inst of Michigan, Ann Arbour, Michigan.

(453) Casasent, D and R Shenoy (1997): Feature Space Trajectory for Distorted-Object Classification and Pose Estimation in Synthetic Aperture Radar, *Optical Eng*, Vol. 36, No. 10, pp. 2719-2728.

(454) Casasent, D and S Ashizawa (1997): Synthetic Aperture Radar Detection, Recognition, and Clutter Rejection with New Minimum Noise and Correlation Energy Filters, *Optical Eng*, Vol. 36, No. 10, pp. 2729-2736.

(455) Christoffersen, T (1990): Klassifisering av Skip i SAR-bilder, FFI/Notat-91/7046, Norwegian Defence Research Establishment, Kjeller, Norway.

(456) Hauter, A, KC Chang and S Karp (1997): Polarimetric Fusion for Synthetic Aperture Radar Target Classification, *Pattern Recognition Letters*, Vol. 30, No. 5, pp. 769-775.

(457) Jacobs, EL and G O'Brien (1998): Investigation of Computational Vision and Principal Component Analysis with Application to Target Classification, *Optical Eng*, Vol. 37, No. 7, pp. 2022-2028.

(458) Klepko, R (1991): Classification of SAR Ship Images with the Aid of a Syntactic Pattern Recognition Algorithm, Tech Note 91-10, Defence Research Establishment Ottawa.

(459) Klepko, R (1991): Overview of Automated Ship Classification Work Within the Airborne Radar Section at DREO, DREO Report in Review.

(460) Meadows, GA and Z Wu (1990): Estimation of a Moving Ship's Hull Shape from Its Wave Spectra, *IEEE Trans on Geosc and Rem Sens*, Special IGARSS'92 issue, Vol. 2, pp.1321-1324, Houston, TX, USA.

(461) Morse, AJ and MA Protheroe (1997): Vessel Classification as Part of an Automated Vessel Traffic Monitoring System Using SAR Data, *Int J Rem Sens*, Vol. 18, No. 13, pp. 2709-2712.

(462) Novak, LM, GJ Owirka and WS Broweri (2000): Performance of 10-and 20-Target MSE C lassifiers, *IEEE Trans on Aerosp and Elect Syst*, Vol. 36, No. 4, pp. 1279-1289.

(463) Sadjadi, F (2002): Improved Target Classification Using Optimum Polarimetric SAR Signatures, *IEEE Trans on Aerosp and Elect Syst*, Vol. 38, No. 1, pp. 38-49.

(464) Touzi, R and F Charbonneau (2003): The SSCM for Ship Characterization Using Polarimetric SAR, *IEEE Int Geosc and Rem Sensing Symp* (IGARSS'03), Toulouse, France.

(465) Yi, JH, B Bhanu and M Li (1996): Target Indexing in SAR Images Using Scattering Centers and the Hausdorff Distance, *Pattern Recognition Letters*, Vol. 17, No. 11, pp. 1191-1198.

(466) Yuan, C and D Casasent (2002): Composite Filters for Inverse Synthetic Aperture Radar Classification of Small Ships, *Optical Eng*, Vol. 41, No. 1, pp. 94-104.

8 HF RADAR

8.1 Overview

The following table gives an overview of publications on the theme “HF Radar” (High Frequency Radar) sorted after publication year. The reports primarily discuss High Frequency radar used for ship detection. Summaries of a selection of some of the most important and available papers are given following the table.

YEAR	TITLE	AUTHOR	PUBLISHED
2003	Calibration of HF Radar Systems with Ships of Opportunity	Fernandez, DM, J Vesecky and C Teague	IEEE Int Geosc and Rem Sensing Symp (IGARSS'03), Toulouse, France.
2002	Suppression of Sea Clutter with Orthogonal Weighting for Target Detection in Shipborne HFSWR	Xie J, Y Yuan and Y Liu	IEE Proc Radar, Sonar and Navig, Vol. 149, No. 1, pp. 39-44.
2001	Detection of Ships with Multi-Frequency and CODAR SeaSonde HF Radar Systems	Fernandez, DM, JF Vesecky, DE Barrick, CC Teague, MM Plume and C Whelan	Can J Rem Sens, Vol. 27. No. 4, pp. 277-290, Canada.
2001	Surveillance of the 200 Nautical Mile Exclusive Economic Zone (EEZ) Using High Frequency Surface Wave Radar (HFSWR)	Ponsford, AM	Can J Rem Sens, Vol. 27. No. 4, pp. 354-360, Canada.
1998	Ship Detection With High-Frequency Phased-Array and Direction-Finding Radar Systems	Fernandez, DM, JF Vesecky, CC Teague, JD Paudan and KE Laws	Proc of IGARSS'98, Piscataway, NJ.
1998	Ship Detection With High-Resolution HF Skywave Radar	Barnum, JR	IEEE J of Oceanic Eng, Vol. 11, No. 2, pp. 196-209.
1994	Target Detection and Tracking with a High-Frequency Ground Wave Radar	Khan, R, B Gamberg, D Power, J Walsh, B Dawe, W Pearson and D Millan	IEEE J of Oceanic Eng, Vol. 19, No. 4, pp. 504-548.
1984	1984 Feasibility Study of HF Ground-Wave Radar of Tracking Ships	Ponsford, AM	Final Report British Admitality by University of Birmingham.

8.2 Detection of Ships with Multi-Frequency and CODAR SeaSonde HF Radar Systems (470)

This paper focuses on the CODAR SeaSonde (which is a high-frequency radar system) and Multi-Frequency Coastal Radar systems (MCR). These systems are designed to measure environmental ocean features like ocean currents, waves and winds, in addition to being able to detect ships and other discrete subjects. Measurements have been done on the east and west coasts of the USA, in addition to measurements over Lake Michigan.

The paper measures ship echoes within Doppler spectra. The data indicates, for the first time, the possibility to detect ships with HF (High Frequency) radar over freshwater lakes. The echoes from ships are determined, and it is shown that the positions measured with HF radar are consistent with visual and GPS observations of ships in the region observed. The radar cross-section values that are measured are consistent with experimental values obtained. The ships' echoes in the Doppler spectrum are compared to those of the first-order ocean Bragg scatter. The maximum ranges for ship detection, for radar cross-sections of approximately 50 dBsm (at 25 MHz) are estimated to be 15-20 kilometres with the MCR HF radar system. Ship estimates that are made simultaneously from both CODAR SeaSonde and MCR systems illustrate higher SNR (Signal to Noise Ratio) associated with the CODAR SeaSonde systems. Signal stationarity, frequency diversity, and peak tracking are used to separate ships from other targets and other noise sources within echoes received from both types of radar systems.

8.3 Ship Detection With High-Frequency Phased-Array and Direction-Finding Radar Systems (469)

The use of High Frequency (HF) radar systems for detection and monitoring of ship and fishing vessel activity is described in the paper. Data used in the experiment was collected during the fall of 1997 south of Chesapeake Bay during the third Chesapeake Outfall Plume Experiment (COPE-3). CODAR SeaSonde and multi-frequency HF radar systems are used. The presence of large tank ships is illustrated. The ability of HF radar to detect and track ships within a near coastal region is demonstrated by comparing data from both radar instruments with ancillary observations. The problem of echoes in multi-frequency HF radar data is addressed, and an approach to remove ship echoes is suggested. A comparison of the ship echo power to the ocean echo power in the Bragg region has shown that the tanker ships' RCS are between 40 dB to 60 dBsm. The effects of ships can be examined in greater detail, by using the combination of multiple HF radar systems and observations on the ground.

8.4 Surveillance of the 200 Nautical Mile Exclusive Economic Zone (EEZ) Using High Frequency Surface Wave Radar (HFSWR) (473)

It is required that nations establish and maintain Administration, Law Enforcement and Environmental Protection over their Exclusive Economic Zone (EEZ). The EEZ is defined as 200 nautical miles (nm) where a country is granted sovereign rights by the United Nations Convention on the Law of the Sea (UNCLOS). The EEZ is much larger than the 12 nm territorial limits, and the question is what kind of sensors is available to monitor this new frontier? The paper presents the High Frequency Surface Wave Radar (HFSWR), which has the spatial and temporal resolution needed for this purpose. The HFSWR is developed and demonstrated to monitor activity within the 200 nm EEZ in a collaborative and cost-shared project between the Canadian Department of National Defence and Raytheon Systems Canada Limited. The HFSWR is proven to be an effective tool for providing all weather, surveillance of surface activity within this the EEZ. The development of a network of two HFSWRs and an Operational Control Centre, measurements of the systems performance and an assessment of the utility to the Canadian Forces are also performed. Extensive testing and verification of parameters have been done since the system started operating in January 1999.

The area coverage is good, and ships are tracked throughout the defined area of coverage (25 nm to 220 nm by the 1200 degrees azimuth). Continuous tracking of the vessels is performed, from the first detection until they leave the coverage area or exceed their maximum detection range. The track accuracy is better than 0.25 nm in range, 0.25 degree in azimuth, and 0.5 knots in velocity. The true advantage is achieved when sensor data is combined such that the HFSWR maintains the target identity with the radar track.

8.5 Literature

(467) Barnum, JR (1986): Ship Detection With High-Resolution HF Skywave Radar, *IEEE J of Oceanic Eng*, Vol. 11, No. 2, pp. 196-209.

(468) Fernandez, DM, J Vesecky and C Teague (2003): Calibration of HF Radar Systems with Ships of Opportunity, IEEE Int Geosc and Rem Sensing Symp (IGARSS'03), Toulouse, France.

(469) Fernandez, DM, JF Vesecky, CC Teague, JD Paudan and KE Laws (1998): Ship Detection With High-Frequency Phased-Array and Direction-Finding Radar Systems, Proc of IGARSS'98, Piscataway, NJ.

(470) Fernandez, DM, JF Vesecky, DE Barrick, CC Teague, MM Plume and C Whelan (2001): Detection of Ships with Multi-Frequency and CODAR

SeaSonde HF Radar Systems, *Can J Rem Sens*, Vol. 27. No. 4, pp. 277-290, Canada.

(471) Khan, R, B Gamberg, D Power, J Walsh, B Dawe, W Pearson and D Millan (1994): Target Detection and Tracking with a High-Frequency Ground Wave Radar, *IEEE J of Oceanic Eng*, Vol. 19, No. 4, pp. 504-548.

(472) Ponsford, AM (1984): 1984 Feasibility Study of HF Ground-Wave Radar of Tracking Ships, Final Report British Admitality by University of Birmingham.

(473) Ponsford, AM (2001): Surveillance of the 200 Nautical Mile Exclusive Economic Zone (EEZ) Using High Frequency Surface Wave Radar (HFSWR), *Can J Rem Sens*, Vol. 27. No. 4, pp. 354-360, Canada.

(474) Xie J, Y Yuan and Y Liu (2002): Suppression of Sea Clutter with Orthogonal Weighting for Target Detection in Shipborne HFSWR, *IEE Proc Radar, Sonar nd Navig*, Vol. 149, No. 1, pp. 39-44.